



UNIVERSITÀ DEGLI STUDI DI SALERNO



UNIVERSITÀ DEGLI STUDI DI SALERNO
Dipartimento di Farmacia

PhD Program
in **Drug Discovery and Development**
XXXI Cycle — Academic Year 2018/2019

PhD Thesis in

***Functional characterization of
Candida albicans Hst3p
histone deacetylase***

Candidate

Anna Maria Petrone

Supervisor

Prof. *Amalia Porta*

PhD Program Coordinator: Prof. Dr. *Gianluca Sbardella*

A mamma, papà e Giulia.

INDEX

Abstract	1
Chapter I: Introduction	5
1.1 Kingdom Fungi	5
1.2 The biology of <i>Candida albicans</i>	6
1.3 The distinct morphogenetic states of <i>C. albicans</i>	7
1.4 <i>C. albicans</i> genome.....	9
1.5 Virulence factors of <i>C. albicans</i>	11
1.5.1 Polymorphism	11
1.5.2 White-opaque transition	14
1.5.3 Biofilm formation.....	15
1.5.4 Adhesion and invasion	19
1.5.5 Hydrolases secretion	22
1.5.6 pH <i>sensing</i>	24
1.5.7 Metabolic adaptation.....	27
Chapter II: Candidiasis and their treatment	29
2.1 Candidiasis	29
2.2 Treatment of candidiasis	30
2.2.1 Polyenes	31
2.2.2 Azoles.....	31
2.2.3 Fluorinated pyrimidine analog 5-FC.....	32
2.2.4 Echinocandins	32
2.2.5 Alkylamines	33
2.3 Antifungal drug resistance	33
2.4 Drug resistance in <i>C. albicans</i>	34
2.4.1 Azole resistance	34
2.4.2 Polyene resistance	37

2.4.3	Flucytosine resistance.....	37
2.4.4	Echinocandin resistance	37
2.4.5	Allylamine resistance	38
Chapter III: Epigenetic mechanisms in the fungal pathogen <i>Candida albicans</i>		
		39
3.1	Chromatin and its dynamic nature.....	39
3.2	Histone acetylation – deacetylation.....	40
3.3	Eukaryotic deacetylases.....	41
3.3.1	HDACs	41
3.3.2	Sirtuins.....	43
3.4	Histone deacetylases in <i>C. albicans</i>	45
3.5	Histone deacetylases regulate <i>C. albicans</i> morphology and pathogenicity	46
3.6	Hst3p regulates acetylation levels of H3K56 in <i>C. albicans</i>	47
Chapter IV: Aim of PhD project.....		51
Chapter V: Materials and Methods		55
5.1	Yeast strains and culture conditions	55
5.2	Monitoring <i>C. albicans</i> growth under NAM treatment.....	56
5.3	<i>Candida</i> histone extraction.....	56
5.4	Analysis of H3K56ac by Nano LC-MS/MS.....	57
5.5	Morphological analysis of <i>C. albicans</i> liquid cultures	58
5.6	Drop-plate assay	59
5.7	MALDI-TOF MS technology.....	59
5.7.1	Characterization of <i>C. albicans</i> phenotype by MALDI-TOF MS	60
5.7.2	Optimizing MALDI-TOF MS protocol for <i>C. albicans</i>	61
5.8	NAM treatment for <i>Candida</i> RNA extraction.....	62

5.9 Total RNA extraction.....	62
5.10 RNA-Sequencing	63
5.11 Recombinant Hst3p purification	64
5.11.1 Bacterial growth conditions.....	64
5.11.2 Transformation of <i>E. coli</i> competent cells.....	64
5.11.3 Expression of recombinant proteins in BLR (DE3) <i>pLysS</i> cells	65
5.11.4 Hst3p purification by affinity chromatography and ion exchange.....	65
5.11.5 Hst3p-short purification from inclusion bodies.....	66
5.12 Hst3p purification using a co-expression system.....	68
5.12.1 Co-expression experiment	68
5.12.2 Protein purification after chaperones co-expression	69
5.13 Western Blot analysis.....	69
5.14 Statistical analysis	69
Chapter VI: Results	71
6.1 Analysis of H3K56 acetylation levels during <i>C. albicans</i> growth....	71
6.2 NAM treatment induces <i>C. albicans</i> phenotypic switching.....	74
6.3 MALDI-TOF technology for <i>C. albicans</i> phenotypic screening.....	82
6.4 RNA-Sequencing data analysis.....	86
6.5 Optimization of protein expression in <i>E. coli</i>	104
6.5.1 Hst3p purification.....	106
6.5.2 Hst3p-short purification	109
6.5.3 Purification of Hst3p from a co-expression system	112
Chapter VII: Discussion	115
Bibliography	125
Appendix: List of publications	137

Papers.....	137
Presentation at conferences	138

ABSTRACT

The unicellular eukaryotic organism *Candida albicans* is one of the most important fungi in medicine, used as experimental model to study fungal pathologies and the underlying biology of dimorphic fungi. This fungus is a component of the human mucosal microbiota; it is normally found as a commensal in vaginal and oral mucosal districts, and in the gastrointestinal tract. However, at these sites it behaves as an opportunistic pathogen: following environmental changes in the host this fungus can become pathogenic, leading to invasive and lethal infections in susceptible individuals. Therefore, during the last decades, *Candida* has emerged as a major human fungal pathogen responsible for an extended variety of mucosal and systemic infections.

The ability of this opportunistic fungus to cause and propagate successfully infections is linked to the expression of different and alternative virulence factors. Its key virulence trait is its morphological plasticity: its ability to shift from oval budding yeasts to elongated cell structures (pseudohyphal and hyphal filaments) responding to diverse and numerous environmental cues.

Adaptive chromatin changes promote *Candida* variability and phenotypic plasticity. Therefore, epigenetic regulation of gene expression is considerably involved in the morphogenesis and virulence of this polymorphic fungus. Adaptation of *C. albicans* to drug pressure, yeast to hyphae transition, biofilm formation, white-opaque switch are important pathogenic mechanisms, in which posttranslational histone modifications play a prominent role. In particular, acetylation – deacetylation of histones modulates morphological switch in *C. albicans* and, consequently, this modification is correlated to fungal virulence.

Histone H3 Lys56 acetylation (H3K56ac) is an important post-translational modification in yeast, that contributes to fungal genome stability.

In *C. albicans*, acetylation levels of H3K56 are regulated by two enzymes with fungal-specific properties: the acetyl transferase Rtt109p and the NAD⁺-dependent histone deacetylase (sirtuin) Hst3p, encoded, respectively, by *RTT109* and *HST3* genes. *HST3* is an essential gene for *C. albicans*: homozygous deletion mutants for this sequence are not viable. The essentiality of *HST3* gene for *C. albicans* viability, combined with fungal-specific properties of its enzyme Hst3p, make it an attractive potential target for antifungal therapy.

Focus of this study was to examine the molecular pathways regulated by Hst3p of *C. albicans*. Considering that deletion of this sirtuin is lethal for this fungus, it is intuitive to understand that it regulates vital process in the fungal cell. As histone deacetylase, Hst3p modulates gene expression, in particular induces the repressive state of chromatin, inhibiting transcriptional activation. Consequently, deletion of this gene or repression of its protein induces dysregulation of gene expression, leading to fungal death. Based on these considerations I focused my interest on this fungal protein, in order to characterize its role in *C. albicans* biology and virulence and its downstream targets, as potential new targets for the treatment of fungal infections.

Substrate of Hst3p is the acetylated histone H3 Lysine 56. To analyse the effect of Hst3p inhibition on its substrate, I grew up *C. albicans* in the presence of nicotinamide (NAM), a non-specific sirtuin-inhibitor. Mass spectrometry analysis allowed me to evaluate, for the first time, acetylation levels of H3K56 during *Candida* growth and their variations upon NAM treatment. Interestingly, nicotinamide treatment induced the accumulation of H3K56 acetylation levels during *C. albicans* growth, demonstrating the inhibitory effect of NAM on Hst3p activity.

One important attribute of *Candida* is its morphological variability, which is the result of the adaptive response to environmental changes which in turn this morphological plasticity triggers infection.

To study the role of Hst3p in fungal virulence, I analyzed the potential involvement of this sirtuin in phenotypic switch. Morphological analyses were performed under NAM treatment to investigate the effect of Hst3p inhibition on cell duplication and filamentation. Hst3p inhibition resulted in a reduction of fungal growth rate and alteration of yeast-hyphae transition in *C. albicans*: NAM induced an abnormal filamentous growth, with formation of V-shaped hyphae under conditions that normally maintain the yeast shape of *Candida*. This phenotypic analysis was performed also on two azole-resistant strains of *C. albicans* to investigate the role of Hst3p in drug resistance. Hst3p inhibition had similar effect on the resistance strains compared to the control wild-type strain, inducing morphological alterations and reducing cell duplication rate.

These phenotypic assays highlighted the effect of Hst3p inhibition on regulation of *Candida* morphology. V-shaped hyphae formation in *Candida* in non-inducing filamentation conditions require the structural rearrangement of the whole cell, which is a result of alteration in gene expression, induced by NAM treatment. Based on these considerations, I analysed the entire transcriptome of *C. albicans* strain SC5314 by RNA-sequencing to investigate whether the inhibition of Hst3p by NAM was responsible for changes in the pattern of expression of Virulence-related Genes. This analysis showed that gene categories most dysregulated upon NAM treatment are those associated with hyphal growth, adherence, white-opaque switch, drug resistance and cell wall maintenance. RNA-Sequencing analysis allowed to identify some dysregulated genes upon Hst3p inhibition; considering that no alteration in gene expression was detected for upstream members of pathways that control these dysregulated genes, to verify if the expression of these genes is regulated epigenetically by H3K56 acetylation, future experiments of chromatin immunoprecipitation (ChIP) will be performed.

To select inhibitors of Hst3p to be used as potential fungicidal compounds, I expressed and purified both the full length and a short sequence of recombinant

Hst3p. These proteins did not show enzymatic activity, due probably to denaturing conditions used during purification, that were necessary considering that both the full length and the short sequence of Hst3p were complexed to the bacterial molecular chaperon GroEL. To improve protein folding in bacterial host and avoid denaturing conditions for purification, I expressed and purified recombinant Hst3p from a bacterial system over-expressing some molecular chaperons. Once determined the enzymatic activity of recombinant protein, an enzymatic assay will be set up, useful to screen and select small molecules, potential inhibitor of the fungal sirtuin Hst3p, which could be used as antifungal compounds.

CHAPTER I

INTRODUCTION

1.1 Kingdom Fungi

Fungi are eukaryotic single-celled or multinucleated organisms, which exist practically in all the environments of Earth, where they reside as free-living organisms. They absorb nutrients from decaying organisms thus playing an important role as ecological decomposers. Fungi are extremely diversified in size; they are represented by microscopic yeasts, which are only several microns in diameter and by large poly-pores, which may reach several meters in diameter (1). Yeasts, molds and the well-known mushrooms are part of the Kingdom of Fungi, which is a separate realm from the other eukaryotic life Kingdoms of Plants and Animals.

As mentioned previously, Fungi are present wherever, in soil, air, water, on plants, and also in organisms as well as on their surfaces. They grow on the skin, in the intestinal tract and mucous membranes of animals and humans. Just a few fungi have established a commensal relationship with humans and are members of the endogenous microbial flora (2, 3). However, they are important pathogens that may cause serious diseases and pose a significant public health risk (4).

Over the last few decades there has been a net increase in opportunistic fungal infections. The increase of organ transplantation practises, the use of novel chemotherapeutic and immunomodulatory agents and the massive use of antimicrobial agents have increased the population of susceptible patients at risk for invasive fungal infection (particularly aspergillosis and candidiasis, and in the USA of histoplasmosis) (5, 6, 7).

Fungi of the *Candida* genus have emerged as major human pathogens and *C. albicans* represents the preponderant cause of invasive candidiasis (8, 9).

1.2 The biology of *Candida albicans*

The creamy and glistening white of yeasts colonies gave rise to the name of *Candida*, that comes from the Latin term “candidus”, meaning “glowing white”.

The heterogeneous genus *Candida* includes fungi which belong to the order Saccharomycetales and to the class Ascomycetes. Approximately 200 species are part of this genus that is the largest genus of clinically important yeast (10).

C. albicans is a eukaryotic organism whose cellular structure is similar, for functions and morphology, to that of animal cells. As eukaryotes, fungal cells contain a nucleus in which DNA is packaged by histone proteins. In addition, fungal cells contain mitochondria and a complex system of internal membranes, including the endoplasmic reticulum and the Golgi apparatus. *C. albicans* has a plasma membrane similar to that of other eukaryotes, except that the bilayer structure is stabilized by ergosterol: a steroid molecule that replaces the cholesterol found in the membrane of animal cells. However, a peculiar feature of fungal cells is the presence, outside the cytoplasmic membrane, of a cell wall. *C. albicans* biology and pathogenicity are influenced by the cell wall because of its ability to provide protection and a physical contact with host and the surrounding environment and to maintain the shape and plasticity of the organism. It was initially considered an almost inert cellular component that protect against changes in osmotic pressure, but now we know that it is a dynamic and plastic structure.

The major components of the cell wall are proteins and fibrillar polysaccharides, glucan and chitin, which are involved with its structural rigidity (11, 12). The expression, secretion, and physical location within the cellular wall structure of wall proteins may vary intensively. These proteins, relevant as antigens, can undergo several and distinct post-translation modifications, such as glycosylation (primarily addition of mannose residues), phosphorylation, and ubiquitination (12). Mannoproteins, located at the cell surface, constitute a

fibrillar outer layer in the cell wall, while the β -glucan/chitin layer is located under the mannoprotein coating (13) (Fig. 1).

C. albicans cell wall proteins mediate interactions with host proteins, such as complement fragments, fibrinogen and several extracellular matrix components. Some glycolytic enzymes and proteins related to the Hsp70 and Hsp90 families are also located in the cell wall (12). *Candida* cell wall is the structure responsible for a specific fungal morphology because of the differential expression of some proteins in the distinct morphological growth form of the fungus (12).

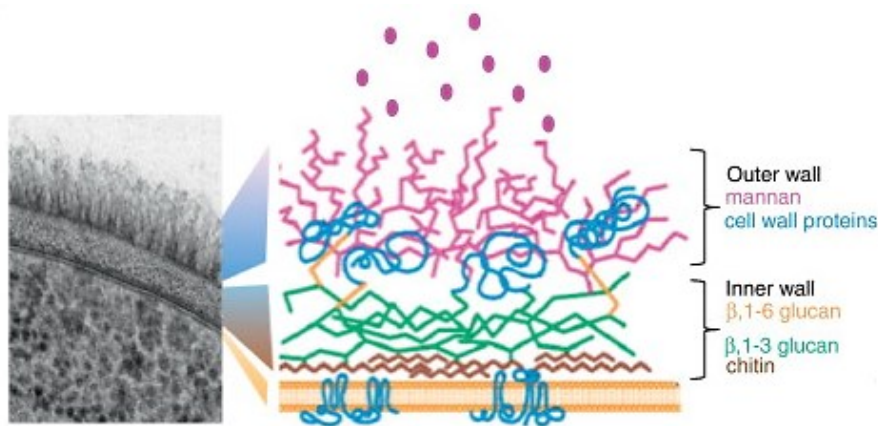


Fig. 1 Structure of the *Candida albicans* cell wall

Section of *C. albicans* cell wall showed by transmission electron micrograph and by a cartoon showing the arrangement of the major components (14).

1.3 The distinct morphogenetic states of *C. albicans*

A striking feature of *C. albicans* is its ability to detect changes in the environmental and to tolerate and respond adequately by changing its morphology and physiology (12). *C. albicans* grows either as a unicellular budding yeast or in a filamentous form. Existing in two distinct morphological forms, it is generally denominated as “dimorphic fungus”. Unlike *Histoplasma capsulatum*, *Penicillium*

marneffeii, other dimorphic fungal pathogens of humans, that grow typically in filamentous forms outside the host and convert to yeast form in human bodies, *C. albicans* is found in both yeast and filamentous forms in the host and switches reversibly between the two forms. The yeast-to-hyphae transition exhibits a multiplicity of intermediate growth forms, that are referred to as germ tube and pseudo-hyphae (9, 15).

C. albicans reproduces by budding, giving rise to yeast cells and to the production of blastospores or blastoconidia. Changes in growth conditions (pH, temperature, nutrients) induces the formation of short germ tubes. The germ tube has parallel-sided walls and do not display constriction at the point of origin of the mother cell. The daughter bud elongates and, after the formation of the septum, the daughter cell remains connected to the blastopore mother cell (15). This process give rise to the formation of pseudo-hyphae, filamentous structures composed of elongated cells with constriction at the septa. Pseudo-hypha can vary considerably in their width and length and can superficially resemble true hyphae when the elongation of buds is so excessive (15).

It is possible to distinguish true hyphae from pseudo-hyphae: true hyphae do not show constriction at the neck of the mother cell, are highly polarized and have parallel sides along their length; pseudo-hyphal cells, on the contrary, have a constriction at the neck of the mother cell and the bud, and at other subsequent septal junction (15). The composition of the cell wall of yeast cells, pseudo-hypha and true hypha is similar, although the percentages of mannan, β -glucans, chitin vary depending on the morphological stage considered. In addition, the content of chitin in hyphal cells is at least three times greater than yeast cells (12).

The yeast-to-hyphae transition occurs in response to a wide variety of environmental conditions that mimic those present in the host, including the presence of serum, body temperature (37°C), high CO₂/low O₂ ratio, neutral pH, some carbon sources (e.g., N-acetylglucosamine) and amino acids (e.g., proline)

(16, 17). On the other hand, temperatures below 30°C, high cell densities, ammonium salts, high concentration of glucose and acid pH favour the yeast-like growth of *Candida* (17) (Fig. 2).

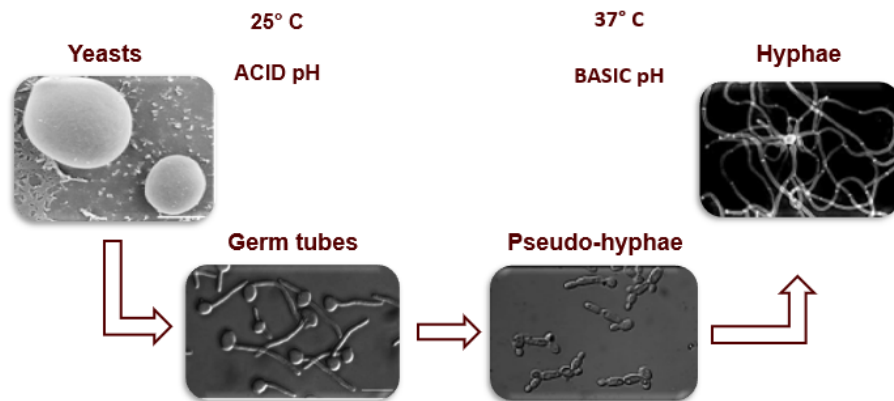


Fig. 2 *C. albicans* yeast-to-hyphae transition

Acid pH and temperatures below 30°C induce yeast form of *C. albicans*. When pH and temperature increase, yeast cells (18) germinate with consequent formation of germ tubes, pseudo-hyphae and true-hyphae (9).

1.4 *C. albicans* genome

The genome of *C. albicans* strain SC5314 has been fully sequenced since this organism is widely used for molecular and genetic analyses all over the world. Generally, the genome of this fungus displays high dynamism and contains many translocations, truncations, and other mutations that occur more frequently than in other microbes (9). Sequencing of the genome of this polymorphic fungus has been performed at the Stanford Genome Technology Center (19).

C. albicans has a diploid genome consisting of eight pairs of homologous chromosomes which are numbered from 1 (largest) to 7 (smallest), with the one

carrying the ribosomal DNA, called R. Its haploid genome size is estimated to be 14.3 Mb, containing 6,419 open reading frames (ORFs) longer than 100 codons, of which some 20% do not show known counterparts in other genomic sequences (19).

This fungus poses great problems for studying gene function because it is diploid and because the codon CUG, which is found at least once in approximately two-thirds of ORFs, is translated abnormally into a serine instead of a leucine (19).

The *Candida* Genome Database (CGD) is constantly updating the information pertaining the functions of unknown ORFs and of other genes. Gene annotation data available in CGD shows that the function of only 27.11% (1,686 genes) of the genes have been experimentally verified, whereas 70.44% (4,380 genes) of the genes remain uncharacterized. Furthermore, 152 genes are still in the “dubious” class for which no experimental evidence is available.

Introns often interrupt eukaryotic genes; these intergenic elements are spliced out yielding gene transcripts for fully expressed coding sequences. Only about 6% of *C. albicans* genes contain introns, most of which typically contain a single intron. Genes involved in specific cellular processes, such as splicing, translation, mitochondrial respiration and protein degradation contain high percentage of introns; thus introns are not randomly distributed in *C. albicans* genome (20).

Several introns are located in 5' UTR regions, suggesting the possibility that translational regulation of certain genes is controlled by alternative splicing.

1.5 Virulence factors of *C. albicans*

C. albicans is a commensal organism normally found in mammals. It asymptotically colonizes the skin and mucosal surfaces of most healthy individuals. However, alteration in host immunity, and/or microbiota and use of antibiotics can lead to the inability to control *C. albicans* colonization and the development of disease.

The pathogenicity of this pleomorphic fungus depends upon three major factors: the immune status of the host, the environmental conditions and the expression of specific virulence factors (9).

The ability to adhere tightly to host cells, switch phenotypes, form biofilm, secrete degradative enzymes (e.g.: phospholipases, secreted aspartyl proteases), escape the immune system are key virulence factors, essential for *C. albicans* survival in hostile conditions and they have been implicated in the pathogenesis. Additionally, the ability of *C. albicans* to infect a host is supported by a wide number of fitness attributes, including metabolic plasticity, rapid adaptation to changes in environmental pH, powerful nutrient supply ability and resistance to stresses imposed by the host (9, 21, 22).

1.5.1 Polymorphism

The ability to undergo a reversible phenotypic transition from budding yeast to pseudo-hyphal and hyphal filaments is one of the most important virulence traits of *C. albicans* which is responsible for its success as a pathogen.

Yeast and true hyphae are regularly observed during infection and have distinct functions; on the contrary, the role of pseudo-hyphae and switching *in vivo* is rather unsettled (22).

A wide variety of virulence-related properties are associated to hyphae development and elongation, including lysis of macrophages, invasion of epithelial cell layer, biofilm formation and thigmotropism (21, 22). Thus, hyphal

form is an active player in tissue penetration and escape from immune cells. As such, virulence of *C. albicans* mutants that are unable to form true hyphae is attenuated (23). However, *C. albicans* yeast cells contribute to fungal virulence by dissemination in tissue and colonization of new sites of infection in the host body.

Many environmental conditions also affect *C. albicans* morphology, including extracellular pH, starvation, presence of serum and amino acids. The quorum sensing, a mechanism of microbial communication, also regulates *Candida* morphogenesis (22). The main quorum sensing molecules produced by *C. albicans* include farnesol, tyrosol and dodecanol. Due to this kind of cell communication, yeast growth is induced at high cell densities ($> 10^7$ cells ml⁻¹), while hyphal formation is promoted at low cell densities ($< 10^7$ cells ml⁻¹) (22).

Extracellular signals (serum, glucose, pH, temperature, nutrients) are transmitted from the medium to internal transcriptional machinery through a series of signal transduction pathways that affect the expression of large number of genes whose products are responsible for the change of *Candida* morphology.

The Cph1p-mediated MAPK pathway and the Efg1p-mediated cAMP pathway are well-known pathways involved in yeast-to-hypha transition (16, 24). In *C. albicans*, *RASI* regulates hyphal development and likely functions upstream of both pathways (Fig. 3) (24).

Nitrogen starvation active MAP kinase pathway promoting *C. albicans* filamentation by induction of the downstream transcription factor *CPH1*, whose expression is regulated by the upstream members of this cascade, the kinases Cst20p, Hst7p, Cek1p (21, 25).

The response to serum, 37°C and CO₂ is mediated by Ras-cAMP-protein kinase A pathway (21). Environment stimuli or *RASI* can trigger *CYR1*, adenylyl cyclase, inducing formation of cAMP. This secondary messenger induces activation of PKA catalytic subunits (Tpk1p and Tpk2p) with subsequent

activation of the downstream effector *EFG1* which promote hyphal growth, inducing hypha-specific genes and repressing yeast-specific genes (Fig. 3) (25).

On the contrary, the dimorphic transition is negatively regulated by several transcription factors: *TUP1*, *NRG1* and *RFG1* (25), which repress filament-specific genes (*ECE1*, *HWPI1*, *RBT1*), encoding secreted or cell surface proteins (25).

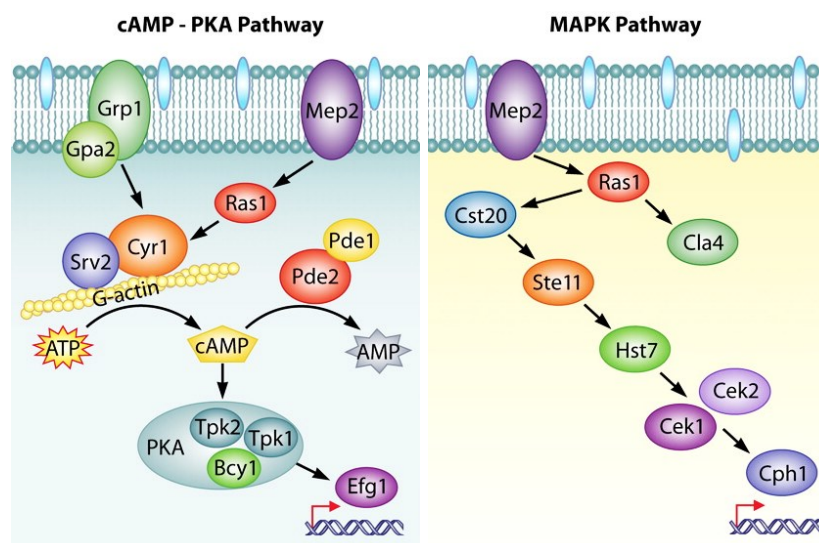


Fig. 3 Cellular signaling cascades involved in *C. albicans* morphogenesis

C. albicans dimorphism is regulated by the Cph1p-mediated MAPK pathway and the Efg1p-mediated cAMP pathway. The GTPase Ras1p functions upstream of both pathways (Figure modified by Ref. 26).

1.5.2 White-opaque transition

EFG1, the major transcription regulator of *Candida* dimorphism, is also involved in the control of white-opaque phenotypic switching, another type of morphological transition which consists in the alternation between white and opaque cells. Differences in gene expression are responsible of distinct features of these two types of cells: white and spherical cells form white smooth colonies while opaque and elongated cells, which are larger than the other one, form grey and flat colonies (27). White and opaque cells differ in expression of specific genes (*WH11* in white type; *OP4* and *SAP4* in opaque type), in their virulence (opaque cells are less virulent than white cells) and sensitivity to immune system (27).

The white-opaque switching is controlled by *MTL* (mating type like) locus, which includes the transcriptional regulators *MTLa1*, *MTLa1* and *MTLa2*, located on chromosome 5 (27). *MTLa1* is located on one chromosome, while *MTLa1* and *MTLa2* are located on the other homolog. The master regulator of the white-opaque transition is the transcription factor *WOR1* (*white-opaque regulator 1*) which is expressed exclusively in opaque cells and is inhibited by the *Mtla1/a2* heterozygous complex; for this reason, only strains of *C. albicans* homozygous in *MTL* locus can switch. However, this process is very rare in *MTL* homozygous strains. *WOR1* regulates transcription levels of other transcription factors, *EFG1*, *WOR2* and *CZF1*, and *WOR1* itself, creating a positive feedback loop (27). Downstream effector of *WOR1* is the opaque and filamentation inducer 1, *OF11*, a zinc finger transcription factor involved in opaque cell formation.

Environment signals (CO₂ and N-acetylglucosamine) activating the *cAMP/PKA* pathway induce formation of opaque cells by *WOR1* (27) (Fig. 4).

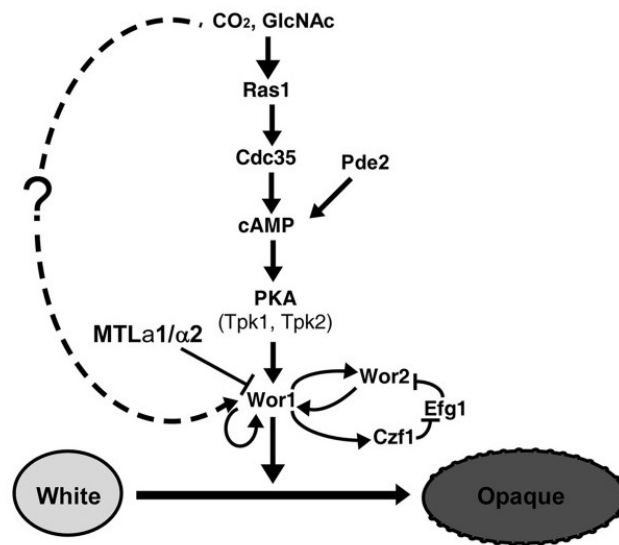


Fig. 4 White-opaque transition in *C. albicans*

CO₂ and GlcNAc activating the cAMP-PKA pathway induce opaque cell formation in *C. albicans*. The white-opaque transition can be triggered also by an uncharacterized pathway mediated CO₂ and GlcNAc sensing (27).

1.5.3 Biofilm formation

To survive to changes in the environment many microorganisms have evolved the capacity to adhere to surfaces and to develop as a multicellular community, such as biofilms (28). A biofilm can be defined as an organized community of adherent cells with a complex three-dimensional architecture and properties that are distinct from those of free-floating (planktonic) cells.

C. albicans has the ability to form biofilm on abiotic or biotic surfaces, such as pacemakers, dentures, catheters and mucosal cell surfaces (29) This capacity is an important virulence factor of *Candida* and it represents a serious problem for human health because the development of biofilms on implanted medical devices has increased the rates of nosocomial infections (9).

C. albicans biofilms are highly structured and heterogeneous due to the presence of a great variety of cell types (budding yeast, pseudohyphal cells, elongated hyphal cells) embedded in an extracellular polysaccharide matrix (29) (Fig. 5).

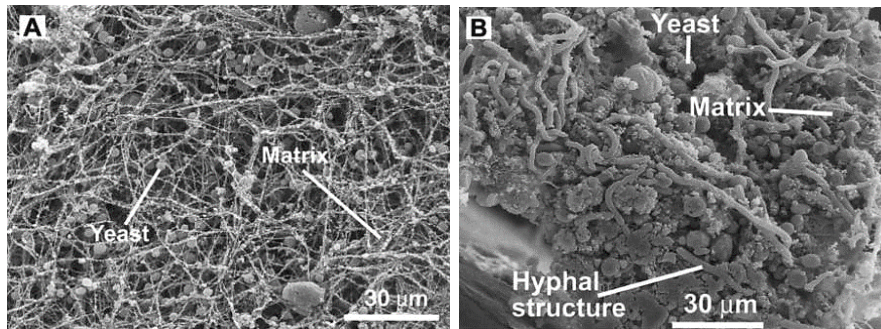


Fig. 5 SEM of *in vivo* *Candida* biofilm

Image A shows the intraluminal surface of biofilm; image B displays a biofilm cross-section. Yeast cells and hyphae are evident along with extracellular matrix material (30).

Formation of biofilm takes place through distinct developmental stages. At first, the budding yeast cells adhere to the substrate and proliferate horizontally forming a basal layer of anchoring cells. Subsequently, yeast cells produce elongated structures (germ tubes) that grow into filamentous forms, including hyphal and pseudo-hyphal cells, forming the upper layer of the biofilm. Then, as biofilm matures there is an accumulation of extracellular matrix material, mainly composed of proteins and carbohydrates, that will cover the biofilm. Finally, non-adherent yeast cells disperse from the biofilm complex colonizing new sites (9, 22, 31). *C. albicans* virulence is promoted by dispersion of yeast cells from the mature biofilm, as dispersed cells display enhanced virulence compared to planktonic cells due their increased ability in adhesion and biofilm formation (22).

Mature biofilms are characterized by an increased drug resistance to different antifungal agents. It has been demonstrated that individual cells dispersed from

biofilms are much more resistant to common drugs and host immune factors than the free-living cells (22, 32). This suggests that the biofilm formation induces changes in the cells and these changes are retained even after the dispersion of the individual cells from the biofilm (9).

Distinct factors are responsible for the biofilm drug resistance (Fig. 6). First, the complex architecture of biofilms impairs diffusion of antifungal drugs (9, 22); the presence of multiple cell types (yeast, pseudo-hypha and true hypha) combined with the high cell density within the biofilm can contribute to biofilm resistance (33). Moreover, variation of the ergosterol content in membranes biofilms can promote azole and polyene resistance (31). Over-expression of enzymes involved in synthesis of ergosterol is responsible of differential response to antifungal compounds (33).

The upregulation of efflux pumps is an additional mechanism of biofilm drug resistance, with consequent reduction of antifungal accumulation in the cell. It is the primary mechanism of azole-resistance in *C. albicans*. Drug exportation in this fungus is regulated by two major classes of efflux pumps: the ATP-binding cassette transporters *CDR1* and *CDR2* and the major facilitator superfamily transporter *MDR1*. It has been demonstrated that during biofilm formation and development the transcription levels of these genes are upregulated (33).

Secreted extracellular matrix represents a physical barrier which protect cells within the biofilm from environmental stresses and antifungal compounds. Biofilm drug resistance is correlated with the activity of the polysaccharide β -1,3 glucan, constituent of the biofilm matrix, which binds to and sequesters azole drugs. The susceptibility of biofilms to fluconazole is increased when biofilm is treated with β -1,3-glucanase (29).

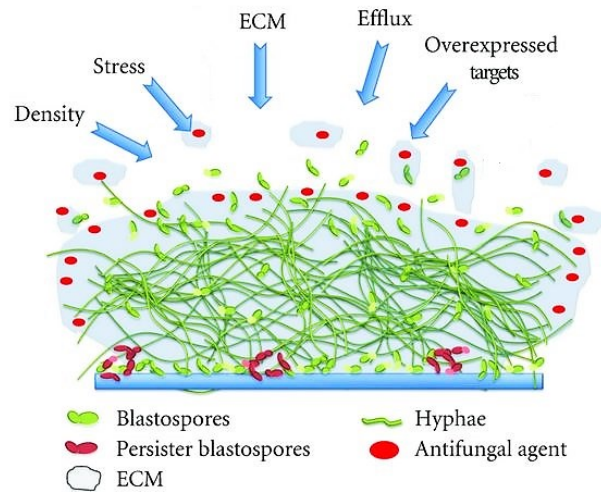


Fig. 6 Biofilm resistance mechanisms in *C. albicans*

The high cell density and complexity of *C. albicans* biofilm is represented. Several factors drive antifungal resistance within the biofilm, including extracellular matrix, cell density, stress, overexpressed targets (Figure modified by Ref. 33).

Six transcription factors, defined master biofilm regulators, are implicated in biofilm formation: *TEC1*, *BCR1*, *EFG1*, *BRG1*, *NDT80*, *ROB1* (9, 22, 29, 31), which regulate transcription of at least 19 gene targets (Fig 7). Deletion of any of these regulators (*BRG1*, *EFG1*, *TEC1*) causes deficient biofilm formation *in vivo* rat infection models (34).

Negative regulator of biofilm matrix synthesis is the transcription factor Zap1, a modulator of zinc acquisition. This Zap1 function suggests that biofilm matrix levels are affected by environment zinc levels (22, 31).

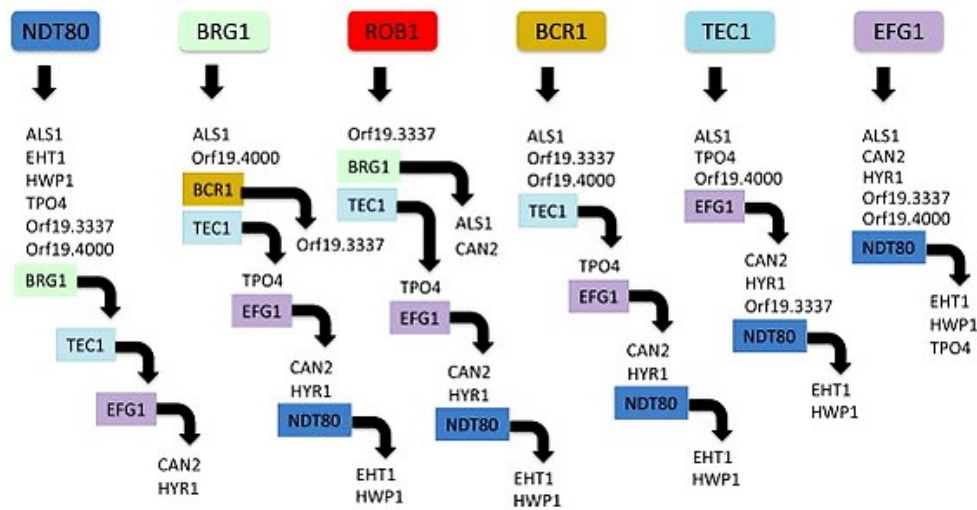


Fig. 7 Master regulators controlling biofilm formation in *C. albicans*

TEC1, *BCR1*, *EFG1*, *BRG1*, *NDT80* and *ROB1* are transcription factors involved in biofilm formation by controlling the expression of at least 19 gene targets, including biofilm-specific genes (*TPO4*, *CAN2*), hypha-specific genes (*HWP1*, *HYR1*) and adhesion genes (*ALS1*) (34).

1.5.4 Adhesion and invasion

Like other pathogens, *C. albicans* virulence requires recognition and binding to host cells. This fungus has the ability to adhere to distinct surfaces like implanted devices in host body, epithelial and endothelial cells and extracellular matrix (35). Adhesion to host cell proteins is an essential early step for colonization and establishment of *Candida* infections (9). This process is mediated by a specialized group of proteins, called adhesins, which promote adherence to other *C. albicans* cells, to other microbes, to host cells and abiotic surfaces (22).

To date, three gene families (*ALS*, *HWP*, and *IFF/HYR*) have been identified as adhesins in *C. albicans* (35). The *ALS* (agglutinin-like sequence) family is composed by eight proteins with a large degree of sequence similarity (Als1 to Als7 and Als9). The *ALS* genes, located on three different chromosomes

(chromosome 3, 6 and R), encode for glycosylphosphatidylinositol (GPI)-linked cell surface glycoproteins (9, 25, 35). The first cell surface protein identified was Als1p, which activated by cAMP-PKA pathway via Efg1p, functions as a downstream regulator of filamentation in *C. albicans* (25). Overexpression of *ALS1* induces flocculation and formation of voluminous aggregates of cells (25). Particularly important for adhesion is the hyphal-cell wall adhesin Als3p (22); it plays crucial role also in other process, such as iron acquisition (Als3p functions as a ferritin receptor), promotion of hyphae endocytosis by clathrin-mediated mechanism and biofilm formation (22, 35).

The *HWP* (hyphal wall protein) family includes three proteins: Hwp1p, Hwp2p and Rbt1p (repressed by Tup1). These genes are expressed exclusively in hyphae and are upregulated during mating of opaque cells; they are involved in adhesion to host cell surface proteins, cell-cell aggregation, mating and biofilm formation (35). Hwp1p, which is among the most well-characterized adhesins in *C. albicans*, is a cell surface mannoprotein that is covalently linked to the out layer of the cell wall glucan via the C-terminal GPI anchor. The extracellular amino-terminal domain of Hwp1p, which looks like mammalian transglutaminase substrates, is recognized by the transglutaminases exposed on host cell surface; this cross-linking between germ tube/hyphae and mammalian epithelial cells determine the formation of stable and covalent attachments to host cells (22, 35). The expression of *HWPI* is regulated by transcriptional regulators of hyphal growth *EFG1*, *TUP1* (25) and by the master regulator of biofilm formation *BCR1* (29).

The *IFF/HYR* gene family (*IFF* standing for IPF family F and *HYR* for hyphally upregulated protein) includes 12 proteins (*HYR1* and *IFF1-11*) with high level of sequence similarity in their N-terminal domains (35). The best-known member of this family is *HYR1*, hypha-specific gene coding a GPI-anchored cell wall protein, whose transcription *EFG1*-dependent is induced during yeast-to-hyphae transition (25). Unlike the other members of this family, *IFF11* encodes a

secretory protein, which does not display the GPI anchor, suggesting an enzymatic function for this protein, which is required for normal cell wall organization and virulence (35).

C. albicans uses two different mechanisms for host cells invasion: induced endocytosis and active penetration. The first mechanism depends upon host cell functions: *C. albicans* hyphae induce their own endocytosis by expression of specialized proteins on their cell surface, called invasins. These proteins induce rearrangements of the host actin cytoskeleton stimulating endocytosis through interaction with E-cadherin on epithelial cells and N-cadherin on endothelial cells (36). Als3p (which also functions as an adhesin) and Ssa1p are two invasins involved in the process of host invasion via induced endocytosis (Fig. 8) (22). The second mechanism is host cell-independent and requires active and viable *C. albicans* hyphae: fungal cells exert force for active penetration and invasion of host cells or substrate (22, 37). Active penetration is facilitated by enzymatic activities of secreted aspartic proteases (Saps) (22).

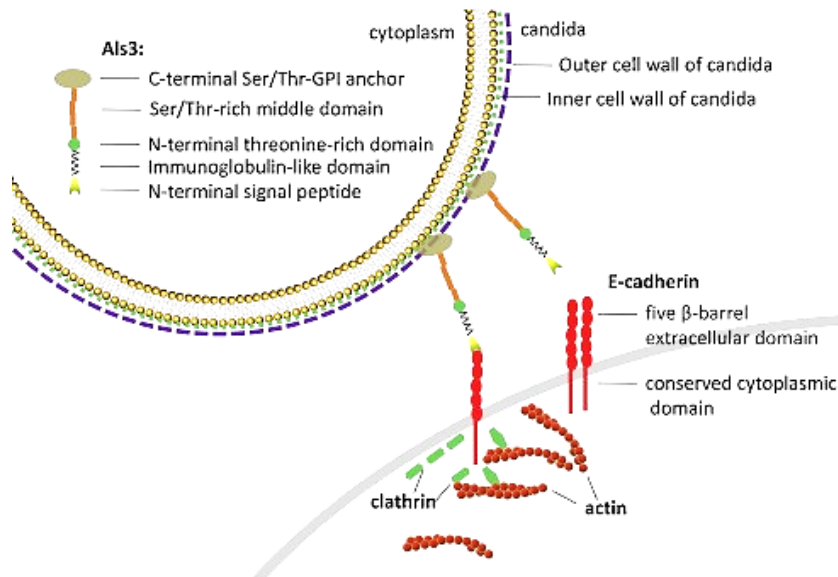


Fig. 8 Clathrin-mediated induced-endocytosis

The image illustrates the interaction between the fungus-expressed Als3p and the host cell-surface E-cadherin. This interaction recruits several cytoplasmic proteins, such as actin and clathrin, to the site of endocytosis (Figure modified by Ref. 38).

1.5.5 Hydrolases secretion

C. albicans is able to secrete distinct hydrolytic enzymes which are considered virulence factors responsible for penetration of the fungus into host cells by digestion of host cell membranes. In addition, these enzymes facilitate the extracellular nutrient acquisition by their degradation activity (39). *C. albicans* exhibits three different classes of secreted hydrolases: proteases, phospholipases and lipases.

Among the hydrolytic enzymes, secreted aspartic proteases (*SAPs*) are key virulence determinants of *C. albicans*, which contribute to adhesion and invasion of this fungus. The *SAPs* family is composed by ten members, Sap1p to Sap10p, with a molecular weight in the range of 35 to 50 kDa. Unlike Sap1p–8p which are

secreted and released into the extracellular space, Sap9p and Sap10p remain bound to the cell-surface by their GPI-anchor (22). Sap enzymes are responsible for all of the extracellular proteolytic activity of *C. albicans* and contribute to fungal success also because of their versatile property: they are active in a wide range of pH. In particular, Sap1p-3p are active at lower pH values and Sap4p-6p show strong activity at higher pH (39). In addition, the expression of the *SAP* genes is differentially regulated according to the type and stage of the disease (40, 41): Sap1p-3p are mainly involved in superficial candidosis, whereas Sap4p-6p are particularly expressed in systemic infection (40). During *C. albicans* yeast-to-hyphae transition the expression of *SAP* genes is regulated according to the morphological stage of the fungus: *SAP1-SAP3* and *SAP8-10* genes are mainly detected in yeast cells, whereas *SAP4* to *SAP6* genes are predominantly expressed in hyphal forms (39, 42). It has been demonstrated that the expression of *SAP* genes and hyphae formation are two processes co-ordinately regulated: the transcription factor Tec1p (expressed mainly in hyphal forms) recognizes consensus sequences in the promoter regions of *SAP4*, *SAP5* and *SAP6*, regulating their transcript levels (39). In summary, *SAP* genes are differentially expressed according to environmental conditions (pH), to morphological form and to the type of disease.

Phospholipases family is composed by four different classes (A, B, C and D) of enzymes which damage cell membrane by hydrolysis of phospholipids, the major component of the biological membranes. They are divided in distinct classes according to the specific ester bond that is cleaved in the phospholipid molecule. Among the phospholipases the most notable are the components of class B which are the only extracellular phospholipases and contribute to *C. albicans* pathogenicity (22).

C. albicans secretes other hydrolases, the lipases, a gene family consisting of 10 members (*LIP1-10*) whose extracellular activity is important for fungal

infection (22). The expression of all 10 lipases during the yeast-hypha transition and the detection of lipases transcripts such as *LIP5*, *LIP6*, *LIP8*, and *LIP9* during experimental infections suggest the contribution of lipases to *C. albicans* virulence (43).

1.5.6 pH sensing

C. albicans has the ability to sense, respond and adapt rapidly to changes of the environment. The transition between different morphologies represents a response of *C. albicans* to these changes. Ambient pH is one of the most relevant environmental variables that changes between different host niches. *Candida* is exposed to broad range of pH stresses during its commensal and pathogenic lifestyles. It can colonize, in fact, any human anatomical sites that vary strongly in ambient pH including the oral mucosa (pH 6), the vagina (pH 4-5) and stomach (pH 2); thus, this fungus is able to proliferate in media ranging from pH 2 to pH 10 (44). Adaptation to the surrounding environmental pH is essential for the biology and pathogenicity of *C. albicans* (22, 44, 45).

C. albicans is not only able to adapt to changing environment pH but it can also actively modify extracellular pH, through metabolism of available nutrients. For example, *Candida* acidifies the medium by glycolysis in presence of glucose. On the contrary, in the absence of glucose, this fungus uses amino acids as carbon source and alkalinizes the extracellular environment by producing ammonia, thereby auto-inducing hypha formation (22).

The two-cell wall β -glycosidases Phr1p and Phr2p are decisive proteins for adaptation of *C. albicans* to changing pH. Expression of these genes is pH-dependent and is oppositely regulated by the major pH-responsive modulator Rim101p. *RIM101* gene encodes a zinc finger transcription factor activated by proteolytic cleavage of its C-terminal domain in neutral-alkaline conditions (25). Once activated in alkaline environment, Rim101p moves into the nucleus where

induces expression of *PHR1* and suppresses *PHR2* transcription (25), genes encoding cell surface glycosidases involved in correct cross-linking of β -1,3 and β -1,6 glucans. Consequently, *PHR1* is expressed at alkaline pH, whereas *PHR2* is expressed at acidic pH (44, 45).

The *RIM101* pathway includes numerous upstream members, such as Rim21p, Dfg16p, Rim9p, Rim20p, Rim13p, Rim8p (25). Rim9p and Rim21p/Dfg16p are two trans-membrane proteins which are responsible for sensing external pH changes. In neutral-alkaline environments, these sensors are stimulated, inducing ubiquitination and phosphorylation of Rim8p; this process leads to endocytosis of the membrane complex and recruitment of the endosomal sorting complexes required for transport (ESCRT) I, II, and III (25, 46). Other two Rim proteins are recruited: Rim20p and Rim13p; Rim20p functions as an adaptor bringing the protease Rim13p in proximity with Rim101, thus promoting Rim101p proteolytic activation. Rim101p active “short form” migrates to the nucleus regulating expression of target genes (25, 46) (Fig. 9). It functions as a repressor of genes expressed at acidic pH, such as *PHR2* (induced at pH below 5.5) and an activator of the alkaline-response genes *PHR1* (strongly induced at pH above 5.5), *PRA1* (coding an antigenic cell wall protein involved in host-pathogen interaction during *C. albicans* infection) and *RIM101* itself (25, 44) (Fig. 10).

Therefore, *RIM101* signaling pathway controls pH-regulated gene expression but also other processes, such as cell wall organization, growth and pH-induced morphogenesis, considering that yeast and hyphal growth of *C. albicans* are favored by acidic and alkaline pH, respectively (44).

External pH adaptation requires cell wall remodelling: the exposure at the cell wall periphery of chitin and β -glucan increases in acidic environment. Reduced expression of the cell wall chitinase encoded by *CHT2* allows increased chitin exposure. Transcription levels of *CHT2* gene are regulated by *RIM101* signaling pathway (Fig. 10): intuitively, Rim101p, activated in alkaline growth conditions,

increase expression of the chitinase Cht2p in the cell wall, with consequent hydrolysis of the growing chitin polymers into short fragments reducing the chitin content in the cell wall (44).

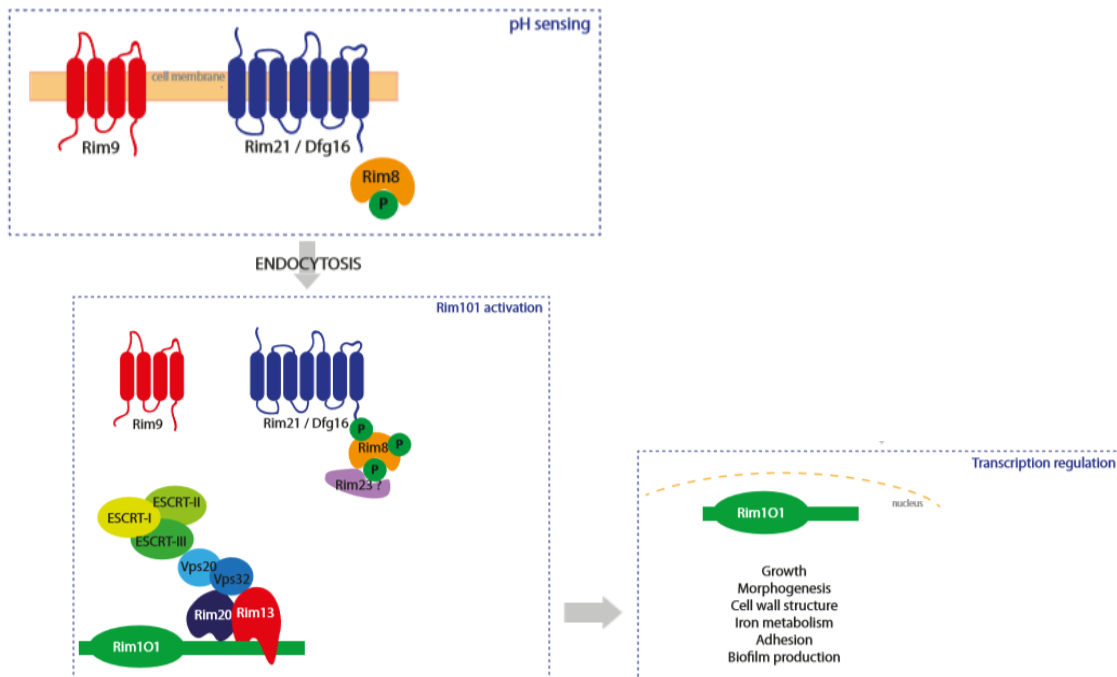


Fig. 9 Rim101p pathway in *C. albicans*

The transmembrane sensor proteins Rim9p and Rim21p/Dfg16p and the arrestin-like protein Rim8p sense variations in pH. In alkaline conditions, the membrane complex undergoes to endocytosis and the ESCRT complexes are recruited, combined to recruitment of Rim20p and Rim13p, leading to Rim101p activation, which migrates to the nucleus (Figure modified by Ref. 46).

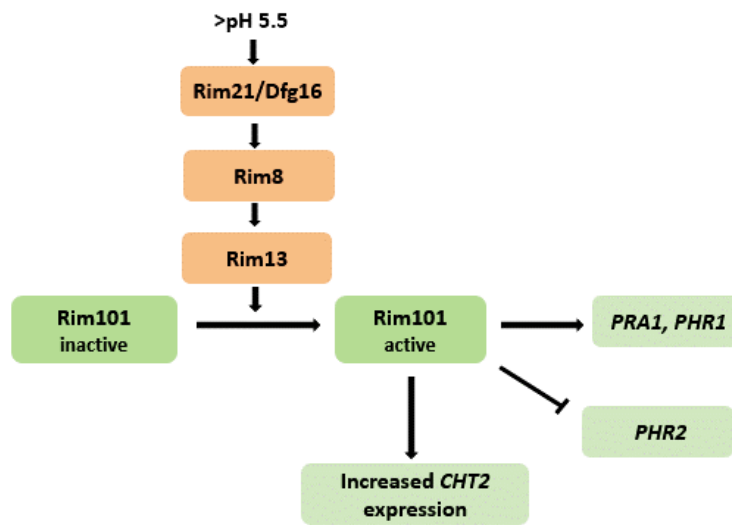


Fig. 10 Downstream targets of Rim101p

Active Rim101p in short form migrates to the nucleus where represses the expression of genes induced at acid pH, such as *PHR2*, and induces the expression of alkaline-response genes, such as *PHR1*, *PRA1* and *CHT2*.

1.5.7 Metabolic adaptation

C. albicans, which can colonize diverse niches, must exhibit adequate metabolic flexibility to use and assimilate the available nutrients in these niches. In healthy individuals *Candida* is mainly found in the gastrointestinal tract. In this host niche the concentration of nutrients is high, but the growth of the fungus is limited by the competition with other microbes which are part of the intestinal microbial flora. When *C. albicans* gains access to the bloodstream during infection, it finds a relatively high concentration of glucose (6-8 mM), the selected nutrient source of most fungi (22). However, the fungus can be phagocytosed by macrophages and neutrophils. Inside the phagocytic cells, in which the amount of available nutrients is reduced, *C. albicans* faces a condition of nutrient starvation (22).

In hostile niches *C. albicans* can adapt, survive and grow using alternative metabolic pathways to exploit host proteins, lipids and amino acids (22). Consequently, this adaptation affects the virulence of this pleomorphic fungus.

CHAPTER II

CANDIDIASIS AND THEIR TREATMENT

2.1 Candidiasis

Fungal infections caused by yeasts belonging to the genus *Candida* are called candidiasis. These infections can be caused by over 20 species of *Candida* yeasts and the most prevalent of which is *C. albicans* (5, 47). In healthy individuals, distinct human body niches (skin, mucous membranes, intestinal tract) (47) are colonized by *Candida* yeasts creating a balance with resident microflora without causing infection. However, when this balance is compromised there is an overgrowth of these yeast cells leading to infection development.

These opportunistic infections can occur in acute or chronic form and they can range from superficial lesions to disseminated and invasive mycoses in immunocompromised patients.

The commonest form of candidal infections is the superficial candidiasis which affects niches where *Candida* lives as a commensal, such as the mucosa and the skin. Illness, debility and temporary reduction of immune defense can predispose to symptomatic mucosal and superficial candidiasis. Superficial infections do not represent always a risk to the life of patients, however they inevitably and significantly lower the quality of life (48).

Patients severely compromised by weakening and malignant diseases and who receive antibiotic and immunosuppressive therapy are easily affected by systemic candidiasis (5, 49, 50). The most frequent form of this invasive and severe yeast infection is candidemia, that occurs when *Candida* enters the bloodstream and disseminate to other organs (49).

To date, the number of drugs available for antimycotic therapy is limited, even if the frequency of *Candida* infections is increasing (48).

2.2 Treatment of Candidiasis

C. albicans is a eukaryotic organism and therefore share many of its biological processes and cellular structures with human cells. Consequently, there is a restricted number of targets which can be exploited for antifungal drug development. Most antifungal drugs cause deleterious side effect on human cells and, at the dose used, are fungistatic rather than fungicidal. For this reason, an important goal in antifungal drug discovery is the identification of new fungal targets.

Antifungals can be subdivided into five classes based on their site and mode of action: polyenes, which interact with fungal membrane sterols altering membrane functions; azoles, which inhibit the enzyme involved in ergosterol synthesis; 5-fluorocytosine, which inhibits RNA and/or DNA synthesis; echinocandins, which inhibit the enzyme responsible for glucan synthesis (the main cell wall polysaccharide); allylamines, which inhibit ergosterol biosynthesis by inhibition of squalene epoxidase (48) (Fig. 11).

Numerous and distinct types of mechanisms have been developed by fungal cells to tolerate antifungals compounds, leading to an increase in the prevalence of drug resistance (48).

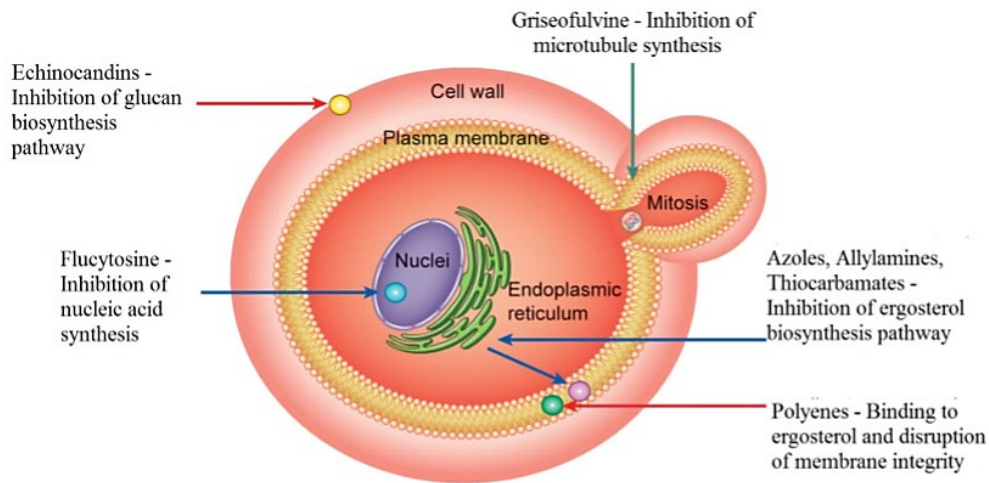


Fig. 11 Traditional antifungal agents and their mechanisms of action

Polyenes bind ergosterol forming holes or channel in the fungal membrane, impairing cellular functions; azole act by inhibition of the enzyme able to convert lanosterol into ergosterol, causing depletion of ergosterol in cell membrane; echinocandins inhibit glucan biosynthesis; flucytosine acts inhibiting RNA and DNA synthesis; griseofulvine inhibits mitosis (51).

2.2.1 Polyenes

Derived from fermentation by *Streptomyces* species, polyene antifungal agents are natural drugs which interact with ergosterol localized in the fungal cell membranes with consequent disruption of membranes. This binding causes the formation of channels through the fungal membrane, leading to altered permeability of this structure, oxidative damage and finally leaking of intracellular components, resulting in fungal death (48, 52).

2.2.2 Azoles

Azoles represent the class of antifungals with the highest number of drugs, including ketoconazole, itraconazole and fluconazole. These compounds are broadly used for mycoses treatment (48). Azole antifungal agents have fungistatic activity against *Candida* spp. and fungicidal activity against *Aspergillus* spp. (48).

Azole interfere with the biosynthesis of ergosterol, the major sterol in fungal cells which functions as a regulator of membrane fluidity and integrity. Target of these drugs is the lanosterol 14 α -demethylase, a cytochrome P450 enzyme, encoded by the *ERG11* gene and involved in converting the lanosterol into ergosterol. The inhibition of Erg11p enzyme causes reduction of ergosterol content in fungal cell membrane with accumulation of aberrant sterol intermediates, leading to the formation of a plasma membrane with alterations in its structure and function (48, 53).

2.2.3 Fluorinated pyrimidine analog 5-FC

Flucytosine, also known as 5-fluorocytosine (5-FC), is a fluorinated derivative of the pyrimidine cytosine. 5-FC is actively transported into the fungal cell by the cytosine permease, encoded by *FCY2* gene; once inside the cells, cytosine deaminase, encoded by *FCY1* gene, converts this compound in 5-fluorouracil (5-FU) which is further converted to metabolites that inhibit fungal RNA and DNA synthesis, causing cell death (48). Considering that mammalian cells do not possess the cytosine deaminase, they are not directly subject to the deleterious effects of 5-FC (48).

2.2.4 Echinocandins

The most recently developed class of antifungal agents is represented by the cyclic lipopeptides, the echinocandins. These drugs interfere with cell wall biosynthesis functioning as non-competitive inhibitors of β -(1, 3)-D-glucan synthase. Inhibition of this enzyme results in depletion of glucan polymers in fungal cells with consequent altered structural integrity of fungal wall, that became weak and unable to resist osmotic pressure leading to cell lysis (54).

2.2.5 Allylamines

A new class of ergosterol biosynthetic inhibitors is represented by allylamines; these agents differ chemically and functionally from the other ergosterol-inhibiting antifungal compounds. Allylamines, such as terbinafine and naftifine, act by inhibition of the squalene epoxidase, enzyme encoded by *ERG1* gene and involved in ergosterol biosynthesis, blocking the conversion of squalene to lanosterol, leading to squalene accumulation and ergosterol depletion in the cell membrane (48). High levels of squalene alter membrane permeability, leading to disorganization of cellular structure and finally fungal death (48).

2.3 Antifungal drug resistance

Over the last decades the incidence of invasive fungal infections has increased considerably, with consequent massive use of antifungals agents (55). A critical risk to the excessive use of antifungals is the acquisition of drug resistance; this risk is aggravated by the exiguous number of antimycotics available for therapy. Consequently, antifungal drug resistance is becoming a serious problem in the control of fungal diseases.

In general, fungi can display intrinsic resistance to antifungal drugs (primary resistance) or can develop resistance following exposure to the drug during treatment (secondary resistance) (55). The development of antifungal resistance is a complex phenomenon and is correlated to multiple microbial and host factors (55), including:

- alteration in drug target,
- overexpression of the antifungal drug target,
- alteration in sterol biosynthesis,
- reduction in the intercellular concentration of target enzyme,
- overexpression of efflux pumps

The diffusion of drug resistance phenomenon requires the development of new alternative therapy for the treatment of fungal diseases.

2.4 Drug resistance in *C. albicans*

The resistance against antifungals compounds has been extensively documented among several *Candida* species (49, 56). The increased insensitivity of *C. albicans* to antifungal drugs as consequence of resistance has been observed with different degree for every currently used drug classes (56).

2.4.1 Azoles resistance

Azole antifungal agents represent the primary treatment choice for antifungal therapy because of their safety profiles and favorable oral bioavailability (48, 49). However, among several *Candida* species the intrinsic and acquired resistance to azole antifungals is increasing (48, 49, 57).

The main azole resistance mechanisms in *Candida* include:

1. Mutation and overexpression of *ERG11*. Azole affinity to the drug target lanosterol 14 α -demethylase (encoded by *ERG11* gene) is reduced when point mutations occur in this gene causing the amino acid substitutions in the target enzyme, which is responsible for the biosynthesis of the ergosterol, an important component of the cell membrane (48, 49). These amino acid substitutions result in structural alteration of lanosterol 14 α -demethylase, reducing its recognition by azole antifungals. Another mechanism of azole resistance involving ergosterol synthesis is represented by the overexpression of *ERG11* gene (caused by gene duplication in some cases), which results in intracellular accumulation of the target protein and intuitively more drug for inhibition is required, reducing fungal susceptibility (48, 49) (Fig. 12, A).

2. Overexpression of plasma membrane efflux pumps. Two types of azole transporters in *C. albicans* have been identified: the major superfamily transporter encoded by *MDR1* and the ATP-binding cassette (ABC) transporters encoded by *CDR1* and *CDR2* (48, 49, 52). These pumps differ in the specificity of the azole molecule and in the source of energy used to translocate the compounds across the cell membrane. The Cdr proteins are primary transporters able to transport all azole compounds using the hydrolysis of ATP; on the contrary, Mdr1p pump is a secondary transporter which uses proton gradient for extrusion of fluconazole (48, 49, 52). Consequently, upregulation of *MDR1* is responsible for fluconazole resistance and upregulation of ABC transporters results in multi azole resistance (48) (Fig.12, B). The effect of overexpression of these efflux pumps is the decreased intracellular concentration of azole available for inhibition of the target enzyme (lanosterol 14 α -demethylase) (48, 49). Mutations in the transcription factors *TAC1* (transcriptional activator of *CDR* genes) and *MRR1* (multidrug resistance regulator 1) are responsible for upregulation of *CDR1/CDR2* and *MDR1*, respectively (48, 49). To date, nineteen point mutations in different domains of *TAC1* have been identified and fifteen mutations for *MRR1* (58).

3. Inactivation of *ERG3* gene. This gene encodes for the sterol $\Delta^{5,6}$ desaturase, enzyme which catalyzes one of the final steps of the ergosterol biosynthesis pathway. Defective $\Delta^{5,6}$ desaturation results in altered sterol content in cell membrane which does not contain ergosterol but other sterols. This alteration is correlated to azole resistance and cross-resistance to polyenes (48, 49, 52) (Fig. 12, C).

4. Alteration of azole influx. Azole can cross the cell membrane via energy-independent facilitated diffusion (48). When fungal cell membrane composition is altered, membrane fluidity and asymmetry are affected,

leading to a decreased uptake of drugs (48, 59). Moreover, among resistant *C. albicans* clinical isolates the azole import levels change, suggesting that drug uptake plays a key role in azole resistance (48).

5. Biofilm formation. *Candida* forms biofilms that are intrinsically resistant to azoles, and the mechanisms that underlie this resistance are multifactorial, involving induction of drug efflux pumps during biofilm formation, reduced penetration of drugs through biofilm matrix, expression of resistance genes, drug sequestration by glucan within the extensive extracellular matrix (48, 58).

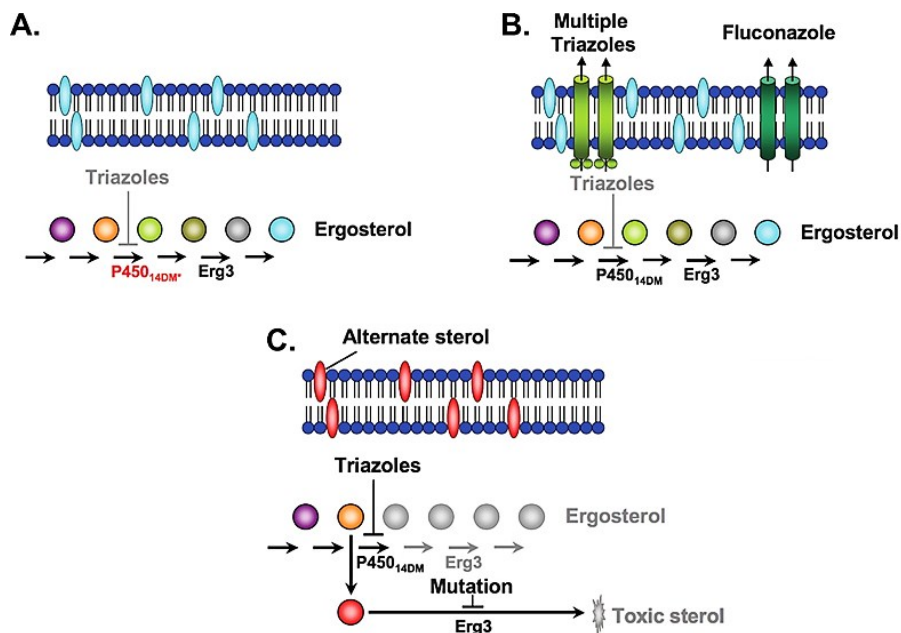


Fig. 12 *C. albicans* azole resistance mechanisms

A) Upregulation or mutation of triazole target, lanosterol 14 α -demethylase (also known cytochrome P450) reduces effect of azole compounds on their target. B) Overexpression of efflux pumps *CDR1* and *CDR2* confers resistance to multiple triazoles and upregulation of *MDR1* confers resistance to fluconazole, reducing intracellular accumulation of these drugs. C) Following cytochrome P450 inhibition by azoles, intermediates of ergosterol biosynthesis are accumulated and converted in toxic sterol by the desaturase Erg3p, inhibiting fungal growth. *ERG3* mutation prevents the accumulation of toxic sterol conferring azole resistance (Figure modified by ref. 60).

2.4.2 Polyenes resistance

In *C. albicans*, the resistance to polyene, in particular to amphotericin B, is less common and generally involves depletion of the target ergosterol in the fungal plasma membrane (48, 49). Defects in genes involved in biosynthesis of ergosterol cause the accumulation in cell membranes of others sterol instead of ergosterol (49). In fact, membranes of polyene-resistant *Candida* isolates have reduced levels of ergosterol, compared to those of polyene-susceptible isolates (49). Decreased sensitivity to polyenes is a consequence of loss-of-function mutations in ergosterol biosynthetic genes, such as *ERG3* (48, 49), *ERG5* (61), *ERG6* (49), *ERG11* (62).

2.4.3 Flucytosine resistance

In vitro, 3–10% of *C. albicans* isolates display resistance to flucytosine, whereas during treatment with 5-FC, 30% of isolates develop resistance (48). The deficiency in enzymes involved in the pyrimidine pathway causes resistance to this drug (48, 49). Point mutations in the *FCY2* gene, which encodes the cytosine permease, decrease the activity of this enzyme preventing the intracellular accumulation of this compound (49). Moreover, point mutations in the cytosine deaminase (encoded by *FCY1* gene) and in uracil phosphoribosyl transferase (encoded by *FURI* gene) alter the metabolism of 5-fluorocytosine (49).

2.4.4 Echinocandins resistance

Among *Candida* species no intrinsic resistance to echinocandin has been identified so far (63). Mutations in the drug target (1,3)- β -D-glucan synthase complex lead to echinocandins resistance (48, 49). This acquired resistance involves point mutations in “hot spot” regions of *FKS* genes, which encode the two subunits of glucan synthase; these mutations result in amino acid changes in

protein sequence, decreasing the sensitivity of enzyme to drug (64). *C. albicans* resistance is mostly linked to mutations in *FKS1* gene, and especially at amino acids 641 to 649 and amino acids 1,345 to 1,365 in hot spot 1 and hot spot 2, respectively (64). On the contrary, in *Candida glabrata* these mutations are mainly found in *FKS2* gene (64).

2.4.5 Allylamines resistance

Allylamines bind to squalene epoxidase (Erg1p), inhibiting ergosterol biosynthesis, without affecting cytochrome P-450 enzymes. Single amino acid substitution in Erg1p is responsible for terbinafine resistance (48). Upregulation of genes encoding membrane transporters (*CDR1*, *AGP2* and *HOL3*) is also linked to terbinafine resistance in *C. albicans* (48).

CHAPTER III
EPIGENETIC MECHANISMS IN THE FUNGAL PATHOGEN
Candida albicans

3.1 Chromatin and its dynamic nature

In all eukaryotes, including the fungal pathogen *C. albicans*, transcriptional activation and repression are affected by specific chromatin structures.

Chromatin is the nucleoprotein complex that houses the genetic information in Eukaryotes. The basic repeat element of chromatin is the nucleosome, composed by 147 bp of DNA wrapped around a histone protein octamer comprised of two histone H2A-H2B dimers and one histone (H3-H4)₂ tetramer. Small segments of linker DNA link each nucleosome to the next. Chromatin is further condensed by formation of a poly-nucleosome fibre which is stabilized through the binding of histone H1 to the linker DNA and to each nucleosome, allowing the formation of an order structure (65).

Histones are relatively small (11-15 kDa), very basic proteins that share the same structure: a globular histone fold domain, composed by three α -helices connected by two loops, critical for nucleosome formation and a flexible N-terminal tail that protrudes from the nucleosome core and is subjected to numerous modifications (66). Histones have a primary role in packaging large genomes into small nuclei. However, nucleosomes are not simply structural elements: they play fundamental roles in regulation of gene expression since they determine the accessibility of DNA and the sequential recruitment of regulatory factors to the DNA. Several molecular mechanisms are used to regulate access to DNA in chromatin: chemical modifications of histones proteins and DNA, remodelling of nucleosome, incorporation of histone variants (67).

Histones undergo a wide variety of post-translational modifications (acetylation, phosphorylation, methylation, ubiquitylation, sumoylation) that, by alteration of histones interaction with DNA, regulate important biological processes such as transcription, DNA repair, nucleosome assembly. Therefore, these covalent modifications modulate chromatin condensation state: they can create or stabilise binding sites for regulatory proteins, like transcription factors, or they can have opposite effect, occluding chromatin-binding sites (68).

Nucleosomes are completely or partially disassembled and moved along the DNA fiber by ATPase remodelling enzymes, exposing or occluding local DNA regions to interactions with transcription factors which regulate gene expression (67).

All together these mechanisms regulate DNA accessibility and, consequently, are all vital biological processes.

3.2 Histone acetylation - deacetylation

Gene transcription is a finely and highly regulated process in Eukaryotes (68). Among the numerous post-translation modifications of histones, the acetylation plays a crucial role in regulation of gene expression. Specifically, acetyltransferase enzymes induce transcriptional activation acting on lysine side chains of histones and other non-histone proteins (68).

Histone acetylation is a dynamic and reversible process; the balance between acetylated and non-acetylated proteins is controlled by the opposing action of two families of enzymes: histone acetyltransferases (HATs) and histone deacetylases (HDACs), respectively (69).

Histone acetyltransferase proteins (HATs) transfer an acetyl group from acetyl-coenzyme A (acetyl-CoA) to the ϵ -amino group of some lysine side chains within the N-terminal tail region of histones, mostly in H3 and H4 (68). These regions

regulate interactions between the nucleosomes and bind DNA through charge interactions: positively charged histone tails interact with negatively charged DNA. Lysine acetylation causes neutralization of this positive charge weakening histone-DNA or nucleosome-nucleosome interactions; consequently, the nucleosome structure is destabilized increasing chromatin accessibility to transcription modulators (68).

Generally, acetylated chromatin is associated with transcriptional activation, whereas deacetylation correlates with repression of gene expression (68).

3.3 Eukaryotic deacetylases

Eukaryotic deacetylases, which act suppressing gene transcription by removing the acetyl groups from the lysine residues, are highly conserved from yeast to human. They modulate the acetylation status of histones and non-histones targets, such as the cytoskeletal protein tubulin (70). These enzymes are divided in two functionally distinct families: Zn^{2+} -dependent histone deacetylases or HDACs and NAD^+ -dependent histones deacetylases or sirtuins, which are homologous to the yeast Sir2 (Silent information regulator 2) family (70). These two families are composed by numerous and distinct proteins with non-redundant functions (70).

3.3.1 HDACs

Histone deacetylases are classified in three main groups in humans based on their homology to yeast proteins. Class I HDACs have high sequence similarity to yeast Rpd3p and include 4 members: HDAC 1-3, and HDAC8. Class II HDACs are similar to yeast Hda1p and include HDAC 4-7, HDAC 9-10. The last group is class IV, which contains the solitary member HDAC11; it has conserved residues in its catalytic site that are shared by both class I and class II deacetylases (70, 71).

Class I, II, IV HDACs share similar function, three-dimensional structure, sequence homology and catalytic mechanism (71). The active sites of these enzymes display a high degree of sequence similarity: they consist of a tubular pocket characterized by two adjacent histidine residues, two aspartic acid residues, one tyrosine residue and a Zn^{2+} ion located at the bottom of this pocket (72). Histidine residues make hydrogen bonding to aspartic acid residues and activate a water molecule coordinated with the zinc ion inducing the nucleophilic attack at the carbonyl of the acetylated substrate (71, 72) (Fig. 13).

Therefore, the catalytic domain of these enzymes, composed by approximately 390 amino acids, deacetylate acetylated substrates by activation of a water molecule with the divalent zinc coupled to the histidine-aspartate charge-relay system (70, 72).

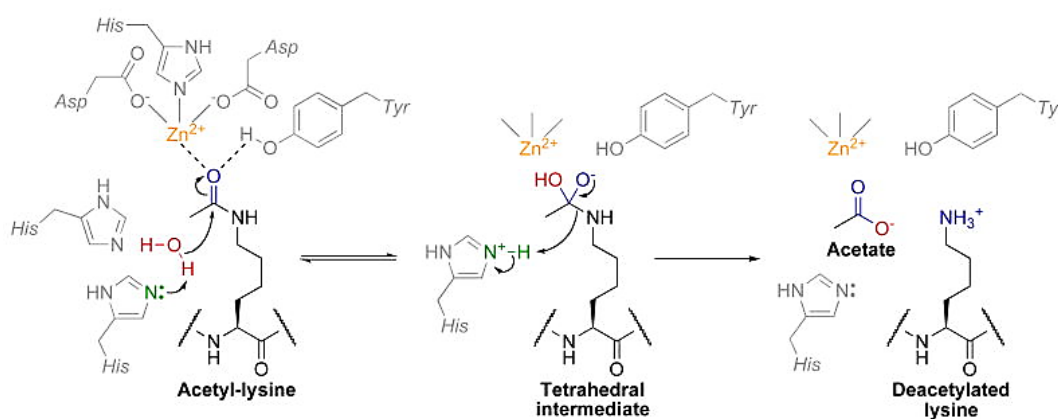


Fig. 13 HDACs catalytic mechanism

The active sites of HDACs is composed by a Zn^{2+} ion and a histidine-aspartate charge-relay system. An activated water molecule attacks the acetyl carbonyl carbon inducing the formation of a tetrahedral intermediate witch collapses forming acetate and deacetylated lysine (73).

3.3.2 Sirtuins

Enzymes of class III HDACs are represented by sirtuins, NAD⁺-dependent histone deacetylases which require NAD⁺ as cofactor for their activity, in contrast to class I, II and IV HDACs which are Zn²⁺-dependent enzymes. These proteins are evolutionarily conserved, with seven homologs in humans (SIRT1-7) and five in yeast (ySir2 and HST1-4) (74). Sirtuins are involved in multiple and vital cellular processes, such as apoptosis, cell cycle regulation and gene silencing (74).

Members of this family of histone deacetylases show some and specific conserved sequence motifs (70, 71). These enzymes are composed of four helices connected by four linking loops (75). These loops give rise to a cleft where a highly conserved catalytic core is found (75). During deacetylation reaction, the acetyl-lysine and NAD⁺ bind this catalytic core occupying opposite sides (75). The catalytic domain of sirtuins differ from that of others HDACs: consists of approximately 275 amino acids and holds two motifs which may function as zinc finger domain, and one or more hydrophobic regions (70).

Sirtuins are structurally different from the HDACs and, moreover, deacetyl their substrates by a very different mechanism that requires NAD⁺ as a substrate (70). In fact, unlike class I, II, and IV HDACs which are sensitive to the inhibitor trichostatin A (TSA) and release the final acetyl group to the aqueous solution, sirtuins are not inhibited by TSA and transfer the acetyl group of the substrate to an ADP-ribose molecule (76).

Sirtuins cleave one single molecule of NAD⁺ for each molecule of acetyl-lysine that is deacetylated, producing deacetylated lysine, nicotinamide (NAM) and 2'-*O*-acetyl-ADP-ribose (OAADPr) as products (70, 74). Kinetic studies reveal that acetyl-lysine substrate binds first the catalytic domain followed by NAD⁺ to form a ternary complex, suggesting that acetyl-lysine binding is necessary for proper position of the nicotinamide ring of NAD⁺ (74).

The reaction is initiated by binding of NAD^+ to the catalytic site in the presence of substrate, suggesting that both substrates must be bound to the active site for deacetylation reaction (70). After NAD^+ binding, in the first step sirtuins break the NAD^+ molecule releasing nicotinamide as first product and α -1'-*O*-alkylamidate intermediate. Two different mechanisms have been proposed to explain the formation of this intermediate (73, 74).

Nicotinamide is a potent product inhibitor of sirtuins: it can rapidly react with the α -1'-*O*-alkylamidate intermediate regenerating NAD^+ and acetylated substrate by the process “nicotinamide exchange” (73, 74). In the subsequent steps, after multiple reactions involving formation of a cyclic intermediate and water attack, the two final products are released, the *O*-acetyl-ADP-ribose and the deacetylated lysine (73, 74). Therefore, the enzymes transfer the acetyl group from the substrate to the ADP-ribose molecule, releasing *O*-acetyl-ADP-ribose (*OAADPr*), that could be a potential second messenger (73, 74) (Fig. 14).

Several reports have suggested that in addition to deacetylase activity, some sirtuins display NAD^+ -dependent ADP-ribosyl-transferase activity (76).

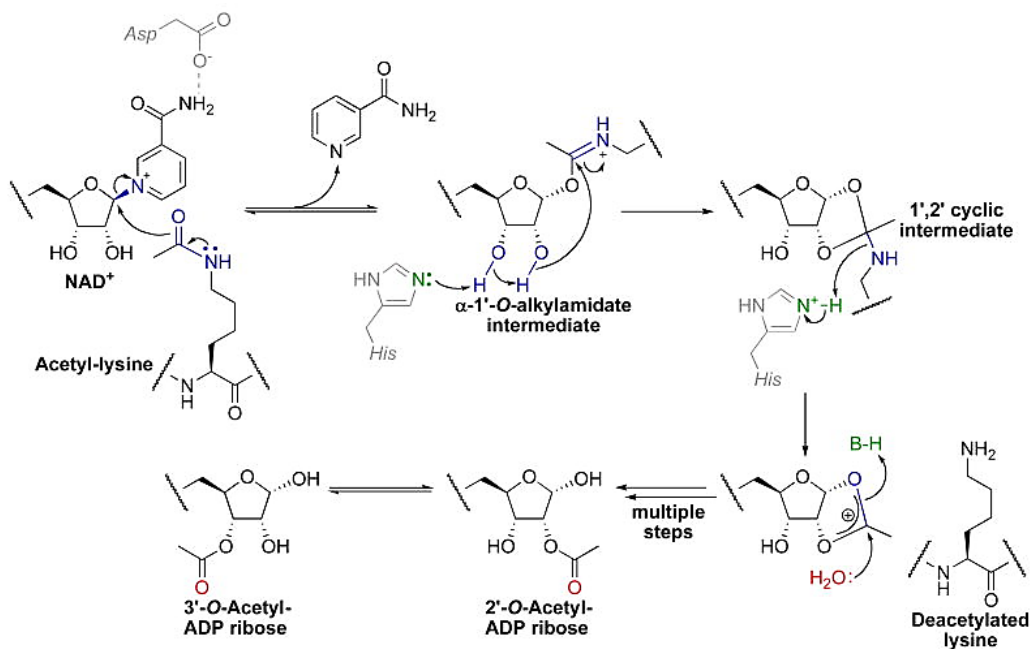


Fig. 14 Sirtuin catalytic mechanism

For deacetylation reaction, sirtuins require the presence of NAD⁺ and acetylated lysine in a 1:1 stoichiometry. Once NAD⁺ molecule is broken, NAM (first product) and α-1'-O-alkylamidate intermediate are released; in subsequent reactions the two final products are released, the O-acetyl-ADP-ribose and the deacetylated lysine (73).

3.4 Histone deacetylases in *C. albicans*

In *C. albicans*, several histone deacetylases have been identified and they are divided in three main classes based on the homology with the key *Saccharomyces cerevisiae* enzymes: Rpd3p is the key enzyme for class I, Hda1p for class II and Sir2p for class III (77, 78).

Class I HDACs in *C. albicans* includes *RPD31*, *RPD32*, *HOS1* and *HOS2*. *C. albicans* genome encodes two genes, *RPD31* and *RPD32*, which are orthologues of *S. cerevisiae* *RPD3*. Proteins of this family have short C-terminal tails and are

usually smaller than those of Class II with the HDAC domain that occupies the major part of these enzymes (77, 78). They play fundamental role in cell survival and proliferation and are principally located within the nucleus (79). Rpd31p and Rpd32p are suppressor of white to opaque transition (78).

HOS3 and *HDA1* are members of class II HDACs. In response to specific cellular signals they shuttle between the nucleus and the cytoplasm (79). Hda1p is involved in regulation of hyphal development (78).

Class III of histone deacetylases, which do not use zinc as cofactor for their activity, is constituted by the sirtuin family which includes *SIR2* gene and *HST* genes: *HST1*, *HST2* and *HST3* (77, 78). The *Candida* Genome database reports Hst1p and Hst2p as putative NAD⁺-dependent histone deacetylases involved in the regulation of white-opaque switching in *C. albicans*. A member of the sirtuin family is the NAD⁺-dependent histone deacetylase Hst3p, which is inhibited by nicotinamide and dynamically controls acetylation levels of lysine 56 on histone H3 (77).

3.5 Histone deacetylases regulate *C. albicans* morphology and pathogenicity

Several biological processes, including yeast-to-hypha transition, drug resistance, biofilm formation and white-opaque switching, are finely regulated by histones deacetylases in *C. albicans* by interaction with specific transcriptional factors (78).

C. albicans has the ability to reversibly switch from yeast to hyphal form. This morphological transition is regulated by changes in chromatin structure, in which HDACs are involved.

Deletion of *HDA1* gene in *C. albicans* impairs hyphal development (77). This result suggests the role of Hda1p in the regulation of fungal filamentation. The

transcription factor Brg1p recruits Hda1p to the promoters of hypha-specific genes, which inhibits the binding of the hyphal repressor Nrg1p allowing the maintenance of hyphal development (78) Therefore, the yeast deacetylase Hda1p changes the chromatin structure of these regions supporting hyphal state (78).

Rpd31p histone deacetylase functions as a repressor and activator of phenotypic transition. In normal conditions for unicellular yeast growth, Rpd31p acts as a repressor of hyphal induction, interacting with repressor complex and deacetylating histone lysine residues in the promoters of hypha-specific genes (*HWPI*, *ECE1*). When environmental conditions induce filamentation, Rpd31p functions as an activator of hyphal extension, inducing expression of the filament-specific transcription factor Ume6p (78).

Recent studies have highlighted the involvement of histone deacetylases in drug resistance process. In particular, it has been demonstrated that sensitivity to some fungistatic compounds can be increased by co-administration of HDACs inhibitors (80) and deletion of *HDA1* and *RPD3* significantly reduces the expression of efflux pumps genes (79).

Therefore, we can conclude that the expression of several fungal virulence factors is epigenetically regulated in *C. albicans* by histone deacetylases activity.

3.6 Hst3p regulates acetylation levels of H3K56 in *C. albicans*

An important posttranslational modification in *C. albicans* is the histone H3 Lysine 56 acetylation (H3K56ac) regulated by *RTT109* and *HST3* genes encoding, respectively, the acetyl transferase Rtt109p and the NAD⁺-dependent histone deacetylase (sirtuin) Hst3p, two enzymes with fungal-specific properties (81). This modification is generally important in yeasts because of contributes to fungal genome stability: altered acetylation levels cause chromosome loss and DNA damage (82).

Acetylation of this lysine residue occurs predominantly during S phase, but when cells enter the G₂/M phase of the cell cycle this modification disappears rapidly (82).

Considering that reduced levels of H3K56ac sensitized *C. albicans* to antifungal and genotoxic agents, it has been investigated the role of this histone modification and of the two enzymes Rtt109p and Hst3p in *C. albicans* viability. For this purpose *C. albicans* deletion mutants were generated.

Deletion of *RTT109* gene, encoding the acetyltransferase responsible for H3K56 acetylation, resulted in a reduction of H3K56ac, increased sensitivity to echinocandins and genotoxic agent (such as hydroxyurea) as consequence of oxidative damage to DNA and reduction of fungal growth rate (81).

On the contrary, the deletion of the two alleles of *HST3* was lethal for *C. albicans*, suggesting that this gene is essential for fungal viability. Only *HST3*+/ Δ heterozygous cells were viable and sensitive to echinocandins and hydroxyurea (81). To study the importance of this gene in *C. albicans*, other mutants were generated in which one copy of *HST3* gene was deleted and the other one was placed under the control of a promoter repressed with doxycycline. Gene repression with doxycycline resulted in strong reduction of *HST3* mRNA levels, increased H3K56 acetylation levels, histones H3 and H4 fragmentation and abnormal filamentation (81). *HST3* repression induced transition to filamentous form under conditions that normally favour the yeast form of *C. albicans*: after 9 and 24 hours of treatment abnormal filaments appeared with a V-shape conformation (“V-shaped filaments”) (81). Moreover, it was examined the effect of *HST3* deletion in *rtt109* Δ/Δ mutants and found that these double mutants were viable, although they grew more slowly compared to the single mutants. Therefore, the lethality of *HST3* deletion mutant is determined by the *RTT109* gene (81).

Considering that nicotinamide is a sirtuins inhibitor, its effect on the fungal sirtuin Hst3p was examined, in order to evaluate whether nicotinamide treatment would mimic *HST3* gene repression effect. Nicotinamide treatment led the same effects of *HST3* gene repression, with increased acetylation of H3K56, reduction of cell proliferation and formation of V-shaped filaments (81).

All together these results demonstrated that *HST3* is an essential gene in *C. albicans*, H3K56 hyper-acetylation is toxic in *C. albicans*, Hst3p has H3K56ac as its physiological substrate and that modulation of H3K56ac reduces *C. albicans* virulence in mice models (81).

On the basis of this consideration and considering that fungal Hst3p family components share sequence motifs that are absent in human sirtuins (Fig. 15), *C. albicans* Hst3p could be a potential target for antifungal therapy.



Fig. 15 Sirtuins homologous to *C. albicans* Hst3p

This figure shows the alignment of Hst3p homologues and orthologs restricted to a small portion of the catalytic core. The human sirtuins SIRT1, SIRT2 and SIRT3 are also included in this comparison. The red box represents residues involved in the interaction with the acetylated substrate. Residues in blue colour are present in all sirtuins, residues in red and brown colour are conserved among fungal Hst3p homologues and orthologs but are different in human sirtuins; on the contrary, residues in green colour are conserved only among human sirtuins (Figure modified by Ref. 81).

CHAPTER IV

AIM OF PhD PROJECT

In recent years, the frequency of *C. albicans* infections as well as the resistance to antifungal therapy have increased due to expansion of susceptible population and to the widespread use of antifungal compounds. In addition, the therapeutic options currently available are limited to few classes of compounds which target fungal cells that display some functional and morphological affinities with human cells. Therefore, the identification of new antifungal targets, novel drugs and strategies for the treatment of fungal infection, is the goal of the current research in this field.

The acetylation homeostasis of H3K56, controlled by Rtt109p and Hst3p, affects *C. albicans* viability and virulence. Previous studies highlighted that aberrant H3K56 acetylation levels cause DNA damage and chromosome loss in *C. albicans*, and that the inhibition of the fungal sirtuin Hst3p activity, by nicotinamide or its gene deletion, reduce fungal virulence and upsets *C. albicans* morphology.

Therefore, the modulation of acetylation levels of H3K56 and Hst3p activity could be a valid and promising strategy for the treatment of *C. albicans* infections.

In the light of the reported data, my PhD project has focused on the functional characterization of the fungal sirtuin Hst3p of *C. albicans*. In particular, this project was intended to examine the molecular pathways regulated by Hst3p of *C. albicans* and to evaluate the possibility of using this protein as a therapeutic target.

For this purpose, the specific objectives of this project were:

- 1) Examine the acetylation levels of histone H3 Lys56 during *C. albicans* growth, with and without nicotinamide, as sirtuin inhibitor.

A previous study demonstrated the effect of the non-specific sirtuin inhibitor nicotinamide (NAM) on *C. albicans* cell viability by Hst3p inhibition (81).

To analyse the variation of H3K56 acetylation during *C. albicans* growth and to investigate the effect of NAM on fungal growth rate and the effect of Hst3p inhibition on its substrate (H3K56ac), I monitored, spectrophotometrically and microscopically, the growth of *C. albicans* for more than 24 hours in the presence and absence of NAM. Once prepared total histone extracts, the acetylation levels of H3K56 of treated and untreated yeasts have been determined by Nano LC-MS/MS.

- 2) Investigate the correlation of Hst3p with the different morphogenetic stages of *C. albicans*. As a dimorphic fungus, *C. albicans* can reversibly switch from the normal yeast morphology to elongated hyphal forms, responding to environmental stimuli. Here, I performed a morphological analysis of the yeast-to-hypha transition of the wild-type control strain SC5314 of *C. albicans*, with and without the sirtuin inhibitor NAM. In order to investigate the effect of NAM on both cellular and colony morphology, this morphological assay has been performed in liquid and solid media, respectively. Moreover, to examine the potential role of Hst3p in resistant strains, I carried out the phenotypic analysis on two fluconazole resistant strains of *C. albicans*, the ATCC 64164 and ATCC MYA 574-GU5 strains.

In order to obtain a characteristic and specific protein profiling of *C. albicans* following Hst3p inhibition I integrated the morphological assays with a mass spectrometry analysis, using the MALDI-TOF technology.

- 3) Analyse the variations in gene expression following Hst3p inhibition with nicotinamide. In order to investigate whether the inhibition of Hst3p by

NAM is responsible for changes in the pattern of expression of Virulence-related Genes (such as those involved in phenotypic switch, adhesion, biofilm formation, etc.) I analysed the entire transcriptome of *C. albicans* strain SC5314 by RNA-Sequencing. Total RNA was extracted from *C. albicans* at time zero, at the initial stage of growth, and from both untreated and treated cells with NAM after 28 hours of incubation.

4) Express and purify both the full length and a reduced form of Hst3p.

The sirtuin Hst3p of *C. albicans* contains sequence motifs conserved among different pathogenic fungi. However, these sequences are different from human sirtuins *SIRT1* and *SIRT2*, responsible for H3K56 deacetylation in human cells (81). Based on this observation, I expressed and purified both the full length and a short sequence of the fungal deacetylase Hst3p, setting up for the first time a protocol for fungal sirtuin purification. Purified protein will be used to set up an enzymatic assay to select inhibitors of Hst3p to be used as potential fungicidal compounds.

CHAPTER V

MATERIALS AND METHODS

5.1 Yeast strains and culture conditions

The wild-type strain SC5314, the fluconazole-resistant strains ATCC 64124 and ATCC MYA 574-GU5 of *C. albicans* were used in this study. Strain SC5314 was kindly provided by Prof. W. A. Fonzi (Georgetown University, Washington, DC, USA), while mutant strains were obtained from the ATCC-LGC Standards partnership.

Stock cultures were routinely maintained on rich YPD (1% Yeast extract, 2% Peptone, 2% Dextrose) solid medium and incubated at 25°C for 48 hours. For liquid culture, very small inoculum from an isolated colony was picked up with a sterile inoculating loop and was suspended in culture medium. Cell suspension was, then, grown with shaking (at 200 rpm) in YPD broth at 25°C over-night. For specific experiments, strains were grown in synthetic YNB (0.17% Yeast Nitrogen Base, without amino acids and ammonium sulfate, Difco) medium, supplemented with 2% glucose and 0.5% ammonia sulfate; M199 medium (containing Earle's salts and glutamine, Sigma-Aldrich), buffered at pH 7.5 with 25 mM HEPES; serum (10% FBS, fetal bovine serum, Euroclone); and Spider medium (2% mannitol, 2% nutrient broth, 0.4% K₂HPO₄, pH adjusted to 7.2 with NaOH). Solid media were prepared by adding 2% agar to liquid broth before autoclaving.

Optical density (OD) was measured with a Beckman DU530 UV/Vis Spectrophotometer at a wavelength of 600 nm (OD₆₀₀). Morphological analysis and yeast to hyphae transition was conducted in liquid and solid media, with and without nicotinamide (NAM, Applichem), as sirtuins inhibitor.

5.2 Monitoring *C. albicans* growth under NAM treatment

Over-weekend culture was diluted to 10^7 /mL in 50 mL YPD medium and allowed to grow at 25°C over-night. The synchronized budding yeast cell culture was used to prepare two cultures of 700 mL YPD medium at cell density of 10^7 /mL. One culture was treated with 75 mM NAM and the other one was used as control. Treated and untreated cells were incubated for more than 24h at 25°C with shaking (200 rpm) and every 2 hours the optical density was measured at 600 nm and cellular pellets of 2×10^9 were collected (4700g for 10 min at 4°C). After washing pellets with water, they were stored at -80°C, for subsequent histone extraction.

5.3 *Candida* histone extraction

Candida pellets were resuspended in three cell pellet volumes of 50 mM Tris-HCl pH 7.5, 30 mM DTT (Bio-Rad) and incubated for 15 min at 30°C with gentle shaking (Incubated Shaker *IST-3075R JEIO* Tech). Samples were harvested at 2,000g for 5 min at room temperature and washed once with three cell pellet volumes of pre-warmed (30°C) Spheroplasting buffer (1.2 M Sorbitol, 20 mM HEPES pH 7.4). Cells were again collected by centrifugation (2,000g for 5 min at room temperature) and were resuspended in five-cell pellet volumes of Spheroplasting buffer, in which zymolyase (Sigma-Aldrich) was added at a final concentration of 100 U/mL. Samples were incubated over-night at 30°C with gentle shaking. The following day, the progress of Spheroplasting was checked by examination under microscope and spheroplasts were harvested at 2,000g for 5 min at room temperature. Cells were lysed by resuspension in three cell pellet volumes of Hypotonic Lysis buffer [10 mM Tris-HCl pH 8, 1 mM KCl, 1.5 mM MgCl₂, 1 mM DTT, 1 mM PMSF (Sigma-Aldrich), 1 mM Protease inhibitor cocktail (Sigma-Aldrich)] and incubation for 1h at 4°C with gentle inversion. The lysate was clarified via centrifugation at 10,000g, 10 min, 4°C. Acid soluble

proteins were extracted from the isolated nuclei by resuspension of nuclear pellet in two lysis buffer volumes of 0.4 N H₂SO₄ and then incubated for 3h at 4°C, with gentle inversion, vortexing occasionally. The insoluble fraction was pelleted (12,000g for 15 min at 4°C) and the histone-rich supernatant was recovered. Histones were acid-precipitated at a final concentration of 25% TCA (trichloroacetic acid, Sigma-Aldrich), overnight at 4°C. Precipitated proteins were collected by centrifugation (12,000g for 15 min at 4°C) and washed twice with ice cold acetone to remove residual acid. The final pellet was air dried, resuspended in Milli-Q H₂O (ca. 50 µL) and incubated over-night at 4°C with gentle inversion. Histones concentration was measured by Bio-Rad protein assay. Histones were resolved by SDS-PAGE (15% polyacrylamide gel) and gel was stained with Coomassie G-250 Brilliant Blue (Sigma-Aldrich) and destained in water.

5.4 Analysis of H3K56ac by Nano LC-MS/MS

Nanoscale liquid chromatography coupled to tandem mass spectrometry (Nano LC-MS/MS) has been successfully applied for histones analysis, in collaboration with Prof. Maria Chiara Monti.

H3 gel bands were cut from the Coomassie-stained gel and subjected to in situ tryptic digestion. Gels pieces, destained using ultrapure water and acetonitrile (ACN), were reduced with 1,4-dithiothreitol DTT at 60°C in a heating block for 60 min. After cooling, gel cubes were alkylated with 54 mM iodoacetamide in 50 mM ammonium bicarbonate (NH₄HCO₃) for 30 min in the dark at room temperature. After washings with ACN, gel slices were covered with trypsin-LysC (Promega) solution 12 ng/mL and incubated for 1h on ice. The excess of trypsin was removed and samples were incubated in 50 mM NH₄HCO₃. Digestion proceeded overnight at 37°C in a heating block (Termomixer Eppendorf). After digestion overnight peptides contained in supernatants were recovered and other peptides were extracted from the gel slides washing twice with 100% ACN.

Extracts were concentrated in Concentrator plus (Eppendorf) and dissolved in 12 μL of 10% formic acid prior to Nano-ESI-LC-MS/MS analysis. Peptides were separated by nano Acquity LC system (Waters Corp. Manchester, U.K) equipped with a BEH C-18 1,7 μm , 75 μm x 250 mm (Waters Corp. Manchester, U.K) column connected to LTQ-ORBITRAP hybrid mass spectrometer (Thermo Scientific). 5 μL of each sample were loaded onto the column and separated at a flow rate of 280 nL/min in a 15% - 40% buffer B linear gradient (Buffer A: 95% H_2O , 5% ACN, 0.1% AA; Buffer B: 95% ACN, 5% H_2O , 0.1% AA) in 55 minutes. Nano LC-MS/MS analyses of H3 tryptic peptides were performed using Selected Reaction Monitoring (SRM) method, on LTQ-ORBITRAP mass spectrometer.

The peptide FQKSTELLIR encompasses the K56 residue, an acetylation site just inside the histone core region. The amount of acetylated peptide of our interest (FQK(ac)STELLIR) was quantified by monitoring its bi-charged ion at m/z 638.82 and the fragmentation that produced two ions (831.54 and 1001.61). H3 peptide YKPGTVALR, a non-modified peptide, was used for normalization of H3 quantities in each gel band. The amount of acetylated peptide was normalized with the amount of YKPGTVALR, monitoring its bi-charged ion at m/z 502.8 and the fragmentation that produced two ions at m/z 616.38 and 713.50.

5.5 Morphological analysis of *C. albicans* liquid cultures

Analysis of single cell morphology was performed in YPD liquid medium at 25°C (yeast-inducing conditions). Cells were pre-grown over-night in YNB medium at 25°C with shaking (at 200 rpm) and were diluted at a final concentration of 10^5 cells ml^{-1} into YPD broth with 25 mM NAM. Cultures were incubated at 25°C for 24 hours and observed over time by inverted microscope, using AMG Evos Imaging System.

Hyphal induction in liquid was carried out in sterile Milli-Q H₂O plus 10% (vol/vol) FBS or in M199 medium, at 37°C, with and without 25 mM NAM. For hyphal growth, 10⁵ yeast ml⁻¹ were inoculated into M199 broth or 10% FBS, with and without 25 mM NAM. Germ tubes and hyphae formation were monitored, by AMG Evos Imaging System, after 3, 5 and 24 hours of incubation at 37°C.

5.6 Drop-plate assay

Colony morphology of the wild-type control SC5314 strain and the two azole-resistant strains of *C. albicans* was examined in both yeast and hyphae conditions by drop-plate assay.

C. albicans cells obtained from over-night cultures in YNB medium were diluted to a cell density of 2 x 10⁷ cells ml⁻¹ and 3 µL of this dilution was spotted onto solid media dispensed in 12-well plates, with and without 25mM NAM.

YPD solid medium was used for colony morphology analysis in yeast-inducing conditions, while filamentation assay was performed on solid media, on M199 medium buffered at pH 7.5, 10% FBS and Spider medium. After incubation for 24, 48 and 72 hours at 25 or 37°C, plates were examined with AMG Evos Imaging System.

5.7 MALDI-TOF MS technology

Mass spectrometry (MS) is an analytical technique in which samples are ionized into charged molecules and ratio of their mass to charge (m/z) is determined. Specifically, in MALDI-TOF mass spectrometry, the ion source is matrix-assisted laser desorption/ionization (MALDI), and the mass analyzer is the time-of-flight (TOF) analyzer. The development of MALDI increased the applicability of MS to large biological molecules such as proteins. This is a “soft ionization” method where ion formation does not cause a significant loss of

sample integrity. MALDI-TOF MS produces singly charged ions, consequently the interpretation of data is easy and rapid.

In MALDI analysis, samples are prepared by mixing with a matrix solution, composed by an energy-absorbent organic compound. The matrix crystallizes on drying and the sample entrapped within the matrix also co-crystallizes. The sample within the matrix is ionized with a laser beam. Desorption and ionization with the laser beam give rise to singly protonated ions from analytes in the sample. Positively charged ions are accelerated through an electrostatic field where they separate from each other on the basis of their mass to charge ratio (m/z). Once ejected through a metal flight tube subjected to vacuum they reach a detector, with smaller ions traveling faster than larger ions. Thus, bio-analytes separated according to their TOF generate a mass spectrum that is composed by mass to charge ratio (m/z) peaks with variable intensities.

5.7.1 Characterization of *C. albicans* phenotype by MALDI-TOF MS

MALDI-TOF technology was used for characterization of distinct morphogenetic states of *Candida*, each phase of yeast growth curve and *Candida* morphology following NAM treatment. The wild-type SC5314 strain of *C. albicans*, grown over-night in YPD at 25°C with shaking (at 200 rpm), was used for this analysis.

- Morphogenetic switching analysis: yeast to hyphae transition was induced in RPMI 1640 medium (with L-Glutamine, Euroclone) where cells from over-night cultures were diluted to a cell density of 10^7 cells ml^{-1} and were incubated with shaking at 37°C. Morphological switch between yeast, germ tube, pseudo-hyphae and hyphae was monitored by microscopy (AMG Evos Imaging System) every 60 minutes. For each morphogenetic state, cells were collected.

- Yeast growth phases analysis: from over-night culture, a fresh inoculum of *Candida* was prepared at a cell density of 10^7 cells ml⁻¹ in YPD. It was incubated at 25°C with shaking and was monitored over time by microscopy (AMG Evos Imaging System). For each phase of growth curve: lag, log and stationary phase, cells were collected.
- *C. albicans* V-shaped hyphae screening: pre-grown culture in YNB was diluted at a cell density of 10^6 cells ml⁻¹ in YPD medium and incubated over-night with and without 25 mM nicotinamide at 25°C with shaking.

5.7.2 Optimizing MALDI-TOF MS protocol for *C. albicans*

MALDI-TOF-MS analysis was optimized on 10^8 cells of *C. albicans* SC5314. Cellular pellets, collected in triplicate for each experiment, were washed three times with sterile Milli-Q H₂O, suspended in 300 µL of de-ionized water to which 900 µL of absolute ethanol was added. After centrifugation at 12,000g for 2 min (13,000g for 3 min, for hyphae) supernatant was discarded and the pellet was dried in concentrator (Eppendorf Concentrator 5301). The pellet was then dissolved in 20 µL of 70% formic acid and 20 µL of methanol and mixed to promote cell lysis. 1 µL of *Candida* extract was spotted in duplicate onto the polished steel MALDI target plate; each spot was overlaid and mixed with 1 µL of HCCA (α -cyano-4-hydroxy cinnamic acid) matrix solution saturated with organic solvent (50% acetonitrile and 0.1% trifluoroacetic acid) and air-dried completely before MALDI-TOF MS measurement.

MALDI-TOF MS analysis was carried out with a Waters MALDI Micro mass spectrometer. Peptide mass fingerprint product ion spectra were acquired in a linear positive mode within a mass range from 2,000 (star mass) to 20,000 Da (end mass). For each spectrum, 240 laser shots in 40 shot steps from different positions of the target spot (random walk movement) were

automatically acquired. The instrument was calibrated for each acquisition with a standard solution of 5 μ M Lysozyme (MW: 14.4 kDa). The list of the best peaks of the spectrum was created automatically by the software (Micromass MassLynx v4.1) after smoothing, normalization, and baseline subtraction. The following parameters were used for MS analysis: Laser Energy 280; Pulse Voltage 850; Detector 2,350 V; Suppression 2,000 mass units. The acquired chromatograms are of the TIC (Total Ion Current) type and lead to a final spectrum representing the sum of the individual spectra acquired over time for each sample.

5.8 NAM treatment for *Candida* RNA extraction

Candida SC5314 cells were inoculated in 50 mL of YPD medium at a cell density of 10^7 /mL and incubated over weekend at 25°C, with shaking (200 rpm). The culture was then diluted at 10^7 cells/mL into fresh YPD medium (50 mL) and incubated over-night at 25°C, with shaking (200 rpm). The day after, 10^6 cells/mL were distributed in Petri dishes of 90 mm diameter (10 mL each). *Candida* was then incubated at 25°C for 28 hours, without shaking. Three independent biological replicates were performed for either control cells or *C. albicans* with 75 mM NAM treatment. A total of 10^8 yeast cells was harvested (8,000g for 10 min at 4°C) at start point (T0) and after 28 h (T28), with and without NAM. Cells were washed with diethyl pyrocarbonate (DEPC)-treated water, and finally stored at -80°C.

5.9 Total RNA extraction

RNA isolation was performed with High Pure RNA Tissue Kit (Roche) following the manufacturer's instructions, modified for fungal lysis. Briefly, yeast cells were disrupted mechanically by using acid-washed glass beads: 1×10^8 yeast

cells were treated with $\sim 100 \mu\text{L}$ of glass beads, resuspended in $400 \mu\text{L}$ of Lysis/Binding buffer (High Pure RNA Tissue Kit) and vortexed 15 times for 1 minute, with 1 minute of interval on ice. Total RNA was, then, isolated according to the kit protocol. RNA quantification was carried out with the instrument Nanodrop 200 Thermo Scientific and its integrity was checked by electrophoresis on 1.5% agarose gel.

5.10 RNA-Sequencing

We performed a transcriptome analysis of *C. albicans* SC5314 under NAM treatment compared to untreated cells. For RNA sequencing, indexed libraries were prepared from $1 \mu\text{g}$ of purified RNA using TruSeq Stranded Total RNA Sample Prep Kit (Illumina Inc.), according to the manufacturer's instructions. A Ribo-Zero Gold rRNA Removal Kit specific for yeasts was used (Illumina Inc.) to remove rRNA. Libraries were pooled and sequenced (paired-end, 2×75 cycles) on NextSeq 550 platform (Illumina Inc.).

Bioinformatic analysis: the raw sequence files generated (.fastq files) underwent quality control analysis using FastQC tool (<http://www.bioinformatics.babraham.ac.uk/projects/fastqc>) and the quality checked paired-end reads were then aligned to the reference *Candida albicans* SC5314 genome (assembly GCA_000182965.3) using STAR (version 2.5.2a), with standard parameters. Using the reads mapped to the genome, the FeatureCount algorithm was used for quantification of each transcript. A given gene was considered expressed when detected by at least 10 reads total in the 3 replicates. Data normalization and differentially expressed transcripts were identified using DESeq2, with standard parameters; differential expression was reported as fold change. A gene with $\text{FDR} \leq 0.05$ (False Discovery Rate) and with a value of Fold Change ≤ -1.5 (for down-regulated genes) or Fold Change ≥ 1.5 (for up-regulated genes) was considered significantly expressed.

5.11 Recombinant Hst3p purification

The full length (aa 1-487) and a short sequence of Hst3p (aa 26-370) of *C. albicans* SC5314 were expressed and purified, using *Escherichia coli* as host strain for recombinant plasmids. Expression plasmids pET28a/Hst3 and pET28a/Hst3-short, purchased from GenScript company, were transferred into BLR (DE3) *pLysS E. coli* cells, where recombinant proteins were synthesized as fusion proteins with N-terminal histidine tag.

In addition, BL21 DE3 *E. coli* cells were used as expression system for co-expression of *Candida* Hst3p and molecular chaperones, that work cooperatively in the protein folding process, increasing the recovery of target protein in the soluble fraction.

5.11.1 Bacterial growth conditions

E. coli cells were grown at 37°C in Luria–Bertani (LB) broth (1% tryptone, 0.5% yeast extract, 0.5 NaCl, pH 7.00) or LB agar plates (1% tryptone, 0.5% yeast extract, 0.5% NaCl, 2% agar, pH 7.00) supplemented with 30 µg mL⁻¹ kanamycin for BLR (DE3) *pLysS* competent cells carrying pET28a vector, or 20 µg mL⁻¹ chloramphenicol for BL21 DE3 *E. coli* cells transformed with chaperone plasmid pG-KJE8 (Takara Bio inc.), carrying a chloramphenicol resistant gene.

5.11.2 Transformation of *E. coli* competent cells

10 ng of plasmid DNA were added to 50 µL of competent cells and, after mixed gently, cells were incubated on ice for 30 min, heat shocked for 45 sec at 42°C and then were immediately placed on ice for 2 min. 500 µL of LB medium were added and cells were incubated at 37°C for 45 min. To be sure to isolate colonies, two quantities of transformed bacteria were plated on LB agar plates containing the appropriate antibiotic. Plates were incubated over-night at 37°C.

5.11.3 Expression of recombinant proteins in BLR (DE3) *pLysS* cells

Optimal conditions for protein expression in BLR (DE3) *pLysS* cells were determined: Hst3p-full length and Hst3p-short were well expressed in the presence of 1 mM isopropyl-b-D-thiogalactopyranosid, IPTG (BioFroxx), at 25°C for 4h.

After determination of optimal temperature and time of induction, proteins expression was performed on large scale. A single colony of each recombinant *E. coli* BLR (DE3) *pLysS* strain was inoculated into 30 mL LB broth supplemented with 30 $\mu\text{g mL}^{-1}$ kanamycin and incubated over-night at 37°C with shaking. The cultures were diluted 1:50 with fresh LB broth supplemented with antibiotic and incubated at 37°C with shaking, to obtain an optical density of 0.8 at 600 nm. Three mL of this non-induced culture was saved as control and induction of expression was carried out by adding 1 mM IPTG. Bacterial cells were then incubated at 25°C for 4h, with shaking. Induced cultures were harvested by centrifugation (Beckman Coulter Avanti J-25) at 5,000g for 15 min at 4°C. Cells were washed with Phosphate Buffer Saline, PBS (Euroclone), harvested by centrifugation at 5,000g for 15 min at 4°C and stored at -80°C before being lysed.

5.11.4 Hst3p purification by affinity chromatography and ion exchange

The cell pellet was resuspended in 30 mL of lysis buffer [20 mM $\text{NaH}_2\text{PO}_4/\text{Na}_2\text{HPO}_4$, 500 mM NaCl, 20 mM Imidazole (BioFroxx), 0.5 mM DTT, pH 7.4] containing 1X protease inhibitors cocktail. The suspension was sonicated for 20 min, at 30% amplitude with 9.9 s on/9.9 s off pulses in a Vibra-Cell (Sonic) ultrasonicator and cell debris were removed by centrifugation (10,000g for 30 min at 4°C) using a Beckman Coulter Avanti J-25 centrifuge. Four M urea (BioFroxx) was added to the cleared lysate and, after complete

dissolution, it was centrifuged at 10,000g for 30 min at 4°C and passed through a 0.45 µm filter before nickel affinity chromatography purification.

Histidine-tagged Hst3p was purified loading cell lysate onto 1 mL His-Trap HP column (GE Healthcare) connected to AKTA purifier FLPC system (Amersham Biosciences) and pre-equilibrated with binding buffer (20 mM NaH₂PO₄/Na₂HPO₄, 500 mM NaCl, 20 mM Imidazole, 0.5 mM DTT, 4 M urea, pH 7.4). After washing the column with the same buffer, proteins were eluted at a flow-rate of 1 mL/min in a 0%-100% linear gradient of elution buffer (20 mM Tris HCl, 10 mM NaCl, 0.25 M imidazole, 0.5 mM DTT, 4 M urea, pH 7.4) in 20 column volumes. The eluted fractions were combined and dialyzed in order to remove urea. Different dialysis steps were performed every 2 h at 4°C against dialysis buffer: 20 mM Tris-HCl, 10 mM NaCl, 0.5 mM ZnCl₂, 0.1 M arginine (Sigma-Aldrich), pH 7.5. Arginine concentration was gradually reduced during dialysis: five buffer changes allowed to reduce finally arginine concentration to 6 mM. In the last two dialysis steps, buffer pH was increased at 9.5. After incubation overnight at 4°C, dialyzed proteins were loaded on a 1 mL Mono Q 5/50 GL column (GE Healthcare) equilibrated with Mono Q binding buffer: 20 mM Tris-HCl, 10 mM NaCl, 6 mM arginine, pH 9.5. Protein elution was performed with a step gradient in Mono Q elution buffer: 20 mM Tris-HCl, 1 M NaCl, 6 mM arginine, pH 9.5. Fraction enriched in Hst3p was stored at -20°C, after addition of 10% glycerol that increases protein stability during storage.

5.11.5 Hst3p-short purification from inclusion bodies

Unlike the full length of Hst3p, the recombinant Hst3p-short of *C. albicans* was not soluble and was purified from inclusion bodies.

The cell pellet was resuspended in 100 mL of lysis buffer (20 mM NaH₂PO₄/Na₂HPO₄, 500 mM NaCl, 20 mM Imidazole, 0.5 mM DTT, pH 7.4) containing 1X protease inhibitors cocktail. Twenty-five mL of cell suspension

were individually sonicated for 10 min, at 30% amplitude with 9.9 s on/9.9 s off pulses in a Vibra-Cell (Sonic) ultrasonicator and insoluble fraction was collected by centrifugation (10,000g for 30 min at 4°C), using a Beckman Coulter Avanti J-25 centrifuge. One hundred mL of cleared lysate (Supernatant 1) was recovered and pellet was resuspended in 20 mL of lysis buffer for subsequent sonication (10 min, 30% amplitude, 9.9 s on/9.9 s off pulses). After centrifugation (10,000g for 30 min at 4°C) the soluble fraction (Supernatant 2) was recovered and inclusion bodies were resuspended in 10 mL of lysis buffer supplemented with 8 M urea and incubated overnight under constant stirring at 4°C. Suspension was centrifuged (10,000g for 30 min at 4°C): supernatant was stored and pellet was solubilized in 5 mL of 6 M guanidine-HCl (Sigma-Aldrich) and 1 mM DTT. After centrifugation (10,000g for 30 min at 4°C) supernatant was recovered and dialyzed to remove the denaturant. Numerous dialysis changes were performed, decreasing to zero guanidine concentration and adding 15 mM arginine-HCl, as stabilizing agent. Protein refolding process was performed as follow:

-1° buffer: 3 M guanidine HCl, 50 mM NaCl, 0.1 mM DTT;

-2°buffer: 1.5 M guanidine HCl, 50 mM NaCl, 0.11 mM DTT, 20 mM Tris-HCl pH 8;

-3° buffer: 0.5 M guanidine HCl, 100 mM NaCl, 0.1 mM DTT, 0.5 M arginine-HCl, 20 mM Tris-HCl pH 8;

-4° buffer: 100 mM NaCl, 0.1 mM DTT, 0.25 M arginine-HCl, 20 mM Tris-HCl pH 8;

-5° buffer: 100 mM NaCl, 0.1 mM DTT, 0.12 M arginine-HCl, 20 mM Tris-HCl pH 8;

-6° buffer: 100 mM NaCl, 0.1 mM DTT, 0.06 M arginine-HCl, 20 mM Tris-HCl pH 8;

-7° buffer: 100 mM NaCl, 0.1 mM DTT, 0.03 M arginine-HCl, 20 mM

Tris-HCl pH 8;

-8° buffer: 100 mM NaCl, 0.1 mM DTT, 0.015 M arginine-HCl, 20 mM

Tris-HCl pH 8.

Buffer changes were performed every 2h at 4°C, under constant stirring.

After dialysis, 10% glycerol was added to pooled fractions that were stored at -20°C.

5.12 Hst3p purification using a co-expression system

100 µL of BL21 DE3 competent cells were transformed with 10 ng of pG-KJE8 chaperon plasmid, as previously described. Transformants were selected from plates containing 20 µg mL⁻¹ chloramphenicol and cultured in LB liquid medium supplemented with 20 µg mL⁻¹ chloramphenicol for preparation of competent cells with standard method. These competent cells were retransformed with pET28a/Hst3 expression plasmid and transformants were selected from plates containing 20 µg mL⁻¹ chloramphenicol and 30 µg mL⁻¹ kanamycin.

5.12.1 Co-expression experiment

Transformants were inoculated in LB medium containing 20 µg mL⁻¹ chloramphenicol and 30 µg mL⁻¹ kanamycin for plasmid selection and 0.5 mg/mL of L-arabinose (Sigma-Aldrich) and 5 ng/mL of tetracycline for induction of chaperone expression. Cells were incubated at 37°C and when OD₆₀₀ of the culture reached 0.8, IPTG was added at a final concentration of 1 mM and culture was incubated overnight at 18°C to induce protein expression. Induced culture was harvested by centrifugation at 5,000g for 15 min at 4°C. Cellular pellet were washed with PBS, harvested by centrifugation at 5,000g for 15 min at 4°C and stored at -80°C.

5.12.2 Protein purification after chaperones co-expression

Cellular pellet from 500 mL of culture was resuspended in 20 mL of lysis buffer (20 mM NaH₂PO₄/Na₂HPO₄, 500 mM NaCl, 20 mM Imidazole, 1 mM ATP, pH 7.4) containing 1X protease inhibitors cocktail. Cell suspension was sonicated for 10 min at 30% amplitude with 9.9s on/9.9s off pulses and insoluble fraction was collected by centrifugation (10,000g for 30 min at 4°C). Cleared lysate, passed through 0.45 µm filter, was loaded onto 1 mL His-Trap HP column for nickel affinity purification. After washing the column with binding buffer (20 mM NaH₂PO₄/Na₂HPO₄, 500 mM NaCl, 20 mM Imidazole, pH 7.4), proteins were eluted at a flow-rate of 1 mL/min in a 0%-100% linear gradient of elution buffer (20 mM NaH₂PO₄/Na₂HPO₄, 10 mM NaCl, 0.25 M imidazole, pH 7.4) in 20 column volumes. Eluted fractions were analyzed by SDS-PAGE.

5.13 Western Blot analysis

The recombinant sirtuin Hst3p purified by chromatography was detected by Immunoblotting. Protein fractions were separated on 12% denaturing polyacrylamide gel and then transferred to nitrocellulose membrane (Bio-Rad). Membrane was stained overnight at 4°C in humidified chamber with the monoclonal primary antibody anti poly-Histidine (clone HIS-1, Sigma-Aldrich). After 45 min at room temperature with the secondary antibodies, immunoreactive protein bands were detected by enhanced chemiluminescence reagents (Elabscience) and analysed by Las4000 (GE Healthcare Life Sciences).

5.14 Statistical analysis

Data are from at least three independent experiments and results are expressed as means ± SD. Data were analysed with GraphPad Prism 4 (GraphPad Software). Two-tailed Student's t test (2-group comparisons) or two-way ANOVA (>2-group

comparisons) were performed as appropriate. P values <0.05 were considered significant.

CHAPTER VI

RESULTS

6.1 Analysis of H3K56 acetylation levels during *C. albicans* growth

The fungal sirtuin Hst3p is responsible for H3 Lys56 deacetylation in *C. albicans*. Being a sirtuin, Hst3p is inhibited by nicotinamide, a non-specific sirtuin inhibitor and a product of NAD⁺-dependent deacetylation reaction. I proposed to determine the variation of acetylation levels of H3K56 during *C. albicans* growth and to examine the effect of Hst3p inhibition on its target H3K56ac during yeast growth.

For this purpose, *C. albicans* growth was monitored for 33 hours with and without NAM. It was necessary to set up a protocol for cell synchronization and to determine the concentration of nicotinamide to be used in shaking cultures that was not lethal for yeast cells. I tested 25, 50, 75 and 100 mM NAM and I found that 75 mM NAM is the appropriate concentration, not toxic but sufficient to induce abnormal hyphae formation in shaking cultures, as reported in literature (81).

The growth curve of *C. albicans*, with and without NAM, was monitored spectrophotometrically at 600 nm for a total of 33 hours. As shown in fig. 16, the duplication time of treated yeasts was slightly reduced upon NAM treatment, causing reduction of cell duplication of approximately 56%, compared to control cells.

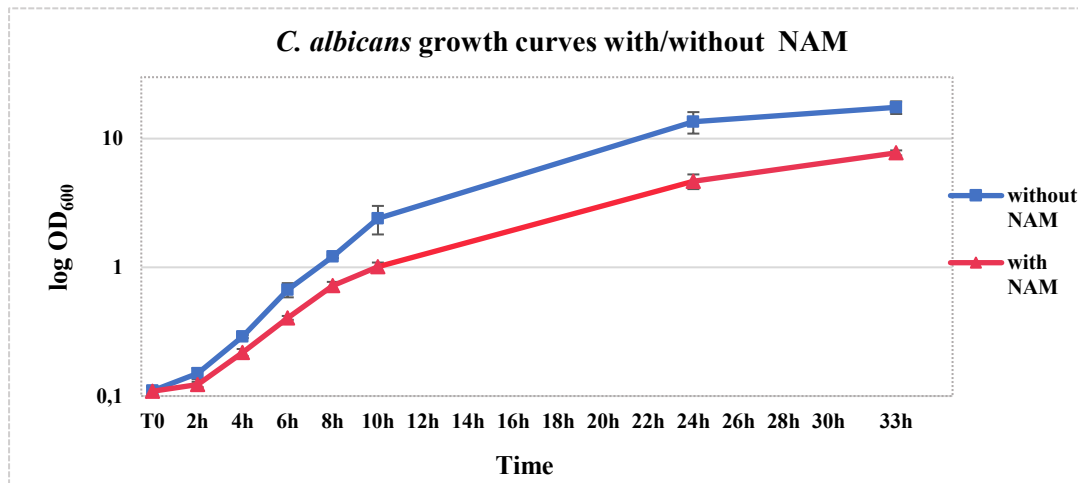


Fig. 16 *C. albicans* growth with and without NAM

Growth curves obtained by growing *C. albicans* alone (blue line) and in the presence of 75 mM NAM (red line) at 25°C, up to 33 hours. Data are means of three independent experiments and are reported as log of the OD₆₀₀ value obtained for each culture at the different time intervals. $p < 0.0001$ (two-way ANOVA test).

Acetylation levels of H3K56 during growth of treated and untreated yeast were then examined. For this purpose, I set up a protocol for total histone extraction from *Candida*, establishing the minimum number of cells necessary and sufficient to extract good amounts of histones (2×10^9 cells), the method for spheroplasts formation (zymolyase digestion), and the type of lysis to be used (hypotonic lysis). Once prepared nuclear protein fractions from each time point of growth curves, the acetylation levels of H3K56 were determined. I firstly examined this histone modification by Immunoblot, using the monoclonal antibody anti-H3K56ac (ab76307, clone EPR996Y, Abcam). Unfortunately, this antibody was no longer marketed and considering that no other antibodies specific for yeast were available against this modification, I had to use an alternative approach to

reach my goal. Specifically, I determined the acetylation levels of H3K56 during *C. albicans* growth by Nanoscale Liquid Chromatography coupled to tandem Mass Spectrometry (Nano LC-MS/MS).

FQK(Ac)STELLIR was the histone peptide of our interest, which was normalized *versus* YKPGTVALR peptide, another peptide of H3 histone chosen because does not show post-translational modifications (81). Nano LC-MS/MS revealed that H3K56 acetylation has a peak at six hours during *C. albicans* growth without NAM and then decreases (Fig.17). On the other hand, H3K56 acetylation of treated yeast increases during the time of treatment and remains almost constant even after 24h of NAM treatment (Fig.17), demonstrating the inhibitory effect of nicotinamide on the fungal sirtuin Hst3p. These experiments allowed us to analyze, for the first time, acetylation levels of H3K56 during *C. albicans* growth and the effect of Hst3p inhibition on its substrate.

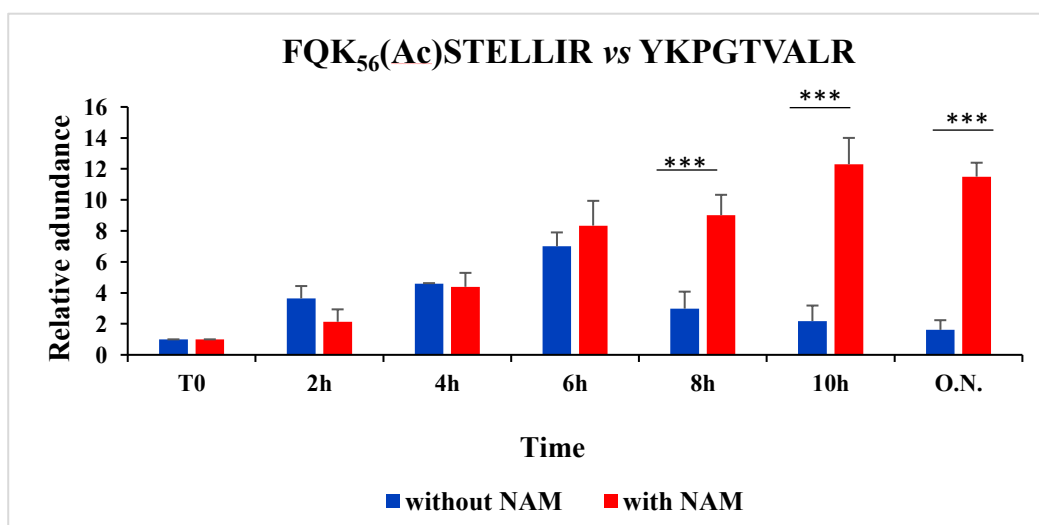


Fig. 17 H3K56 acetylation levels in *C. albicans* with and without NAM

Variation of H3K56ac levels during *C. albicans* growth, with and without NAM, was determined by Nano LC-MS/MS. Data represented are from three independent experiments and represent mean \pm SD. *** p <0.001 (t-test).

6.2 NAM treatment induces *C. albicans* phenotypic switching

A striking feature of *C. albicans* is its dynamic morphogenesis. Its ability to shift from unicellular budding yeast to a multicellular filamentous form, including pseudo-hypha and true hypha, responding to diverse environmental cues, is considered its predominant virulence trait.

Once analysed the effect of Hst3p inhibition on H3K56ac, I decide to examine the effect of sirtuin inhibition on *C. albicans* morphology. Therefore, in order to investigate the correlation of Hst3p with different morphogenetic stages of *C. albicans*, I analysed, *Candida* morphological transition in the presence of NAM. In addition, to study the potential involvement of Hst3p in the fungal resistance this morphological analysis was also performed on two azole-resistant strains of *Candida*. As representative fluconazole-resistant strain, I used the Darlington strain, *C. albicans* ATCC 64124, with mutations in *ERG11* gene and which shows cross-resistance to other azoles, and *C. albicans* ATCC MYA-574, overexpressing the ABC transporter genes *CDR1* and *CDR2* which encode ATP-dependent efflux pumps (83). These strains were grown in different culture media, both solid and liquid, to study colony and cell morphology, respectively, at various temperature and pH, with and without inhibitor of sirtuins.

Firstly, the minimum and sufficient concentration of NAM with effect on *Candida* morphology in static cultures was determined and, moreover, the effect of NAM pre-treatment in liquid culture before spotting cells on solid medium was evaluated. As shown in fig. 18, which displays sections of *Candida* colonies, 25 mM NAM is sufficient to inhibit filamentation in hyphae-inducing solid medium (10% serum, 37°C) and, in addition, pre-treatment of liquid culture with NAM for 5 hours has no effect on germination when cells are spotted on 10% serum agar plate, suggesting that the presence of NAM in solid medium is responsible for alterations of *Candida* morphology. After setting these conditions, all experiments were performed using 25 mM NAM without pre-treatment of cells.

I analyzed the effect of NAM on colony and single cell morphology of *Candida* in hyphae-inducing conditions, using different culture media, such as 10% serum, M199 and Spider medium. These media with neutral-basic pH and an incubation temperature of 37°C induced germination of wild-type strain SC5314 and fluconazole-resistant strains, both in liquid and solid conditions of growth (Fig. 19, panel A, B, C). *C. albicans* ATCC MYA-574 showed an intrinsic reduced germinative ability in 10% serum and Spider medium.

However, addition of 25 mM NAM to wild-type and resistant cells led to a great alteration in *Candida* morphology with a robust inhibition of growth and filamentation in liquid culture and preventing the formation of hyphal crown around the macro-colonies on solid media (Fig. 19, panel A, B, C).

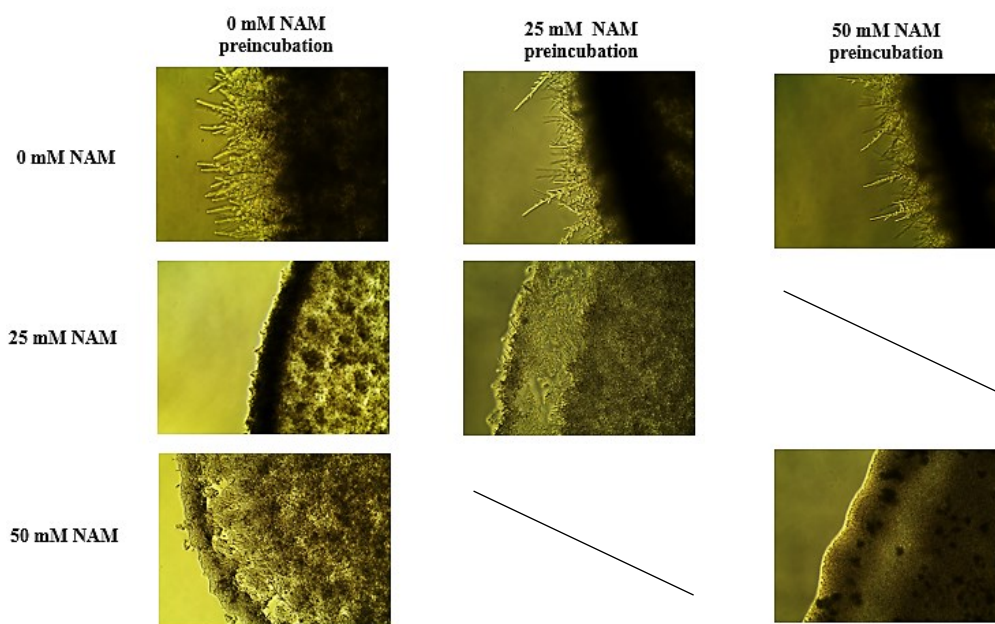


Fig. 18 Drop plate assay on 10% serum

Section of macro-colonies of *C. albicans* SC5314 on 10% FBS agar plate, with and without NAM. Yeasts cells were untreated and treated for 5 hours in liquid media with and without NAM and then spotted on solid medium.

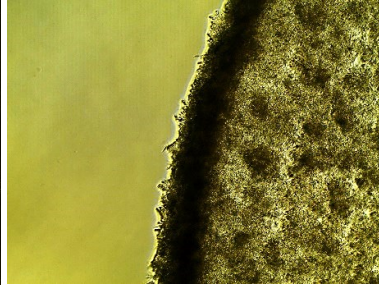
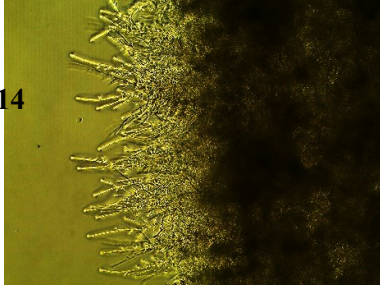
10% FBS

PANEL A

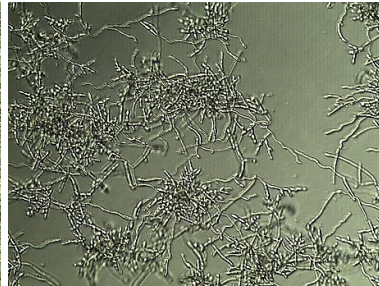
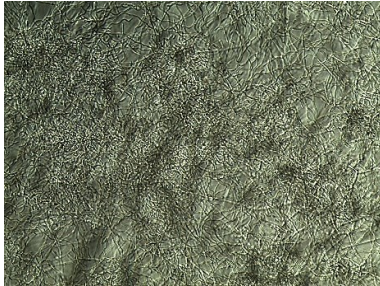
0 mM NAM

25 mM NAM

C. albicans wild-type SC5314

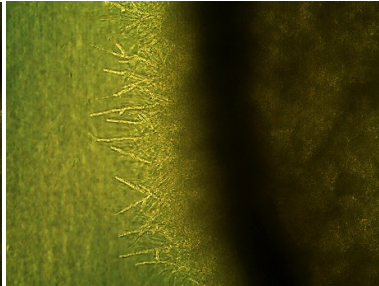
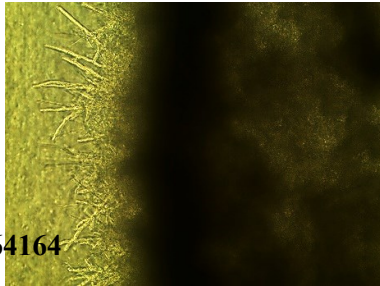


Solid medium



Liquid medium

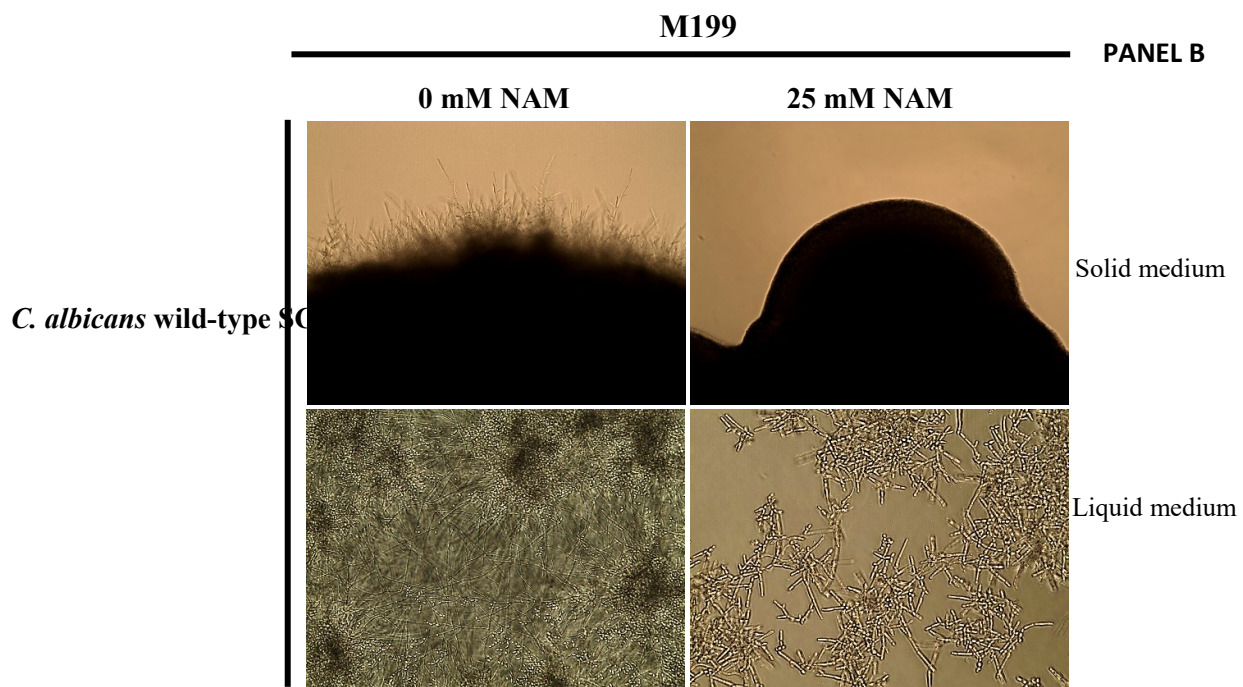
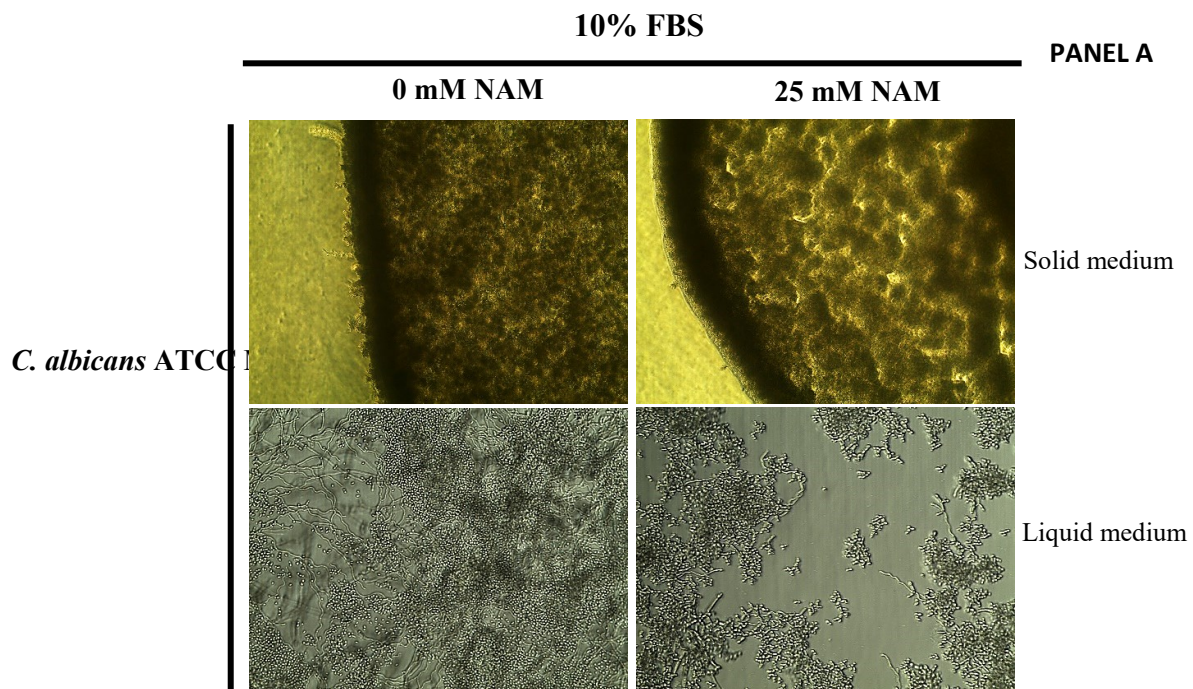
C. albicans ATCC 64164



Solid medium



Liquid medium



M199

PANEL B

0 mM NAM

25 mM NAM

C. albicans ATCC



Solid medium

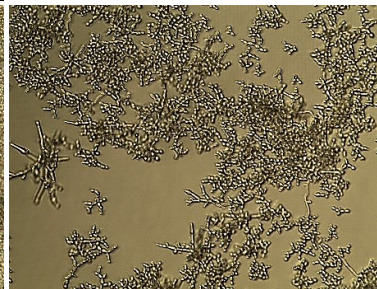


Liquid medium

C. albicans ATCC



Solid medium



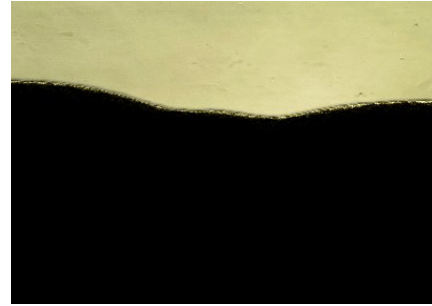
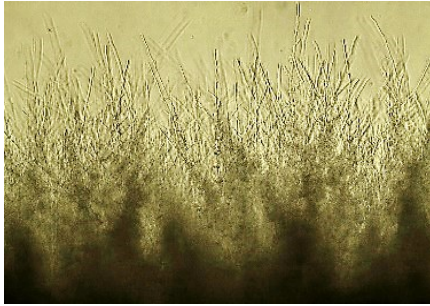
Liquid medium

SPIDER SOLID MEDIUM

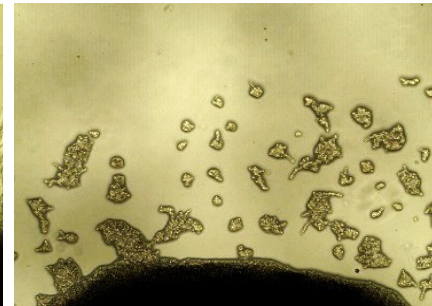
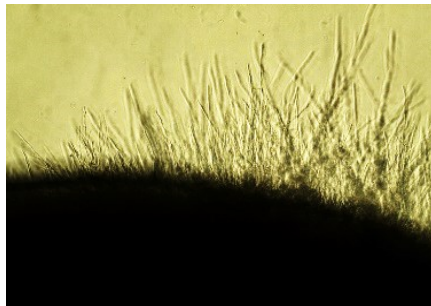
PANEL C

0 mM NAM

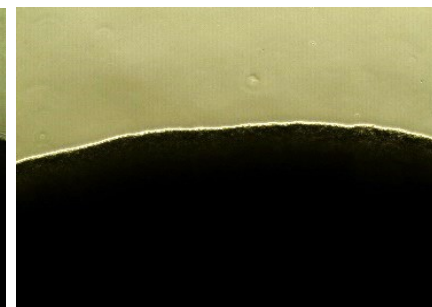
25 mM NAM



C. albicans wild-type SC5314



C. albicans ATCC 64164



C. albicans ATCC MYA 574-GU5

Fig. 19 Morphologies of *C. albicans* strains in hyphae inducing conditions.

Colony and single-cell morphology of *C. albicans* SC5314 and azole-resistant strains ATCC 64124 and ATCC MYA-574-GU5 of *C. albicans* in liquid and solid 10% serum (Panel A), M199 (Panel B) and in solid Spider medium (Panel C).

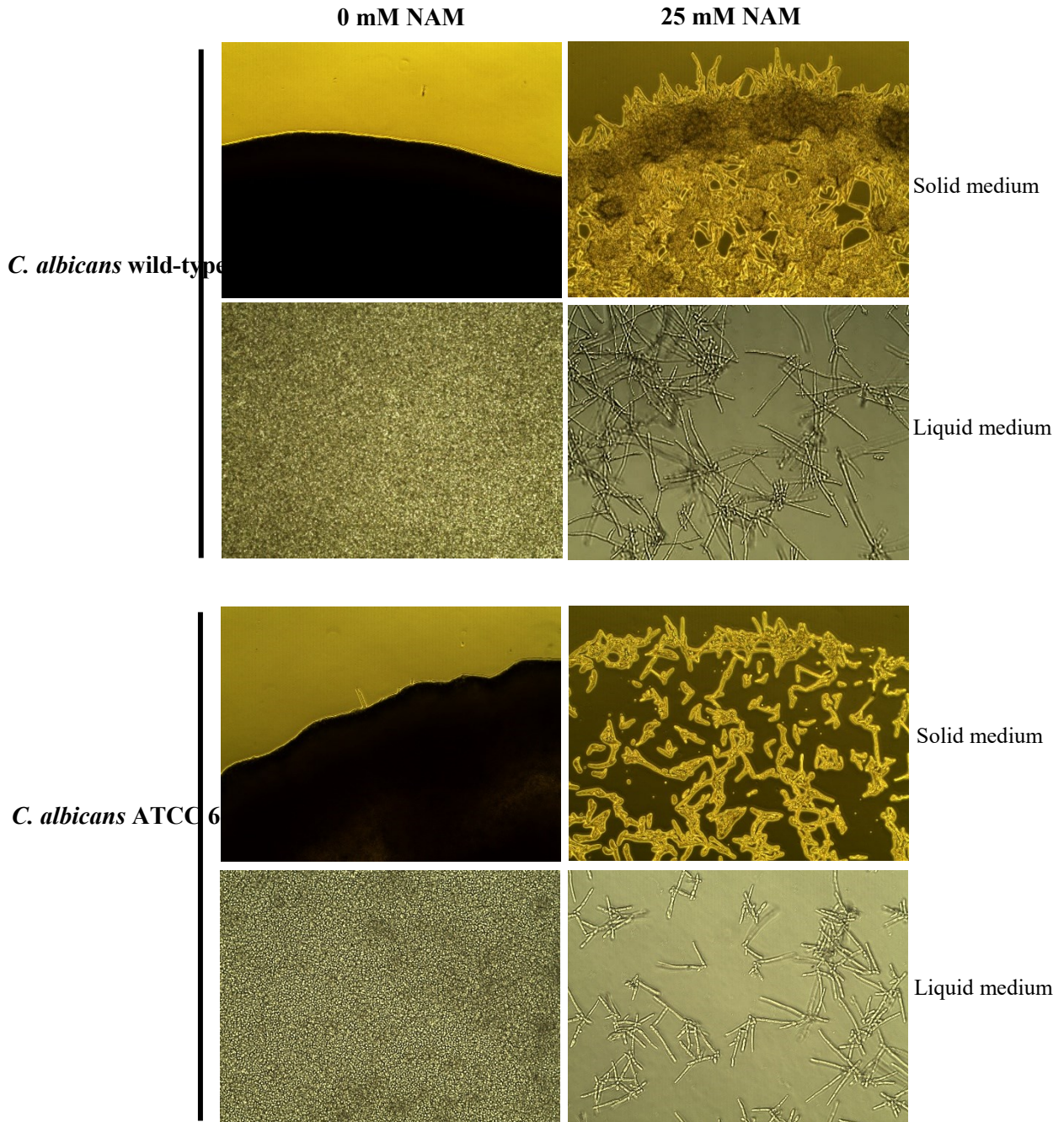
Moreover, I investigated the consequences of NAM-induced inhibition of sirtuin under conditions that normally maintain the yeast form of *C. albicans*, performing morphological analyses in reach YPD medium at 25°C. In this case, NAM treatment triggered the transition to filamentous growth causing the formation of abnormal filamentous structure, called hyphae V-shaped for their conformation. In particular, after 6h of incubation at 25°C I observed pseudohyphae-like cells (not shown) which at later time appeared as ‘V-shaped’ filaments (Fig. 20). NAM treatment resulted, also in this case, in a slowdown of cell duplication, evident in liquid culture and in solid medium, in which cell density of microcolonies is reduced (Fig. 20).

In conclusion, Hst3p inhibition by nicotinamide results in reduction of duplication time, inhibition of germination in hyphae-inducing conditions, and in abnormal filamentous growth under conditions that normally maintain the yeast form of *C. albicans*.

Such morphological observations highlight the influence of NAM on growth rate of the wild-type control strain and the two azole-resistant strains of *C. albicans*, and the effect of Hst3p inhibition on the yeast to hyphae transition and, consequently, on fungal morphology.

YPD

PANEL D



YPD

PANEL D

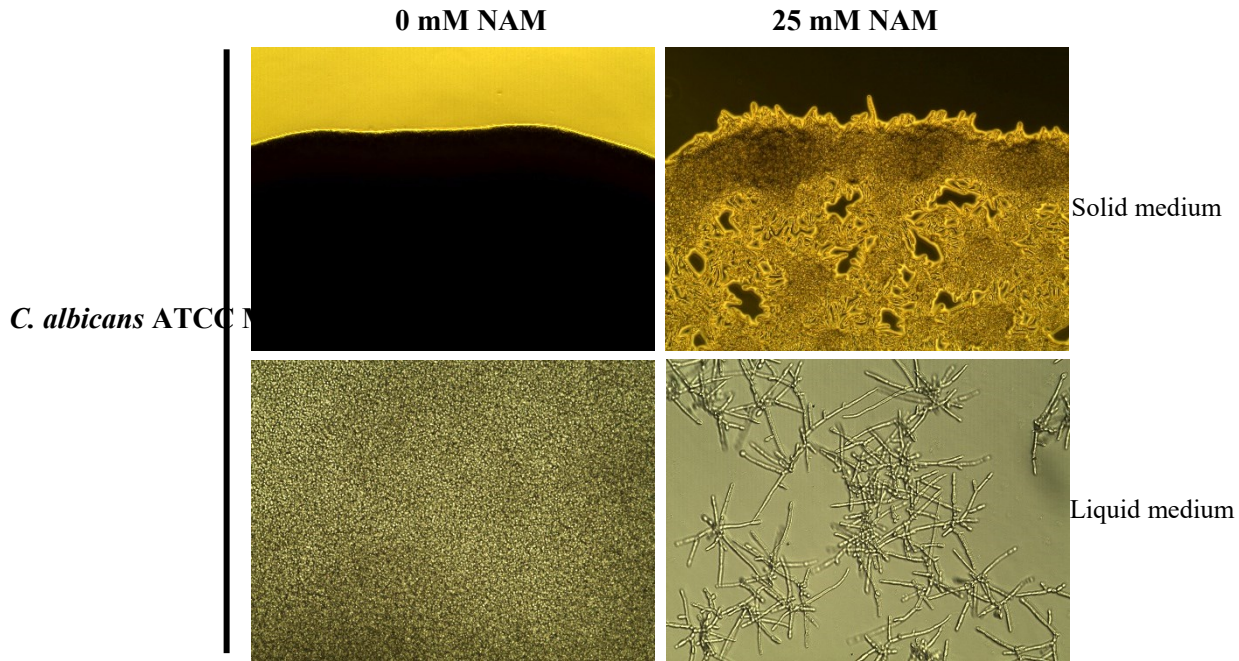


Fig. 20 *C. albicans* morphology in non-inducing hyphae conditions

Colony and single-cell morphology of *C. albicans* strains in YPD, solid and liquid medium, with and without 25 mM NAM (Panel D).

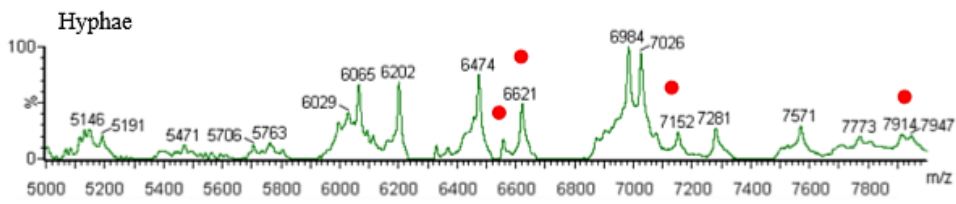
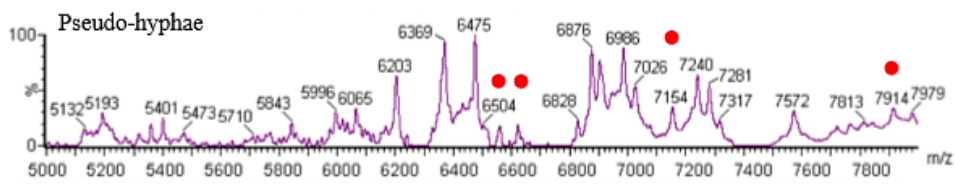
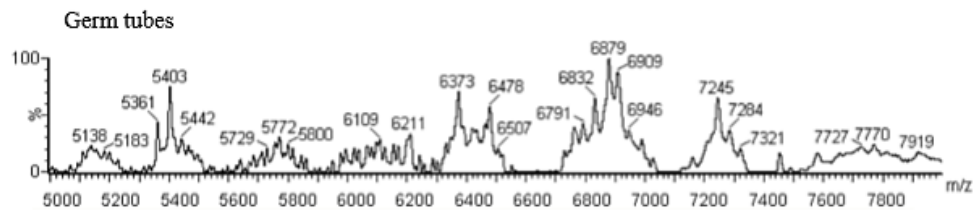
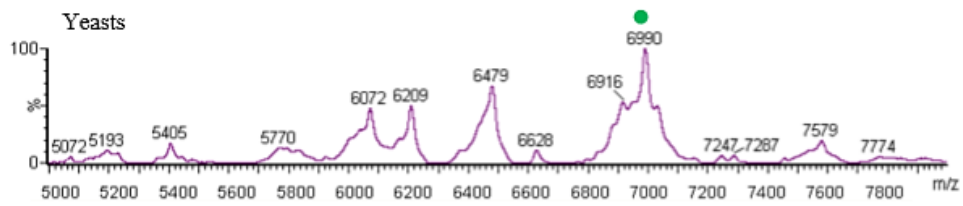
6.3 MALDI-TOF technology for *C. albicans* phenotypic screening

As a complementary approach to our morphological assays, MALDI-TOF MS analysis was performed to document and identify a characteristic protein profiling of *C. albicans* SC5314 associated with Hst3p inhibition. This procedure has proved to be, in this study, a practical and useful tool for differentiation of fungal morphology.

Yeast growth phases (data not shown) and morphogenetic switch of *Candida* were examined acquiring characteristic and specific spectra for each

morphogenetic stage, as consequence of variation in protein expression corresponding to the morphological transition (Fig. 21).

The acquired spectra highlighted a specific molecular profile for yeast (in log, lag e stationary phases) and hyphae morphogenetic stages (yeast, germ tubes, pseudo-hyphae and true hyphae). Comparing these profiles with that obtained after treatment with NAM, which is responsible for V-shaped filaments formation, similar protein profiles can be identified: ions with specific mass to charge ratio (m/z) are shared among NAM-treated yeast and true-hyphae, and moreover ions with distinct m/z ratio are exclusive of V-shaped hypha phenotype (Fig. 22). These data further confirm the effect of nicotinamide on cell morphology, inducing formation of V-shaped hypha which display a protein profiling similar to those of true-hypha but at the same time characteristic of this V-shaped morphology. Moreover, the MALDI-TOF technology has proved to be very useful for rapid screening of *C. albicans* morphologies.



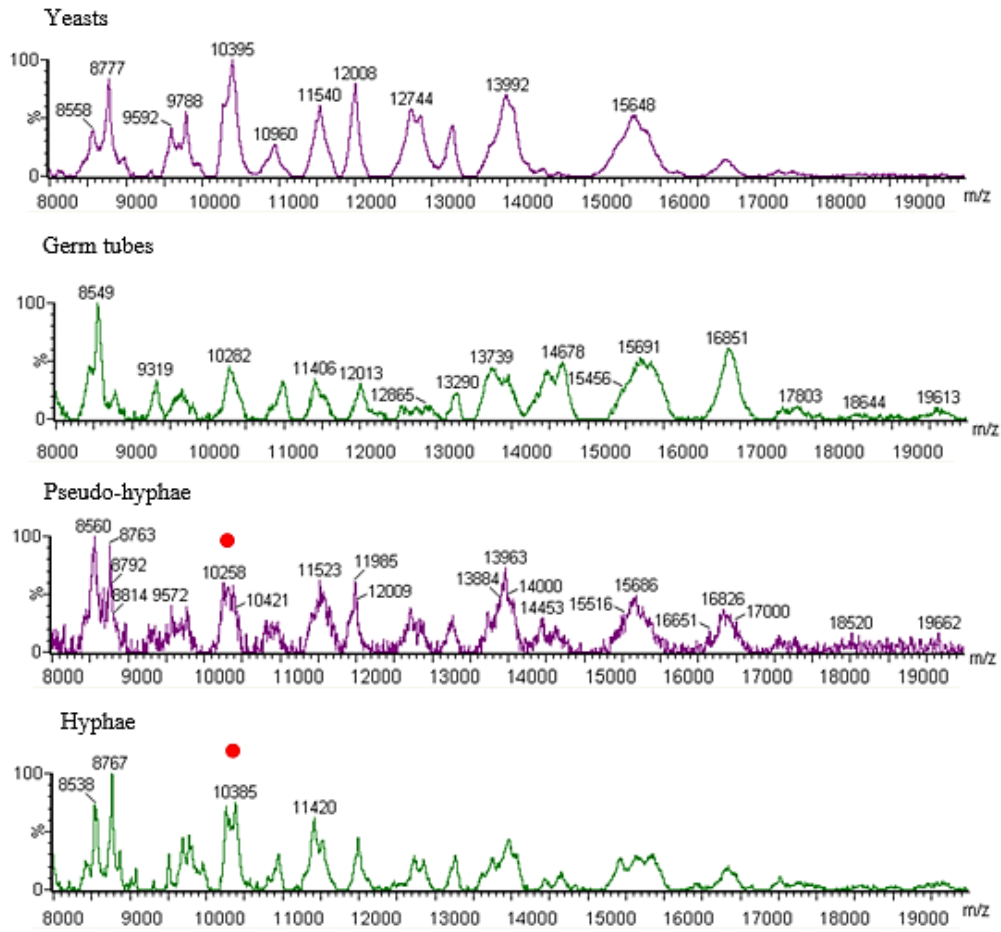


Fig. 21 MALDI-TOF analysis of morphogenetic switch of *Candida*

Representative spectra of yeasts, germ tubes, pseudo-hypha and true-hyphae. Spectra are divided in two mass range (5,000-8,000 and 8,000-20,000 m/z) to appreciate small differences in mass. Red spots indicate protein profiling shared by pseudo-hyphae and true hyphae.

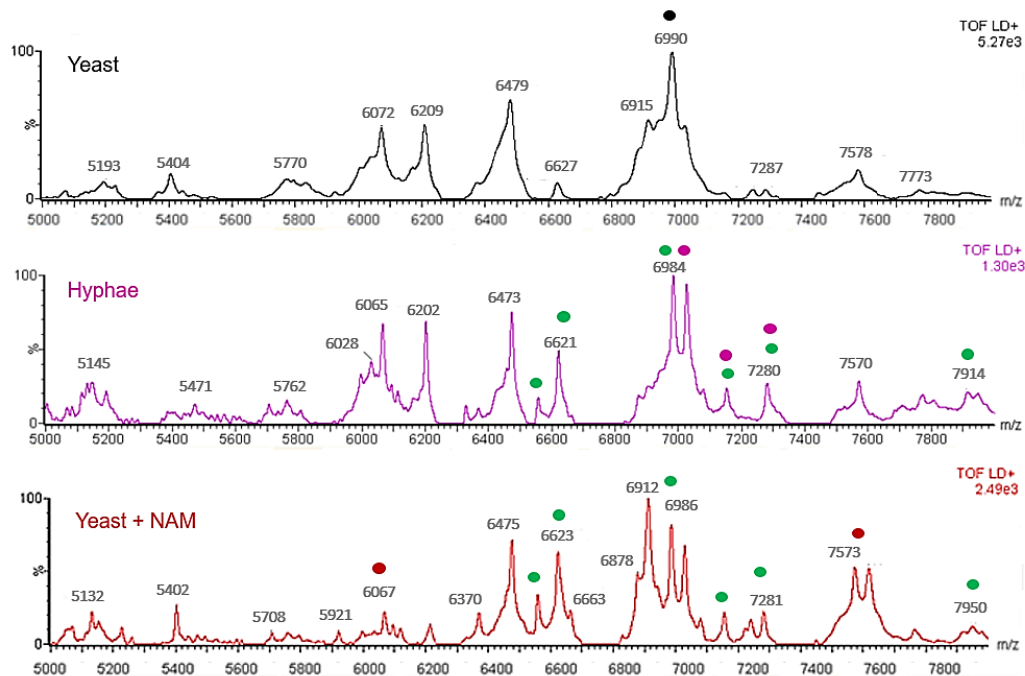


Fig. 22 Representative spectra of yeasts and hyphae compared with spectra of V-shaped hyphae, induced by NAM.

Specific protein profiling is identified for each morphological stage (as indicated by black spots for yeasts, purple for hyphae, red for V-shaped hyphae NAM-induced). Green spots represent ions with m/z ratio shared by hyphae and yeast treated with NAM.

6.4 RNA-Sequencing data analysis

In all Eukaryotes, including *C. albicans*, gene expression is directly influenced by the position of nucleosomes relative to regulatory sequences, by the compartmentalization of function domains within the nucleus and by the packaging of nucleosomal fiber (84). Because all three aspects of chromatin organization are regulated by post-translational histone modifications, various histone modifying enzymes are involved in the switch between permissive and repressive chromatin state (84).

Among various histone modifications, an important post-translational modification in *C. albicans* is the histone H3 Lys56 acetylation (H3K56ac) regulated by *RTT109* and *HST3* genes encoding, respectively, for the acetyl transferase Rtt109p and the sirtuin Hst3p. Increased acetylation of histone lysine residues is, likely, a hallmark of active chromatin because histone acetylation causes chromatin relaxation and gene transcription (85).

Hst3p has NAD⁺-dependent deacetylase activity *in vitro*, and I have shown that NAM treatment leads to an increased H3K56 acetylation in *C. albicans*.

Based on these considerations, I analyzed the entire transcriptome of *C. albicans* strain SC5314 by RNA-sequencing to investigate whether the inhibition of Hst3p by NAM is responsible for changes in the pattern of expression of Virulence-related Genes (such as those involved in phenotypic switching, adhesion, biofilm formation, etc.). For this purpose, total RNA was isolated from *Candida* at the starting point (time zero, T0) and from cells both untreated and treated with 75 mM NAM after 28 hours (T28h) of incubation at 25°C. Isolated RNA was used for transcriptomic analysis of *C. albicans* response to NAM treatment.

To ease the reading of the text, I used the following abbreviations: CaT28N, CaT28 stand for cells grown for 28 h, respectively, with and without NAM, and CaT0 stands for *Candida* at the starting point before incubation. The data analyzed include 3 replicates, corresponding to 3 biological replicates (RNA from independent cultures), and simultaneous examination of over 6,500 *C. albicans* gene transcript levels, representing the entire genome, revealed several genes differentially regulated (Table 1).

	Up-regulated genes*	Down-regulated genes*
CaT28 vs CaT0	453	649
CaT28N vs CaT28	1,315	1,090
CaT28N vs CaT0	1,001	853
*we considered only genes whose transcription levels changed at least 1.5 folds		

Table 1 Differentially regulated genes in untreated and treated yeasts

My analysis shows that gene categories most dysregulated upon NAM treatment are those associated with hyphal growth, adherence, drug resistance and cell wall maintenance.

SAP family genes

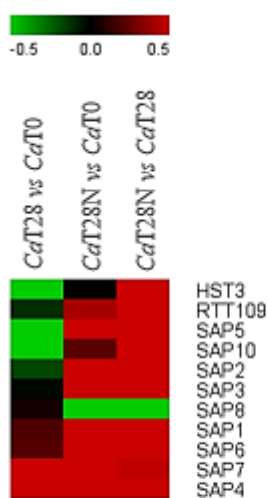


Fig. 23 Heatmap of SAP genes differentially expressed in response to 75 mM NAM in the control strain SC5314 of *C. albicans*.

To date, 10 different secreted aspartic proteinases (*SAP1-10*) have been reported for *C. albicans*. This is a class of secreted hydrolases with extracellular proteolytic activity of particular interest for their role as virulence factors. The high number of similar genes could provide *C. albicans* with the ability to secrete a specific and appropriate enzymatic response at distinct stages of infection (86). Transcript profiles reveal a global up-regulation of *SAP*

genes ranging from +1.69 to +24.67 folds in response to NAM treatment (Fig. 23).

In particular, in CaT28N the expression of:

- *SAP1* increases +2.07 folds compared to CaT28 and +2.47 folds compared to CaT0;
- *SAP2* increases +24.67 folds compared to CaT28 and +21.06 folds compared to CaT0;
- *SAP3* increases +9.79 folds compared to CaT28 and +9.55 folds compared to CaT0;
- *SAP4* increases +1.69 folds compared to CaT28 and +4.19 folds compared to CaT0;
- *SAP5* increases +6.62 folds compared to CaT28 and +3.01 folds compared to CaT0;
- *SAP6* increases +3.23 folds compared to CaT28 and +3.89 folds compared to CaT0;
- *SAP7* increases +2.49 folds only when compared to CaT0;
- *SAP10* slightly increases +1.86 folds only when compared to CaT28.

Interestingly, *SAP8* is the only gene significantly down-regulated upon NAM treatment: transcript level is -1.9 folds in CaT28N compared with CaT28 control, while it is not reduced significantly compared to CaT0. The down-regulation of *SAP8* in treated yeasts is complemented by the increased expression of the other genes.

In CaT28 the expression of all *SAP* genes, except *SAP4* and *SAP5* is not remarkably different compared to CaT0. In CaT28 compared to CaT0 control, *SAP4* is up-regulated (+2.47 folds), while *SAP5* is down-regulated (-2.20-folds).

My results show that NAM treatment induces up-regulation of most of *SAP* genes that is in agreement with the morphological alteration induced in *C. albicans* by sirtuin inhibitor. *SAP* expression is associated with hyphal formation,

adhesion, and phenotypic switching (39). The increased expression of these proteinases upon nicotinamide treatment reflects the role of these enzymes in adherence during formation and elongation of V-shaped hypha induced by NAM.

My data suggest that NAM treatment could increase chromatin accessibility facilitating the binding of transcription factor to *SAP* genes' promoters.

Cell surface and adhesion genes

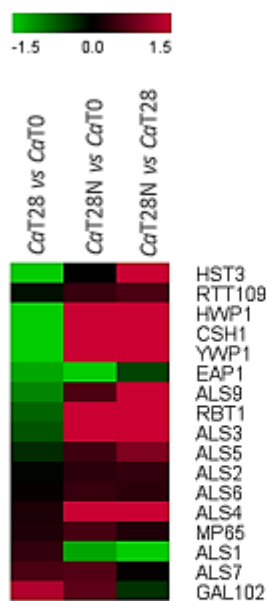


Fig. 24 Heatmap of cell surface and adhesion genes differentially expressed in response to 75 mM NAM in the control strain SC5314 of *C. albicans*.

Candida pathogenicity is a complex process consisting of several steps, among which an important role is played by the ability of *Candida* to adhere to host cells. Adhesion occurs through the expression of various antigens on the cell wall. One of the best characterized groups of cell-surface proteins in *C. albicans* is the *ALS* family (agglutinin-like sequence), consisting of eight glycoproteins with a large

degree of sequence similarity (Als1p to Als7p and Als9p) (25). Different growth stage and morphological form promote differential expression of *ALS* genes (87).

Upon NAM treatment transcript abundance of *ALS1* gene is reduced in CaT28N compared to both CaT28 and CaT0 (-3.03 and -2.20 folds, respectively). On the other hand, NAM treatment increases expression of other *ALS* genes. In CaT28N

compared to CaT28 and CaT0, I found upregulation of *ALS3* (+5.61 and +3.47 folds, respectively), *ALS4* (+2.55 and +3.07 folds, respectively) and *ALS9* (+3.14 and +1.57 folds, respectively) and slight increase of transcription level of *ALS5* (+1.94 and ca.+1.50 folds, respectively). This result supports the hypothesis that adhesins may have overlapping functions. On the contrary, in CaT28 compared to CaT0, the expression of *ALS3*, *ALS5* and *ALS9* is downregulated, -1.61, -1.32 and -1.99 folds, respectively. *ALS1*, *ALS2*, *ALS4* and *ALS6* are not significantly regulated, in untreated cultures (CaT28 vs CaT0). *ALS7* expression is slightly increased in CaT28 compared to CaT0.

Upon NAM treatment, *C. albicans* switches from yeast to abnormal hyphal form. True hyphae are highly hydrophobic, particularly at the apical tip, to facilitate the host cell and tissue penetration (88). Indeed, expression of cell surface hydrophobicity (CSH) by *C. albicans* enhances adherence to host cells. Csh1p protein, detected on the *C. albicans* cell surface, significantly affects the overall CSH status of this fungus. In this study, NAM induces yeast-to hypha transition and, as expected, induces overexpression of *CSH1*, resulting in increase of hydrophobicity in V-shaped hyphae. In CaT28N, *CSH1* transcription levels are +8.79 and +2.90 folds compared to CaT28 and CaT0, respectively. This gene is significantly downregulated (-3.02 folds) in CaT28 compared to CaT0.

The expression of other cell surface proteins is upregulated upon NAM inhibition: comparing CaT28N to CaT28 and CaT0, *FAV2* expression (gene encoding an adhesin-like protein) is increased +4.24 and +2.49 folds, respectively; *RBE1* transcription is increased +2.64 folds only compared to CaT28, while it is reduced -2.69 folds comparing with CaT0. In untreated cells the expression of *FAV2* is not significantly changed, while those of *RBE1* is downregulated (-6.94 folds).

Interestingly, the expression of the yeast-specific gene *YWPI* (Yeast Wall Protein 1) is not downregulated during NAM treatment. This gene encodes a GPI-

anchored glycoprotein of *C. albicans* cell wall, with an antiadhesive effect (with a possible role in yeast dispersal), highly expressed in yeast cells. Moreover, yeast lacking Ywp1p are more adhesive and form thicker biofilms. As expected, since under NAM treatment *Candida* does not form biofilm, *YWPI* transcript is upregulated, +7.70 and +2.55 folds, in CaT28N compared to CaT28 and CaT0, respectively; while it is downregulated -3.01 folds in CaT28 compared to CaT0.

Inhibition of Hst3p by NAM induces strong alteration in *C. albicans* morphology and, as expected, significantly changes the expression of genes involved in adherence (*ALS3*, *ALS4* and *ALS9*) whose transcript levels are upregulated (Fig. 24).

Dimorphism genes

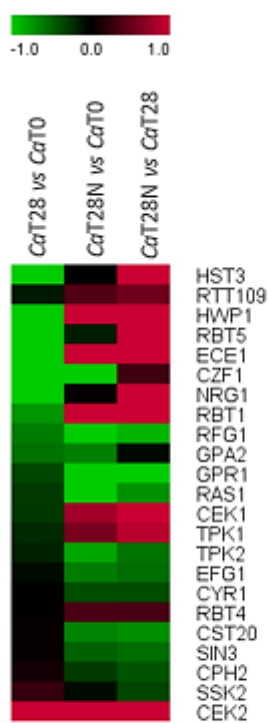


Fig. 25 Heatmap of dimorphism genes differentially expressed in response to 75 mM NAM in the control strain SC5314 of *C. albicans*.

Cph1p-mediated MAPK pathway and Efg1p-mediated cAMP pathway are well-characterized pathways involved in yeast-to-hypha transition. In *C. albicans*, *RAS1* is an important regulator of hyphal development and functions upstream of both pathways (25). The cAMP-PKA pathway is activated by *GPR1* (G-protein coupled receptor) and *GPA2* (G α protein) genes, which regulate the activity of *TPK1* and *TPK2*, two catalytic subunits of *PKA* (cAMP-dependent Protein Kinase), whose activities depend on increasing concentration of

cAMP, produced by adenylate cyclase *CYR1* (25). The downstream effector transcription factor *EFG1* promote hyphal growth, inducing hypha-specific genes and repressing yeast-specific genes; in addition, by induction of cell proteins (*HWP1*, *HWP2*, *HYR1*, *RBE1*, *ECE1*) *EFG1* regulate cell wall dynamics (25). In this study, I did not identify strong differential expression of upstream genes of cAMP-PKA pathway. Weak downregulation is found upon NAM treatment in *GPR1* and *RAS1*: transcript levels are reduced, respectively, -2.36 and -1.71 folds in CaT28N compared to CaT28; -3.18 and -2.19 folds compared to CaT0. The two isoforms of *PKA*, *TPK1* and *TPK2*, are differentially regulated upon NAM treatment: in CaT28N compared to CaT28, *TPK1* is upregulated (+1.91 folds), while *TPK2* is downregulated (-1.56 folds); compared to CaT0, *TPK1* is overexpressed (+1.59 folds) and *TPK2* is downregulated (-1.81-folds). This result suggests redundant role of these two proteins. Downstream component of PKA pathway is *EFG1*, which does not show remarkable differential expression; slight reduction of expression, -1.53 and -1.60 folds, is found in CaT28N compared to CaT28 and CaT0, respectively (Fig. 25).

Expression of filament-specific genes is repressed by *TUP1*, which functions by recruiting the DNA-binding proteins Nrg1p and Rfg1p. NAM induces upregulation of *NRG1*: transcription levels of this gene are +2.60 in CaT28N compared to CaT28, while compared to CaT0 are not statistically significant. On the other hand, the expression of *RFG1* is constantly downregulated over time: -1.88- and -3.04-folds in CaT28N compared to CaT28 and CaT0, respectively (Fig. 25).

As expected from the V-shaped morphology, NAM induces upregulation (ranging from +2.49 to +77.91 folds) of *HWP1*, *HWP2*, *HYR1*, *IHD1*, *RBT1* and *ECE1* genes involved in filamentation and adherence. *HWP1* is upregulated +68.88 folds in CaT28N compared to CaT28 and +4.41 folds compared to CaT0; moreover, in CaT28N transcript levels, of *HWP2* are upregulated +24.69 and

+12.77 folds compared to CaT28 and CaT0 respectively. Transcript levels of *ECE1* in CaT28N is +86.19 folds compared to CaT28, and +29.75 folds compared to CaT0 (Fig. 25).

Several GPI-anchored cell wall proteins are highly overexpressed in CaT28N compared to CaT28 and CaT0: *HYRI* (hyphally regulated gene) involved in core filamentation response, is increased +15.72 and +4.62 folds, respectively; *IHDI*, hyphal specific gene, normally up-regulated during yeast to hyphae transition, is expressed +9.18 folds only comparing with CaT28, while compared to CaT0 no statistically significant variation is detected; ORF19.4653 (encoding a protein similar to GPI-linked cell-wall proteins) transcription levels are strongly increased +48.66 and +77.91 folds, respectively.

RBT1 and *RBT5*, encoding cell wall proteins, are induced during NAM treatment: +4.48, and +4.56 folds, respectively, in CaT28N compared to CaT28; compare to CaT0, *RBT1* is upregulated (+2.57 folds) and no significant variation was detected for *RBT5*.

Comparing CaT28 to CaT0, the expression of most of previously described genes is not statistically significant, while genes upregulated by NAM are downregulated in CaT28 compared with CaT0: *HWPI* (-15.61 folds), *RBT5* (-5.20 folds), *ECE1* (-2.89 folds), *NRG1* (-2.53 folds), *RBT1* is downregulated -1.73 folds, *HYRI* (-3.39 folds), *IHDI* (-7.49 folds).

Genes involved in hyphal morphology and cell wall maintenance are highly represented and upregulated upon Hst3p inhibition by NAM treatment. Upstream genes of pathways controlling *C. albicans* dimorphism are not highly and significantly differential expressed; on the contrary, downstream genes, such as *HWPI*, *ECE1*, *RBT1*, *RBT5*, are overexpressed after NAM treatment.

These results suggest that NAM treatment, inhibiting the activity of Hst3p, increases chromatin accessibility facilitating the binding of transcription factor to promoters of hypha-specific genes.

Alkaline pH-induced genes

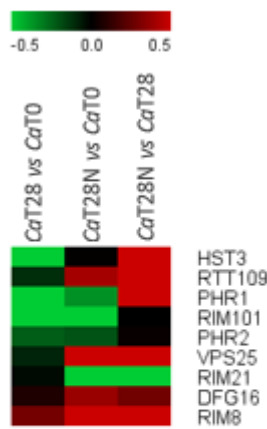


Fig. 26 Heatmap of alkaline-response genes differentially expressed in response to 75 mM NAM in the control strain SC5314 of *C. albicans*.

C. albicans has the ability to colonize different niches whose environmental conditions can change constantly and dramatically. Distinct mechanisms have been developed by this organism to sense, adapt, and respond to external stresses, including variations in the surrounding pH (89). Adaptive response to pH is related to morphological and physiological

changes: fungal dimorphism is induced by alkaline pH which leads to alterations in cell wall architecture and adhesion properties. Rim101p signal transduction pathway controls the response to a neutral-to-alkaline pH change (90). Proteolytically activated in neutral-alkaline pH, the transcription factor *RIM101* expresses alkaline response genes (*PHR1*, *PRA1*) and represses acid response genes (*PHR2*) (90).

I analyzed the expression of alkaline pH-induced genes after NAM treatment, since it induces abnormal hyphae filamentation in *Candida*. Under my experimental conditions, I did not observe significant variations in gene expression for some upstream members of *RIM101* pathway, such as *RIM13*, *RIM20*, *SNF7*, *VPS20*, *VPS23* which are responsible for proteolytic activation of Rim101p (25). However, I found moderate alteration in transcript levels for other upstream members: *RIM21*, *RIM8*, *DFG16* and *VPS25* genes. Comparing CaT28N with CaT28 and CaT0, the expression of the plasma membrane receptor *RIM21* is slightly reduced, -1.52 and -1.56 folds respectively; on the contrary, the

expression of the other plasma membrane pH-sensor *DFG16* is slightly increased, +1.28 and +1.37 folds compared to CaT28 and CaT0, respectively.

However, NAM induces up-regulation of *RIM8* and *VPS25*: in CaT28N compared to CaT28 and CaT0, transcript levels of *RIM8* are +1.55 and +1.99 folds, and those of *VPS25* (part of endosomal sorting complex) are +3.28 and +3.01 folds, respectively.

No statistically significant variation in gene expression is detected for *RIM21*, *RIM8*, *DFG16* and *VPS25* in CaT28 compared to CaT0 (Fig. 26).

PHR1, a gene that at pH above 5.5 codes for a cell surface glycosidase involved in maintenance of hyphal growth, is upregulated (+3.07 folds) only in CaT28N compared to CaT28; on the contrary, the same gene is downregulated (-4.17 folds) in CaT28 compared to CaT0 (Fig. 26).

CHT2 gene, coding for the cell wall chitinase Cht2p, is downregulated, in CaT28N, -4,61 folds compared to CaT28, and -4,74 folds compared to CaT0, resulting in enhanced chitin exposure.

Overall, NAM treatment results in a structural modification of *Candida* cell wall that may play an important immunogenic role that, in turn, may affect the immune recognition of the pathogen.

Biofilm genes

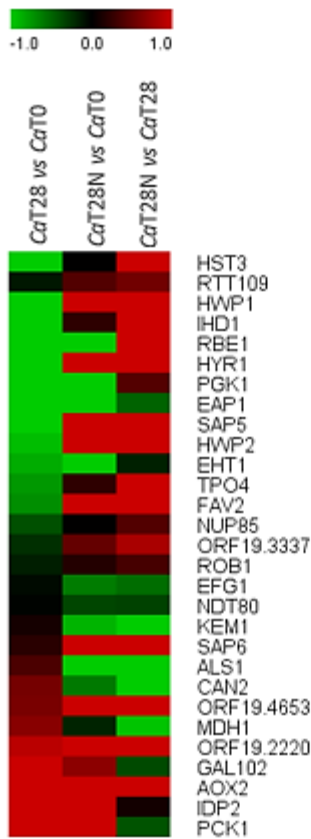


Fig. 27 Heatmap of biofilm-regulated genes differentially expressed in response to 75 mM NAM in the control strain SC5314 of *C. albicans*.

An additional adaptation response used by *C. albicans* to survive in hostile environments consists in multicellular community development. Communities of filaments and yeast cells attached to a solid surface and embedded in an extracellular matrix give rise to a biofilm. Several transcription factors are implicated in the regulation of biofilm formation including the six master biofilm regulators Tec1p, Bcr1p, Bgr1p, Efg1p, Ndt80p, Rob1p (22, 31), with at least 19 target genes, eight of which (*ORF19.3337*, *ALS1*, *TPO4*, *ORF19.4000*, *EHT1*, *HYR1*, *HWP1*, and *CAN2*)

are expressed at higher levels during biofilm formation, compared to planktonic wild-type cells (34). Each regulator controls the other five, and most target genes are controlled by more than one master regulator.

Under NAM treatment *Candida* does not form biofilm, indeed transcription of the six master biofilm regulators is not influenced (*TEC1*, *BCR1*, *BGR1*) or slightly affected (*EFG1*, *NDT80*, *ROB1*) under my testing conditions (Fig. 27). Interestingly, the fungal-specific gene *TPO4*, regulated by *TEC1* and *NDT80* and

encoding a transmembrane transporter involved in biofilm formation, is upregulated (+2.14 folds) in Cat28N compared to CaT28.

Considering that NAM not induces biofilm formation, the increased expression of this gene suggests that its transcription could be regulated epigenetically by Hst3p.

Drug resistance genes

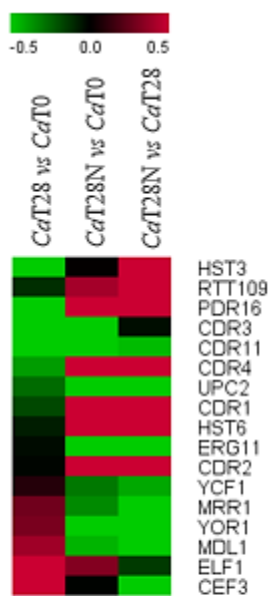


Fig. 28 Heatmap of drug response genes differentially expressed in response to 75 mM NAM in the control strain SC5314 of *C. albicans*.

Azole antifungal drugs are commonly used for treatment of *C. albicans* infections. They prevent ergosterol biosynthesis by inhibition of *ERG11* gene. However, resistance to these antifungal compounds has increased in recent years. Mutations in *ERG11*, overexpression of this gene and upregulation of genes encoding multidrug efflux pumps, *MDR1* and *CDR1/CDR2*, are associated with azole resistance in *C. albicans* (91). The constitutive overexpression of these genes is

usually caused by mutations in the transcription factors *UPC2*, *MRR1*, and *TAC1*, respectively (91).

The current study did not identify differential expression in *TAC1*. *UPC2* and *MRR1* are weakly expressed upon NAM treatment: *UPC2* and *MRR1* expression

is, respectively, -1.51 and -1.71 folds in CaT28N compared to CaT28; -1.91 and -1.33-folds, respectively, compared with CaT0. The expression of *ERG11* is strongly downregulated upon NAM treatment: -3.62 and -3.72 folds in CaT28N compared to CaT28 and CaT0, respectively. This result is in line with the transition to hyphal morphology (NAM-induced) which involves reduction of ergosterol content and increase of chitin amount in hyphal cell wall (92).

The ABC gene superfamily includes both membrane transport proteins which confer a drug-resistance phenotype, and the accumulation of proteins whose functions are associated with protein translation, such as *ELF1* (Elongation Like Factor) and *CEF3* (Elongation Factor-3) (93). *CEF3* is an essential component of the translational system; the encoded protein is detected on surface of yeast cells but not in hyphae. In agreement with the phenotype obtained by NAM treatment, the expression of this gene is reduced (-1.72 folds) in CaT28N compared to CaT28, while, compared to CaT0, is not statistically significant. Gene expression of *ELF1* is not significantly altered by NAM treatment. Mildly downregulation of ABC transporters *MDL1* and *YOR1* is revealed after Hst3p inhibition by NAM treatment: expression levels are -2.01 and -1.99 folds, respectively, in CaT28N compared to CaT28 (Fig. 28).

On the other hand, this study identified upregulation upon NAM treatment of *CDR1*, *CDR2* and *CDR4* whose expression is increased, respectively, +6.79, +3.00 and +4.23 folds, in CaT28N compared to CaT28; compared with CaT0, expression is upregulated +5.77, +2.96 and +3.05 folds, respectively. The expression of *CDR3* and *CDR11* is constant and very weak overtime, with slight reduction of *CDR11* transcript in CaT28N compared to CaT0 (-2.42-folds). Concomitant to *CDR1* and *CDR2* overexpression, I found upregulation of *PDR16* gene which encodes a phosphatidylinositol transfer protein involved in azole resistance. *PDR16* transcript levels are +4.62 and +1.89 folds in CaT28N compared to CaT28 and CaT0, respectively. NAM induced upregulation also of

HST6 (ABC transporter related to mammalian P-glycoproteins): +2.39 and +2.23 folds in CaT28N compared to CaT28 and CaT0, respectively.

Without treatment, no statistically significant variation of gene expression was detected for most of the gene described above, except for *PDR16* (-2.44 folds), *CDR3* (-178 folds), *MDL1* (+1.39 folds), *ELF1* (+1.51 folds) and *CEF3* (+1.71 folds).

NAM administration alters transcriptional drug response, substantially upregulating expression of efflux pumps *CDR1*, *CDR2* and *CDR4*, and downregulating expression of other transporters, such as *MDL1* and *YORI* (Fig. 28). The differential expression of these genes could be related to fungal attempt to expel the drug or, alternatively, their expression is modulated by Hst3p.

Osmotic and stress response genes

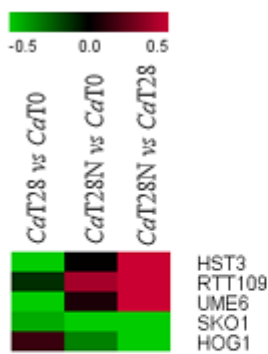


Fig. 29 Heatmap of stress and osmotic response genes differentially expressed in response to 75 mM NAM in the control strain SC5314 of *C. albicans*.

C. albicans has the ability to adapt quickly to host-imposed stresses contributing significantly to its survival and virulence. Different signal transduction pathways allow the detection and the adaptation to such stresses. The response to osmotic, oxidative, and heavy metal

stresses is regulated by the mitogen activated kinase (MAPK) cascade known as the High Osmolarity Glycerol (HOG) pathway, which controls also filamentation and cell wall stability (94). Upstream members of this cascade are the protein

kinases Pbs2p (MAPKK) and Ssk2p (MAPKKK). The key player of HOG pathway is the MAPK Hog1p, which following osmotic stress phosphorylates the transcription factor Sko1p, culminating in expression and repression of osmotic stress-response genes (94).

RNA-Seq data did not highlight significant alteration in transcript levels of upstream genes of HOG pathway, as *SSK1* and *PBS2*. NAM slightly reduces expression of *HOG1* and *SKO1*: -1.50 and -1.70 folds, respectively, in CaT28N compared to CaT28; -1.31 and -2.42 folds, respectively, compared to CaT0.

The *HOG* pathway can drive, also, filamentous growth by activation of specific transcription factors: when Hog1p is inactive it fails to keep the repressor Sko1p on the promoter of *BRG1*, allowing the expression of Brg1p and hyphal elongation. *HOG1-BRG1* can regulate expression of *UME6*, transcription factor which play an important role in hyphal filament extension (95). In this study, NAM treatment supports hyphal development by slight reduction of expression of hyphal repressors *HOG1* and *SKO1*, and by increasing expression of *UME6*: in CaT28N compared to CaT28, *UME6* expression is increased +1.90 folds, while compared to CaT0 there is no statistically significant change (Fig. 29). On the other hand, without NAM, in yeast cells *UME6* expression levels are downregulated, -1.70 folds, and transcript levels of other genes are not significant.

White-Opaque transition genes

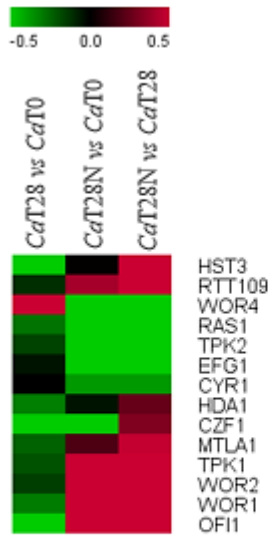


Fig. 30 Heatmap of white-opaque transition genes differentially expressed in response to 75 mM NAM in the control strain SC5314 of *C. albicans*.

C. albicans shows another form of phenotypic switching: the white-opaque transition, in which white and oval cells, forming domed colonies, switch to grey and elongated cells forming flat colonies. The homozygosity for the *MTL* locus that controls cell type is responsible for switching to opaque state. Most *C. albicans* cells are unable to switch because of their heterozygosity for the *MTL* locus

(*MTLa/MTLa*) (96). The Ras-cAMP/PKA pathway regulates filamentous growth and opaque transition in *C. albicans* (27). White-opaque switching in *C. albicans* is regulated by epigenetic mechanisms (27) and is controlled by the positive regulators *WOR1*, *WOR2*, and *CZF1* and the negative regulator *EFG1* (97). *WOR1*, the master regulator of white–opaque switching in *C. albicans*, binds to the promoter regions of *EFG1*, *CZF1*, *WOR2* and *WOR1* itself, controlling their and its own expression (96).

In this study, analysing expression levels of genes involved in white-opaque transition upon NAM treatment, I found induction of genes of opaque growth: strong and significant upregulation of *WOR1* and *WOR2* is detected. Transcript levels of *WOR1* and *WOR2* are +14.02 and +9.76 folds, respectively, in CaT28N compared to CaT28, and compared with CaT0, the expression is +10.75- and +8.47-folds, respectively. On the contrary, the expression of the other activator of

opaque cell type *WOR4*, positioned upstream of *WOR1*, is significantly downregulated upon NAM treatment: -3.44 and -2.23 folds in CaT28N compared to CaT28 and CaT0, respectively (Fig. 30).

The main effect of *WOR4* on regulation of *WOR1* probably occurs during the transition between white and opaque cells. *WOR1* binds to the promoter regions of *WOR2*, inducing upregulation of this gene that regulates transcription of *CZFI*. *CZFI* normally represses a repressor of the opaque state, *EFG1*. The cAMP/PKA pathway induces opaque cell formation by *WOR1* activation mediated by PKA phosphorylation (isoforms *TPK1* and *TPK2*). Downstream of *WOR1* the zinc-finger transcription factor *OFII* (opaque and filamentation inducer 1) is present and whose expression is strongly increased in my experiments. NAM-mediate Hst3p inhibition induces upregulation of *WOR1* and consequently of *OFII*: transcript levels of this gene are +629.34- and +8.54-folds in CaT28N compared to CaT28 and CaT0, respectively (Fig. 30).

On the other hand, in CaT28 compared to CaT0, the expression of *OFII* is strongly downregulated (-73.63 folds), while those of *WOR4* is slightly increased (+1.53 folds); the expression of other genes is not significant.

The upregulation of genes of white-opaque transition, upon Hst3p inhibition, confirms, as reported in literature, that epigenetic mechanisms regulate their transcription, among which Hst3p may be a potential regulator.

The sirtuin inhibitor NAM induced morphological switch in *C. albicans*. Transition to the hyphal morphology intuitively requires differential regulation of gene expression. In the present study, I revealed high up-regulation of several genes in response to nicotinamide treatment. Hypha-specific genes (*HWP1*, *HWP2*, *HYR1*), genes involved in cell adhesion (*ALS3*, *ALS4*, *ALS9*), regulation of cell surface hydrophobicity (*CSH1*), drug transport (*CDR1*, *CDR2*, *CDR4*,

PDR16), cell wall metabolism (*SAPs*) and white-opaque transition (*WOR1*, *WOR2*, *OF11*) are strongly over-expressed in *C. albicans*, upon NAM treatment.

6.5 Optimization of protein expression in *E. coli*

Functional characterization of sirtuin Hst3p and selection of its inhibitors that can be used for therapeutic purpose requires purification of the fungal protein.

Considering that the homologous Hst3p of *S. cerevisiae* (98) was not purified in its full-length but only in its short form (which showed enzymatic activity *in vitro*) I intended to express and purify both the full length and a short form of Hst3p.

The entire sequence coding for aa 1-487 and a short sequence coding for aa 26-370 of *C. albicans* SC5314 Hst3p (Fig. 31) were cloned in pET28a expression vector, expressed and purified, using *Escherichia coli* as host strain for recombinant plasmids.

```

1  MISIDLLDNS GTSMPADTSI KLHEV IKFIS KSKKMTVLTG AGISCNAGIP
51  DFRSSDGLYN MVKAKHPKAV VRGQDLFDIS LFRDEMSSLSV FCTFMESLYK
101 SSLNAKPTET HKFIKILKDK NKLLRCYTQN IDCIEQHINL KLGINLQEFD
151 NNKFKQVWNQ LDVVQLHGNL HKLSCTNCFS QFNWNEEFQT LLANGLNPEC
201 SKCMDKYQQR LYSGKRLTGQ TIGLLRPDIV LYGEHHPQME ILTQGLNSDL
251 KSRPDCLIIM GTSLKVAGVK SLVKSLSKII HNKGGKVIYV NKTCLSASSW
301 KNYIDYEVVS DCDEFVRMLK TEIPDLFLTQ EQLDSEKLNQ VAVKGSSLNK
351 PIVKPEAKVK IEPGIKQEDA IQYSPEREVT IKQEVNIKQE PIVKREVESV
401 SVKEEPIPTP PTPHKPKQA TKLKRKSPDE ISANEVHSRV KRLRPRNDQL
451 SSPASSINGS EEEEEDEPV AKVLFENARK GITLDQH*
```

Fig. 31 Amino acid sequence (aa 1-487) of Hst3p of *C. albicans*

Green boxes represent amino acids not present at N- and C-terminal of Hst3p truncated form (aa 26-370).

Expression plasmids pET28a/Hst3 and pET28a/Hst3-short were transferred into BLR (DE3) *pLysS E. coli* cells; after selecting transformants, optimization

of protein expression was set up changing temperature and time of induction. In detail, transformed *E. coli* cells were grown at 37°C to 0.8 OD₆₀₀ before the addition of 1 mM IPTG, cultures were then incubated at 25° or 35°C for up to 4h. 1.5 mL samples were collected every hour and soluble proteins were analysed by SDS-PAGE and Western blot using an anti-HisTag antibody. Figure 32 shows that both Hst3p-full length (57 kDa), and its short form (42 kDa), were better expressed at 25°C after 4h induction.

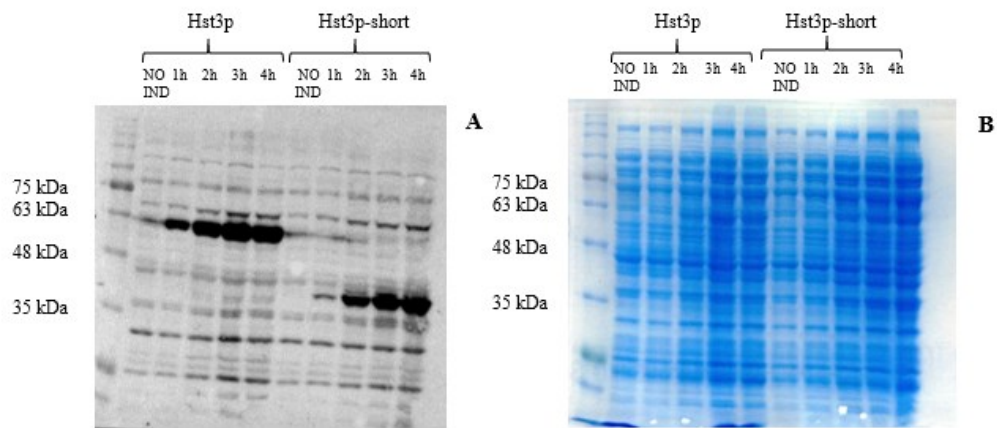


Fig. 32 Analysis of Hs3tp and Hst3p-short expression conditions

Panel A and Panel B represent, respectively, Western Blot and SDS-PAGE analysis of expression conditions of Hst3p full length (57 kDa) and its short form (42 kDa).

6.5.1 Hst3p purification

I tried to purify Hst3p full-length by a first step of affinity chromatography taking advantage of the His-Tag and a second step of anion exchange. Western blot and SDS-PAGE analysis of chromatographic fractions showed Hst3p with a good degree of purification (Fig. 33). Unfortunately, the mass spectrometric analysis of the gel slice corresponding to the prevalent protein around 60 kDa revealed the presence of the chaperonin GroEL associated to Hst3p. Bacterial chaperon GroEL was, therefore, co-purified with the fungal sirtuin and co-migrated with Hst3p. This result highlighted that, when expressed in bacterial host, Hst3p encounters so many folding difficulties to remain trapped in the chaperonin barrel.

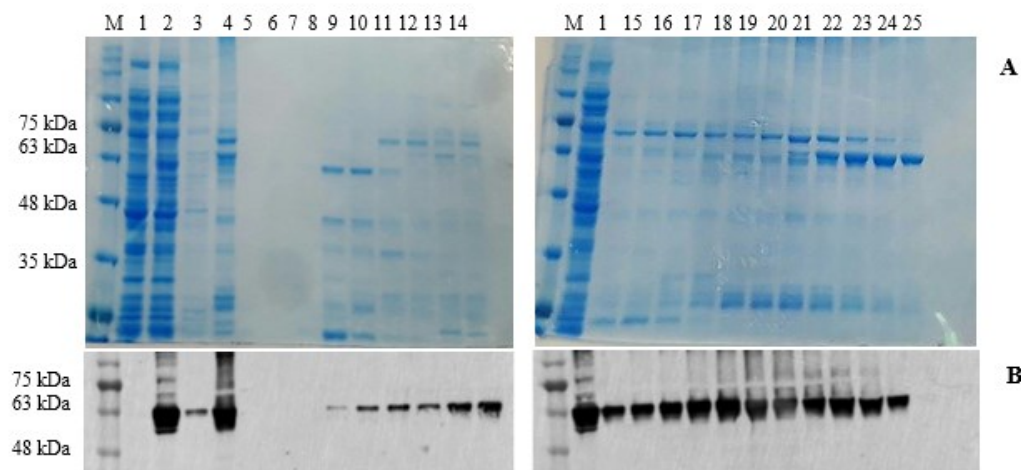


Fig 33. Analysis of ion exchange chromatographic fractions

Panel A: SDS-PAGE of Hst3p purification by anion exchange chromatography, using a Mono Q 5/50 GL column. Panel B: Western Blot analysis of Hst3p purification, using an anti-HisTag antibody. Lane: 1) not induced cell lysate, 2) induced cell lysate, 3) affinity chromatography flow through, 4) pool of dialyzed fractions, 5) ion exchange chromatography flow through, 6-25) ion exchange chromatography fractions.

For effective purification of folded 6xHis-tag Hst3p, I tried to dissociate the chaperonin complex working under denaturing conditions.

After verifying that Hst3 protein was more abundant in the soluble fraction rather than precipitated in inclusion bodies, cells were resuspended in lysis phosphate buffer and sonicated. Cleared lysate was mixed with 4 M urea in order to dissociate Hst3p-GroEL complex and, after complete dissolution of urea, histidine-tagged Hst3p was purified by affinity chromatography (Fig. 34). Once mass spectrometry analysis confirmed the dissociation of the chaperon-Hst3p complex and the presence of only Hst3p in the gel slice corresponding to about 60 kDa, the eluted fractions containing the fungal sirtuin were combined and dialyzed in order to remove urea. To facilitate refolding of recombinant protein after denaturation in urea, dialysis buffer contained 0.1 M arginine, to prevent protein aggregation and 0.5 mM ZnCl₂ to facilitate protein folding, considering that Hst3p has a Zn²⁺-binding domain. Arginine concentration was gradually reduced during dialysis up to 6 mM; dialyzed proteins were loaded on a 1 mL Mono Q 5/50 GL column for further purification by anion exchange chromatography. Eluted fractions were analyzed by SDS-PAGE and mass spectrometry analysis confirmed the presence of Hst3p in one fraction (Fig. 35). Hst3p was purified but was quite degraded. A histone deacetylase assay was performed using the purified protein and a synthetic peptide fragment of histone H3 [NH₂ – GTVALREIRRFQK(Ac)STELLIRK(Biotin) – OH], as substrate. MALDI-TOF technology was used to measure the enzymatic activity of fungal sirtuin Hst3p, which unfortunately did not display any activity.

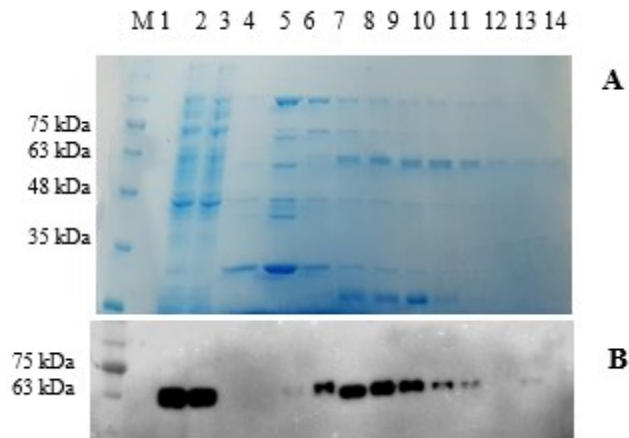


Fig. 34 Affinity chromatography of denatured Hst3p

Panel A: SDS-PAGE analysis of denatured Hst3p purification by affinity chromatography. Panel B: Western Blot analysis of Hst3p purification. Lane: M) Protein marker, 1) not induced cell lysate, 2) induced cell lysate, 3) affinity chromatography flow through, 4-14) affinity chromatography fractions.

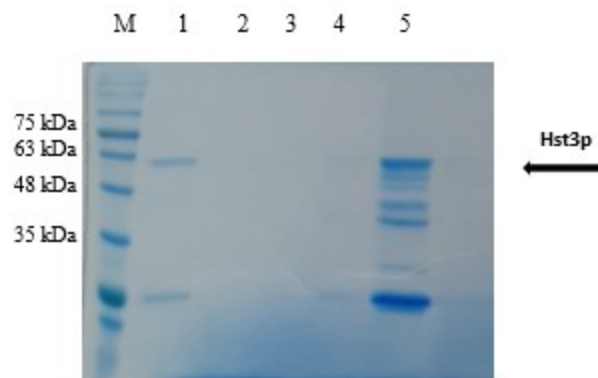
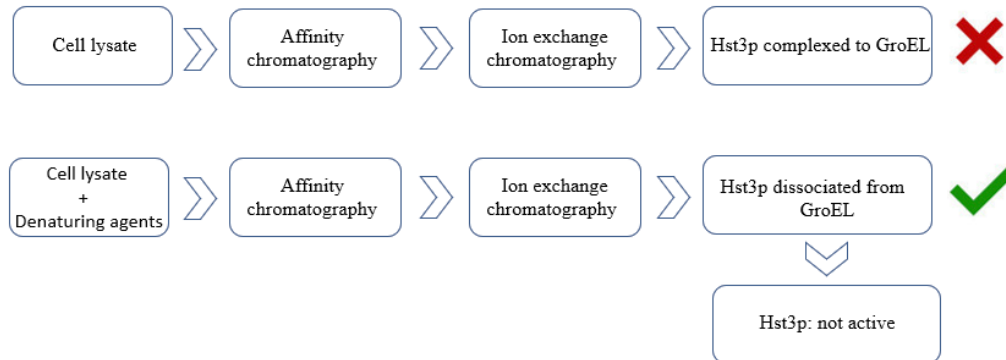


Fig. 35 Analysis of anion exchange chromatography of refolded Hst3p

SDS-PAGE of anion exchange chromatography fractions. Lane: M) Protein marker, 1) dialysed fractions, 2) ion exchange chromatography flow through, 3-5) eluted fractions.

The workflow of Hst3p purification was depicted below:



6.5.2 Hst3p-short purification

Considering that the homologous Hst3p of *Saccharomyces cerevisiae* was purified in its short form and was active, I proceeded trying to purify the short sequence of Hst3p of *C. albicans*. Initially, two chromatographic steps were sequentially performed for Hst3p-short purification: affinity chromatography and anion exchange chromatography. The analysis of these purification steps revealed that, as Hst3p full-length, also the short sequence of this protein was complexed to GroEL: in this case it was evident since the Coomassie staining of chromatographic fractions showed a prevalent protein band at higher molecular weight (ca. 60 kDa) than the expected (42 kDa) (Fig. 36). Mass spectrometry analysis confirmed the co-purification of Hst3p-short with bacterial GroEL.

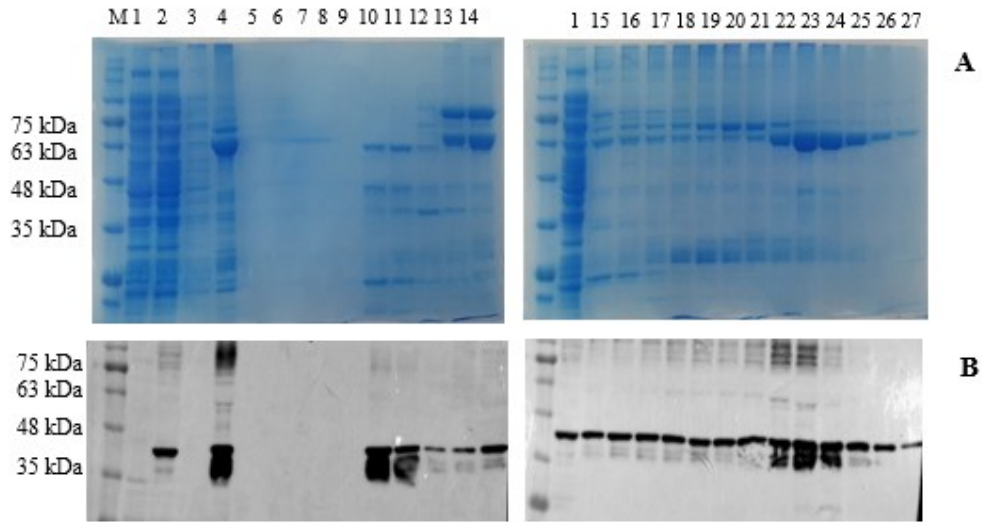


Fig. 36 Analysis of ion exchange chromatography fractions

Panel A: SDS-PAGE of Hst3p-short purification by anion exchange chromatography, using a Mono Q 5/50 GL column. Panel B: Western Blot analysis of Hst3p-short purification, using an anti-HisTag antibody. Lane: M) Protein marker, 1) not induced cell lysate, 2) induced cell lysate, 3) affinity chromatography flow through, 4) pull dialysed fractions, 5) ion exchange chromatography flow through, 6-27) chromatography fractions.

Considering the folding difficulties of this protein, I investigated its solubility. Unlike the full length of Hst3p of *C. albicans*, the recombinant Hst3p in short form was mainly precipitated as insoluble inclusion bodies in the bacterial host (Fig. 37).

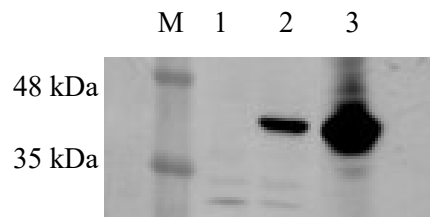


Fig. 37 Analysis of Hst3p-short solubility

Western Blot analysis of Hst3p-short solubility, using an anti-HisTag antibody. Lane: M) Protein marker, 1) Not induced soluble cell lysate, 2) Induced soluble cell lysate, 3) Insoluble protein fraction (inclusion bodies).

The process to obtain Hst3p from inclusion bodies was very laborious. Sonication and centrifugation cycles allowed the isolation of the inclusion bodies. Solubilization of protein aggregates was carried out in empirical ways using high concentration of denaturants and chaotropes. In particular, after overnight solubilization of inclusion bodies at 4°C in 8 M urea, once demonstrated that Hst3p short was still in the pellet obtained by centrifugation, this was resuspended in 6 M guanidine hydrochloride, which allowed the complete solubilization of Hst3p short.

High concentrations of urea and guanidine hydrochloride resulted in complete denaturation of protein, thus subsequent protein refolding steps were necessary. Solubilized protein was refolded by removal of denaturing agent; in particular, several dialysis changes were performed, decreasing to zero guanidine concentration and adding 15 mM arginine-HCl as stabilizing agent and 1 mM DTT as reducing agent. After this extensive process, Hst3p short showed to be in a pure and soluble form (Fig. 38). Unfortunately, this Hst3p-short did not display enzymatic activity.

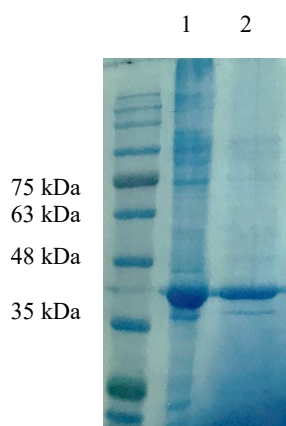
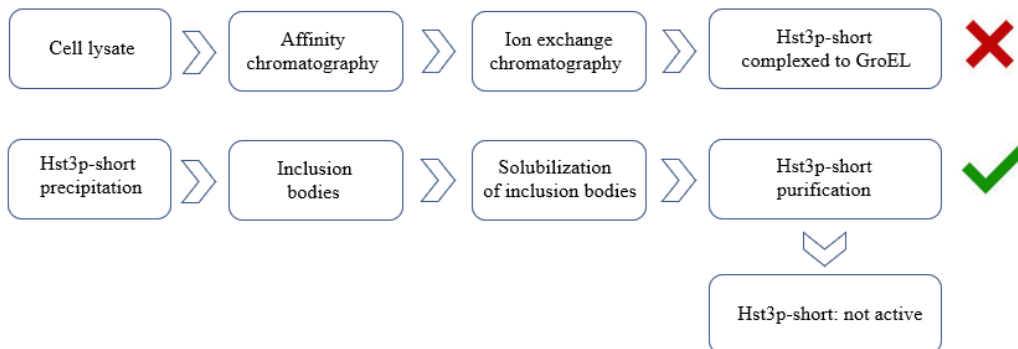


Fig. 38 Analysis of dialyzed Hst3p-short

SDS-PAGE of solubilized Hst3p-short (42 kDa) from inclusion bodies. Lane: 1) Inclusion bodies, 2) Dialyzed Hst3p-short.

The workflow of Hst3p-short purification was depicted below:



6.5.3 Purification of Hst3p from a co-expression system

Both the full length and the short form of the fungal sirtuin Hst3p were unable to fold correctly: co-purification of Hst3p with the bacterial chaperonin GroEL evidenced the misfolded conformation acquired by these proteins when expressed in *E. coli* cells. Denaturing conditions allowed me to solubilize protein aggregates and purify the two proteins, but not to obtain them in an active form.

To improve protein folding in the cell and avoid protein denaturation I tried a second method for protein purification: the co-expression of target protein with molecular chaperones, that operates cooperatively in the protein folding. *E. coli* BL21 (DE3) cells were firstly transformed with the chaperone plasmid pG-KJE8 (coding for *dnaK* – *dnaJ* – *grpE* – *groES* – *groEL* chaperons) and then with the expression plasmid pET28a containing Hst3p sequence of *C. albicans*. After induction of chaperone expression (at 37°C) and Hst3p expression (over-night at 18°C), cells were lysed and protein purification was carried out by nickel affinity chromatography. One single step of purification was successful, obtaining Hst3p in a high pure form (Fig. 39). Mass spectrometry analysis confirmed the presence of the protein without the chaperonin.

Future experiments will be needed to assess the activity of the protein.

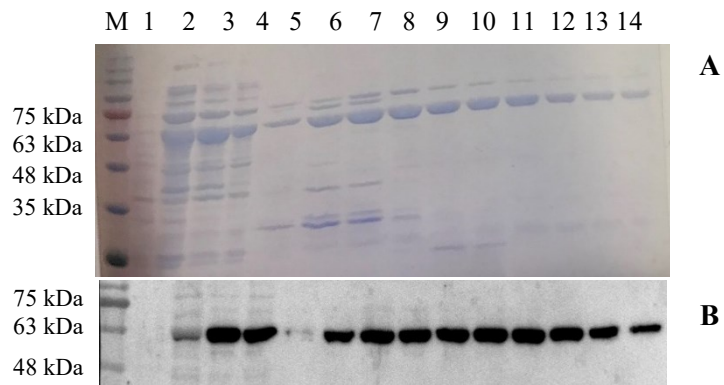


Fig. 39 Analysis of Hst3p purification from a co-expression system

Panel A: SDS-PAGE of Hst3p purification by affinity chromatography after co-expression of target protein with molecular chaperons. Panel B: Western Blot of chromatographic fractions. Lane: M) Protein marker, 1) Cell lysate before induction of molecular chaperons, 2) Cell lysate before induction of recombinant Hst3p, 3) Cell lysate after Hst3p induction, 4) Flow through, 5-14) Chromatographic fractions.

CHAPTER VII

DISCUSSION

The suggestive feature of the polymorphic fungus *C. albicans* is its phenotypic plasticity: this fungus adapts its physiology and morphology to the mutable environmental conditions. The unicellular budding yeasts or the white and round cells can rapidly switch to hyphal filaments or opaque and elongated cells. The yeast-to hypha transition and the white-opaque switching, as well as adaptation to drug pressure and biofilm formation are well-known virulence traits of *C. albicans*, which are regulated epigenetically. Chromatin modifying enzymes, including histone acetyl transferases and histone deacetylases, are involved in fungal morphogenesis and virulence.

The acetylation and deacetylation of histone H3 Lysine 56 is a post-translation modification particularly important in *C. albicans* and in other yeasts, contributing to genome stability. The fungal-specific enzymes Rtt109p and Hst3p orchestrate the acetylation levels of H3K56 in *C. albicans* (81).

HST3 is an essential gene in *C. albicans* and H3K56ac is the physiologic substrate of the sirtuin Hst3p, whose inhibition induces histone degradation and reduction of cell viability (81). Therefore, the modulation of acetylation levels of H3K56 could be an intriguing strategy for the treatment of *C. albicans* infections.

On the basis of these considerations, this research project focused on the functional characterization of the sirtuin Hst3p of *C. albicans* that could be a potential therapeutic target, considering that it is a highly specific enzyme and whose protein sequence contains motifs that are absent in human sirtuins (81).

The fungal sirtuin Hst3p is responsible for H3 Lys56 deacetylation in *C. albicans*. As sirtuin, Hst3p is inhibited by nicotinamide, a product of NAD⁺-dependent deacetylation reaction. In this project I examined the variation of acetylation

levels of H3K56 during *C. albicans* growth and the effect of Hst3p inhibition on its target H3K56ac. *C. albicans* cultures, untreated and treated with 75 mM NAM, were monitored overtime: NAM reduced cell duplication of approximately 56%, compared to control cells, after 33 hours of treatment. Therefore, the inhibition of Hst3p strongly reduced the duplication time, highlighting the role of this sirtuin in the maintenance of cell viability. The acetylation levels of H3K56 were determined for each time point of *C. albicans* growth curve. During fungal growth, this acetylation increased during the time with a typical Gaussian shape: with an acetylation peak at six hours and subsequent reduction, reaching the acetylation levels characteristic of the initial stage of growth. On the contrary, H3K56 acetylation of NAM treated yeasts increased overtime remaining almost constant also after 24h of NAM treatment. I demonstrated for the first time the variations of H3K56ac during *C. albicans* growth, finding an abundant acetylation in exponential phase, in which cell proliferation and gene transcription are normally very active. At the same time, I demonstrated that Hst3p inhibition caused an accumulation of its substrate (H3K56ac).

Moreover, once determined the effect of Hst3p inhibition of its substrate, I investigated the correlation of Hst3p with the different morphogenetic stages of *C. albicans* carrying out a morphological analysis of the yeast-to-hypha transition of the wild-type control strain SC5314 of *C. albicans*, with and without nicotinamide. The potential role of Hst3p in resistant strains was assessed extending these examinations to two fluconazole resistant strains of *C. albicans* (ATCC 64164 and ATCC MYA 574-GU5 strains). Different growth conditions were tested (different pH, temperature, media) examining the effect of Hst3p inhibition by NAM at a single cell and colony level and allowing me to analyze several biological processes, such as cell duplication, germination, hyphae and biofilm formation. The filamentation was induced by 10% serum (used to reflect the response to cues that may be present in the *C. albicans* host environment) or

by alkaline conditions, using M199 (complex medium, able to induce the yeast-to-hypha transition) and Spider medium (rich medium strongly stimulating hyphal growth, used to assess biofilm formation). These media with neutral-basic pH strongly induced, at 37°C, germination, in liquid and solid media, of both the wild-type strain and the resistant strain ATCC 64164 of *C. albicans*. The fluconazole resistant strain of *C. albicans* over-expressing efflux pumps (ATCC MYA 574-GU5), probably because of the elevated membrane rigidity, showed almost no filamentation in liquid and solid media, except in solid M199 medium in which a thick hyphal crown around the macro-colony was formed. The difference found in M199, between liquid and solid medium, may be due to the fact that liquid filamentation is performed at the single cell level, whereas solid filamentation is assessed at the population level, in which the filamentation effect could be enhanced. On the other hand, NAM treatment in the same culture conditions determined severe morphological alterations, arresting the formation, in hypha-inducing condition, of the hyphal crown around the macro-colonies of *C. albicans* strains and blocking the germination of each liquid culture. Moreover, to investigate the effect of Hst3p inhibition under conditions that normally maintain the yeast form of *C. albicans*, morphological analyses were performed in rich YPD medium at 25°C. In this case, NAM treatment triggered the transition to filamentous growth causing the formation of abnormal filamentous structures (V-shaped hypha) in the three examined strains.

Among the resistance strains, the ATCC MYA 574-GU5 strain of *C. albicans* showed less sensitivity to Hst3p inhibition. The mild response to NAM of this strain is correlated to the over-expression of drug transporters.

These morphological analyses demonstrated the effect of NAM on fungal morphology and intuitively, the involvement of Hst3p in the regulation of the yeast-hyphae transition in *C. albicans* strains. Hst3p inhibition by nicotinamide caused reduction of the cell duplication time, inhibition of germination in hyphae-

inducing conditions, and activation of filamentation in yeast-inducing environment, with formation of V-shaped hyphae, whose virulence is reduced in mouse model, as reported in literature (81).

In addition, these morphological analyses were performed along with mass spectrometry, exploiting the potential of the MALDI-TOF technology. This method resulted very useful to differentiate the morphogenetic states of *C. albicans* and for the characterization of the protein profiling of *C. albicans* treated with NAM. The V-shaped hyphae obtained upon NAM treatment showed spectra with some ions with specific mass to charge ratio (m/z) in common with those of true-hyphae; but this analysis highlighted also the characteristic protein profiling of V-shaped hyphae, with some ions with mass to charge ratio (m/z) specific and exclusive of this phenotype. This result confirmed the morphological alteration induced by NAM as consequence of sirtuin inhibition and gave us a mass spectral fingerprinting of *C. albicans* upon Hst3p inhibition.

NAM treatment induced formation of V-shaped hypha in yeast-inducing condition, highlighting the massive effect of Hst3p inhibition of gene transcription. Therefore, to study the transcriptional landscape of the pathogenic fungus *C. albicans* after Hst3p inhibition induced by NAM and to permit a comparison between the phenotypic and the transcriptional response, a RNA-Sequencing analysis was performed. The analysis of over 6,500 gene transcript levels, representing the entire genome of *C. albicans*, revealed several genes differentially regulated: genes involved in adhesion, hyphal growth, drug resistance and cell wall maintenance were mostly dysregulated upon Hst3p inhibition.

The transcriptional expression of genes involved in the regulation of H3K56 acetylation levels, *RTT109* and *HST3*, was firstly examined: following Hst3p inhibition the expression of *HST3* was upregulated (+2.99 folds), probably as compensatory mechanism for the inhibited enzymatic activity, or alternately, the

expression of this gene is regulated epigenetically by Hst3p itself. The expression of *RTT109* was not particularly and significantly affected upon NAM treatment, with very slight increase just in one treated condition (+1.56 folds).

Hst3p inhibition by NAM triggered the phenotypic switching in *C. albicans*, with formation of V-shaped hypha. The transition to hyphal morphology intuitively required huge and complete rearrangement of the cellular structure and properties, and consequently required differential regulation of gene expression to promote hyphal formation.

The V-shaped hypha development and elongation was supported by NAM via over-expression of secreted hydrolases with extracellular proteolytic activity, encoded by *SAP* genes. Global up-regulation was found for almost all ten *SAP* genes, ranging from +1.69 to +24.67 folds in response to Hst3p inhibition. This general up-regulation suggests that Hst3p can regulate the expression of *SAP* genes: the inhibition of the fungal sirtuin could increase chromatin accessibility facilitating the binding of transcription factors to promoters of *SAP* genes.

NAM treatment increased adhesive features of *C. albicans*, inducing expression of innumerable cell surface glycoproteins. The expression of most of genes involved in adherence, downregulated in untreated yeast cells, was up-regulated upon NAM treatment, including genes of *ALS* family (*ALS3*, *ALS4*, *ALS5* and *ALS9*), with expression ranging from +1.57 to +5.61 folds, *FAV2* (adhesin-like protein) and *RBE1* genes. Adhesion to host cell is facilitated also by the cell surface hydrophobicity (CSH), that is a peculiar feature of filamentous structures. NAM triggered the yeast-to-hypha transition inducing, as expected, overexpression of *CSH1* gene, resulting in increase of hydrophobicity in V-shaped hyphae, fundamental for their elongation.

HWP1, *HWP2* (hyphal cell wall proteins), *HYR1* (hyphally regulated gene), *RBT1*, *ECE1* are hypha-specific genes, encoding cell wall proteins expressed exclusively on hypha structures, required for filamentation and adhesion, which

were strongly up-regulated (ranging from +2.49 to +77.91 folds), upon NAM treatment in *C. albicans*, as expected, considering that NAM induced fungal dimorphism. In this study, I did not identify strong differential expression of upstream genes of pathways which control the expression of these hypha-specific genes. Interestingly, the transcriptional repressor of filamentation *NRG1* was up-regulated (+2.60 folds) upon Hst3p inhibition, suggesting that also the transcription of this gene could be affected by the fungal sirtuin Hst3p. On the other hand, the expression of the other filamentation repressor *RFG1* is constantly downregulated (-1.88- and -3.04-folds), in agreement with abnormal hypha formation under NAM treatment. Another hypha-specific gene whose expression was increased by NAM treatment is *PHR1* (+3.07 folds), downstream effector of *RIM101* pathway involved in maintenance of hyphal growth. Under my experimental conditions, I did not observe significant variations in gene expression for some upstream members of *RIM101* pathway, which are involved in response to a neutral-to-alkaline pH change and consequently they regulate fungal dimorphism. The maintenance of hyphal growth and adaptation to environmental pH need cell wall remodelling with enhanced chitin exposure at the cell periphery. This process requires reduced expression of *CHT2* gene, coding for a cell wall chitinase. In this study, I found downregulation (-4.61 folds) of this gene upon Hst3p inhibition; this result is in line with the phenotype generated by NAM, considering that more chitin is required in V-shape hyphal filaments, compared to yeast cells.

Although the pharmacological inhibition of Hst3p by NAM induced hyphal formation, it did not determine *Candida* biofilm formation, as verified by our morphological analyses and also by transcription profiling: the expression of the six master biofilm regulators was not influenced (*TEC1*, *BCR1*, *BGR1*) or slightly reduced (*EFG1*, *NDT80*, *ROB1*) under my testing conditions.

The drug transcriptional response was altered following Hst3p inhibition, with up-regulation of several ABC transporters (*CDR1*, *CDR2*, *CDR4* and *HST6*) and downregulation of other transporters (*MDL1*, *YOR1*) and *ERG11* (ca. -3.7 folds). The increased expression of these genes suggests that Hst3p inhibition is correlated to a relaxed chromatin state, favouring gene transcription or simply drug treatment is responsible for the up-regulation of efflux pumps; reduced levels of *ERG11* transcript reflects the transition to hyphal morphology, in which the ergosterol content in fungal cell membrane is decreased with increased of chitin amount.

Hyphal filament extension is supported under NAM treatment by slight downregulation of some members of *HOG* pathway (which control stress response and filamentation) with consequent upregulation of the transcription factor *UME6*, involved in hyphal elongation.

As reported in literature, epigenetic mechanisms regulate white-opaque transition in *C. albicans*. In my experimental conditions, the expression of genes regulating this phenotypic switch changed upon NAM treatment, finding a strong up-regulation of *WOR1* and *WOR2*, combined with high overexpression of *OF11*, the downstream effector of *WOR1*. Considering that the upstream members of Ras-cAMP/PKA pathway regulating the white-opaque transition were not affected by NAM treatment and the downstream effector *WOR1* was strongly overexpressed confirm the involvement of epigenetic mechanisms in regulation of these genes, demonstrating that Hst3p could be a modulator of transcription of white-opaque genes.

The transcriptional profiling allowed me to identify genes whose expression could be regulated epigenetically by the fungal sirtuin Hst3p. Interestingly, I did not find alterations in gene expression in upstream members of most of examined pathway; however, changes in transcription levels were detected in the downstream effectors of these pathway, suggesting that the inhibition of Hst3p

activity interferes with the expression of these regulators. Specifically, Hst3p inhibition induced the expression of genes involved in regulation of hyphal morphology and cell wall remodelling; in particular hypha-specific genes (*HWP1*, *HWP2*, *HYR1*, *RBT1*, *PHR1*), genes involved in cell adhesion (*ALS3*, *ALS4*, *ALS9*), regulation of cell surface hydrophobicity (*CSH1*), cell wall metabolism (*SAPs*) and white-opaque transition (*WOR1*, *WOR2*, *OF11*) were up-regulated in *Candida albicans*, upon Hst3p inhibition. This study allowed the identification of some potential targets of Hst3p which will be validated by further studies, via chromatin immunoprecipitation experiments (ChIP) or ChIP-on Chip technique.

In order to select potential inhibitor of Hst3p to be used as potential fungicidal compounds, I expressed and purified the fungal sirtuin. Considering that the homologous Hst3p of *S. cerevisiae* was purified only in its short form, I decided to purify the full-length and a truncated form of Hst3p of *C. albicans*. The process of purification was very challenging due to the misfolding of the fungal deacetylase: both the full length and the short forms were unfolded and complexed to the bacterial chaperon GroEL. Following several steps of denaturation, dialysis and renaturation I purified the recombinant proteins, which did not display any enzymatic activity. To improve protein folding I purified the fungal sirtuin from a bacterial system overexpressing some molecular chaperons, which cooperated for the correct protein folding. The enzymatic activity of this recombinant Hst3p is under investigation.

This project has provided new and interesting insight on the fungal sirtuin Hst3p of *C. albicans*, which could be a promising therapeutic target, on the basis of its fungal specific properties and its functions related to *Candida* viability, morphology and virulence.

For the first time, the variations of acetylation levels of H3K56 during the growth of *Candida* were characterized demonstrating that the acetylation of

H3K56 increases with increasing inhibition of Hst3p. The increased inhibition of the fungal sirtuin, as reported in literature, is responsible of fungal death due to the accumulation of acetylated H3K56 that causes histone fragmentation.

The involvement of the fungal deacetylases in *Candida* yeast-to-hypha transition was demonstrated. Its pharmacological inhibition causes strong alteration of fungal morphology, with formation of abnormal filaments in yeast-inducing conditions and arrest of germination in hypha-inducing environment. These morphological alterations are coupled to heavy reduction of fungal growth rate. These alterations reflect the vigorous change in gene expression induced by Hst3p inhibition: the massive up-regulation, upon NAM treatment, of hypha-specific genes, genes regulating cell adherence, cell wall metabolism suggest that these genes could be regulated by epigenetic mechanisms in which an important key player could be Hst3p. Future experiments of chromatin immunoprecipitation will allow to verify if the expression of some selected genes (*SAPs*, *HST3*, *TPO4*, *NRG1*, *WOR1*, *OFI1*), dysregulated in this transcriptomic analysis, is directly regulated by the acetylation of H3 Lys 56 and consequently, by the sirtuin Hst3p.

Moreover, the purified recombinant Hst3p will allow to set up an enzymatic assay useful for screening of small molecules, potential inhibitor of Hst3p, that could be used as antifungal compounds.

BIBLIOGRAPHY

1. Singh S. P., Pandey S., Shukla R., Singh P.C., Mishra A. Chapter 3 Diversity, systematics and application of Fungi. In *Plant Taxonomy & Biosystematics, classical and modern methods*; Rana T. S., Nair K. N., Upreti D.K., Eds. New India Publishing Agency. 2014: pp 41-70 .
2. Underhill D. M., Iliev I. D. The mycobiota: interaction between commensal fungi and the host immune system. *Nat Rev Immunol.* 2014; 14 (6): 405-416.
3. Hallen-Adams H. E., Suhr M. J. Fungi in the healthy human gastrointestinal tract. *Virulence.* 2017; 8(3): 352–358.
4. Warnock D. W. Fungal diseases: an evolving public health challenge. *Med Mycol.* 2006; 44(8):697-705.
5. Bongomin F., Gago S., Oladele R.O., Denning D. W. Global and multi-national prevalence of fungal diseases-Estimate precision. *J Fungi (Basel).* 2017; 3(4): 57.
6. Singh N. Trends in the Epidemiology of Opportunistic Fungal Infections: Predisposing Factors and the Impact of Antimicrobial Use Practices. *Clin Infect Dis.* 2001; 33: 1692-1696.
7. Armstrong P.A., Jackson B.R., Haselow D., Fields V., Ireland M., Austin C., Signs K., Fialkowski V., Patel R., Ellis P., Iwen P. C., Pedati C., Gibbons-Burgener S., Anderson J., Dobbs T., Davidson S., McIntyre M., Warren K., Midla J., Luong N., Benedict K. Multistate Epidemiology of Histoplasmosis, United States, 2011-2014. *Emerg Infect Dis.* 2018; 24(3): 425-431.
8. Pfaller M.A., Diekema D. J. Epidemiology of invasive candidiasis: a persistent public health problem. *Clin Microbiol Rev.* 2007; 20, 133-163.

9. Kabir M. A., Hussain M. A., Ahmad Z. *Candida albicans*: A Model Organism for Studying Fungal Pathogens. *ISRN Microbiol.* 2012; 2012: 538694.
10. Brandt M. E., Lockhart S. R. Recent Taxonomic Developments with *Candida* and Other Opportunistic Yeasts. *Curr Fungal Infect Rep.* 2012; 6(3): 170–177.
11. Chaffin W. L. *Candida albicans* Cell Wall Proteins. *Microbiol Mol Biol Rev.* 2008; 72(3): 495–544.
12. Chaffin W. L., López-Ribot J. L., Casanova M., Gozalbo D., Martínez J. P. Cell Wall and Secreted Proteins of *Candida albicans*: Identification, Function, and Expression. *Microbiol Mol Biol Rev.* 1998; 62(1): 130–180.
13. Gow N. A., Hube B. Importance of the *Candida albicans* cell wall during commensalism and infection. *Curr Opin Microbiol.* 2012; 15 (4): 406-12.
14. Gow N.A., van de Veerdonk F. L., Brown A. J., Netea M. G. *Candida albicans* morphogenesis and host defence: discriminating invasion from colonization. *Nat Rev. Microbiol.* 2011; 10(2):112-22.
15. Sudbery P., Gow N., Berman J. The distinct morphogenic states of *Candida albicans*. *Trends Microbiology.* 2004; 12(7): 317-24.
16. Lu Y., Su C., Liu H. *Candida albicans* hyphal initiation and elongation. *Trends Microbiol.* 2014; 22(12): 707-14.
17. Nadeem S. G., Shafiq A., Hakim S. T., Anjum Y., Kazm S. U. Effect of Growth Media, pH and Temperature on Yeast to Hyphal Transition in *Candida albicans*. *Open Journal of Medical Microbiology.* 2013; 3, 185-192.
18. Polonelli L., Ciociola T., Elviri L., Zanella P.P., Giovati L., Arruda D.C., Muñoz J.E., Mortara R.A., Morace G., Borghi E., Galati S., Marin O., Casoli C., Pilotti E., Ronzi P., Travassos L.R., Magliani W., Conti S. A Naturally Occurring Antibody Fragment Neutralizes Infectivity of Diverse Infectious Agents. *Sci Rep.* 2016; 6: 35018.

19. Odds F. C., Brown A. J., Gow N. A. *Candida albicans* genome sequence: a platform for genomics in the absence of genetics. *Genome Biol.* 2004; 5(7):230.
20. Mitrovich Q.M., Tuch B.B., Guthrie C., Johnson A.D. Computational and experimental approaches double the number of known introns in the pathogenic yeast *Candida albicans*. *Genome Res.* 2007; 17(4): 492-502.
21. Kadosh D. Control of *Candida albicans* morphology and pathogenicity by post-transcriptional mechanisms. *Cell Mol Life Sci.* 2016; 73(22): 4265-4278.
22. Mayer F. L., Wilson D., Hube B. *Candida albicans* pathogenicity mechanism. *Virulence.* 2013; 4(2): 119-128.
23. Lo H. J., Köhler J. R., DiDomenico B., Loebenberg D., Cacciapuoti A., Fink G.R. Nonfilamentous *Candida albicans* mutants are avirulent. *Cell.* 1997; 90: 939-949.
24. Leberer E., Harcus D., Dignard D., Johnson L., Ushinsky S., Thomas D. Y., Schropfel K. Ras links cellular morphogenesis to virulence by regulation of the MAP kinase and cAMP signalling pathways in the pathogenic fungus *Candida albicans*. *Mol. Microbiol.* 2001; 42: 673- 687.
25. Biswas S., Van Dijck P., Datta A. Environmental Sensing and Signal Transduction Pathways Regulating Morphopathogenic Determinants of *Candida albicans*. *Microbiol Mol Biol Rev.* 2007; 71(2): 348–376.
26. Shapiro R. S., Robbins N., Cowen L. E. Regulatory Circuitry Governing Fungal Development, Drug Resistance, and Disease. *Microbiol Mol Bio Rev.* 2011; 75(2): 213–267.
27. Huang G. Regulation of phenotypic transitions in the fungal pathogen *Candida albicans*. *Virulence.* 2012; 3(3): 251–261.
28. Murillo L. A., Newport G., Lan C. Y., Habelitz S., Dungan J., Agabian N. M. Genome-Wide Transcription Profiling of the Early Phase of Biofilm Formation by *Candida albicans*. *Eukaryot Cell.* 2005; 4 (9): 1562–1573.

29. Nobile C., Johnson A. D. *Candida albicans* Biofilms and Human Disease. *Annu Rev Microbiol.* 2015; 69: 71-92.
30. Andes D., Nett J., Oschel P., Albrecht R., Marchillo K., Pitula A. Development and Characterization of an In Vivo Central Venous Catheter *Candida albicans* Biofilm Model. *Infect Immun.* 2004; 72(10): 6023–6031.
31. Finkel J. S., Mitchell A. P. Genetic control of *Candida albicans* biofilm development. *Nat Rev Microbiol.* 2011; 9 (2): 109-118.
32. Baillie G.S., Douglas L.J. Effect of growth rate on resistance of *Candida albicans* biofilms to antifungal agents. *Antimicrob Agents Chemother.* 1998; 42 (8): 1900-5.
33. Ramage G., Rajendran R., Sherry L., Williams C. Fungal biofilm resistance. *Int J Microbiol.* 2011; doi:10.1155/2012/528521.
34. Nobile C. J., Fox E.P., Nett J. E., Sorrells T. R., Mitrovich Q.M., Hernday A.D., Tuch B.B., Andes D.R., Johnson A.D. A recently evolved transcriptional network controls biofilm development in *Candida albicans*. *Cell.* 2012; 148(1-2): 126-38.
35. De Groot P. W. J., Bader O., De Boer A. D., Weig M., Chauhan N. Adhesins in Human Fungal Pathogens: Glue with Plenty of Stick. *Eukaryotic Cell.* 2013; 12(4):470-81.
36. Phan Q.T., Myers C.L., Fu Y., Sheppard D.C., Yeaman M.R., Welch W.H., Ibrahim A.S., Edwards J.E. Jr., Filler S.G. Als3 is a *Candida albicans* invasin that binds to cadherins and induces endocytosis by host cells. *PLoS Boil.* 2007; 5(3): e64.
37. Zhu W., Filler S.G. Interactions of *Candida albicans* with epithelial cells. *Cell. Microbiol.* 2010; 12 (3): 273–282.
38. Yang W., Yan L., Wu C., Zhao X., Tang J. Fungal invasion of epithelial cells. *Microbiol Res.* 2014; 169 (11): 803-10.

39. Naglik J.R., Challacombe S.J., Hube B. *Candida albicans* secreted aspartyl proteinases in virulence and pathogenesis. *Microbiol Mol Biol Rev.* 2003; 67 (3): 400–28.
40. Schaller M., Januschke E., Schackert C., Woerle B., Korting H.C. Different isoforms of secreted aspartyl proteinases (Sap) are expressed by *Candida albicans* during oral and cutaneous candidosis in vivo. *J Med Microbiol.* 2001; 50(8):743-7.
41. Fradin Ch., Kretschmar M., Nitchterlein T., Gaillardin C., Ch. d’Enfert and Hube B. Stage-specific gene expression of *Candida albicans* in human blood. *Mol. Microbiol.* 2003; 47: 1523–1543.
42. Argimón S., Wishart J.A., Leng R., Macaskill S., Mavor A., Alexandris T., Nicholls S., Knight A.W., Enjalbert B., Walmsley R., Odds F.C, Gow N.A.R., Brown A.J. Developmental regulation of an adhesin gene during cellular morphogenesis in the fungal pathogen *Candida albicans*. *Eukaryotic Cell.* 2007; 6: 682–692.
43. Park M., Do E., Jung W. H. Lipolytic enzymes involved in the virulence of human pathogenic fungi. *Mycobiology.* 2013; 41(2): 67–72.
44. Sherrington S. L., Sorsby E., Mahtey N., Kumwenda P., Lenardon M. D., Brown I., Ballou E. R., MacCallum D. M., Hall R. A. Adaptation of *Candida albicans* to environmental pH induces cell wall remodelling and enhances innate immune recognition. *Plos Pathogens.* 2017; 13(5): e1006403.
45. Du H., Huang G. Environmental pH adaption and morphological transitions in *Candida albicans*. *Curr Genet.* 2016; 62: 283-286.
46. Garnaud C., García-Oliver E., Wang Y., Maubon D., Bailly S., Despinasse Q., Champlébourg M., Govin J., Cornet M. The Rim Pathway Mediates Antifungal Tolerance in *Candida albicans* through Newly Identified Rim101 Transcriptional Targets, Including Hsp90 and Ipt1. *Antimicrob Agents Chemother.* 2018; 23: 62(3).

47. Sawant B., Khan T. Recent advances in delivery of antifungal agents for therapeutic management of candidiasis. *Biomed. Pharmacother.* 2017; 96:1478-1490.
48. Bondaryk M., , Kurzątkowski W., Staniszewska M. Antifungal agents commonly used in the superficial and mucosal candidiasis treatment: mode of action and resistance development. *Postepy Dermatologii i Alergologii.* 2013; 30(5):293-301.
49. Spampinato C., Leonardi D. *Candida* Infections, Causes, Targets, and Resistance Mechanisms: Traditional and Alternative Antifungal Agents. *BioMed Research International.* 2013; 2013: 204-237.
50. Zupanić-Krmek D., Nemet D. Systemic fungal infections in immunocompromised patients. *Acta Med Croatica.* 2004; 58 (4): 251-61.
51. De Oliveira Santos G. C., Vasconcelos C. C., Lopes A. J. O., de Sousa Cartágenes M., Filho A. K. D. B., do Nascimento F. R. F., Ramos R. M., Pires E. R.R. B., de Andrade M. S., Rocha F. M. G., de Andrade Monteiro C. *Candida* Infections and Therapeutic Strategies: Mechanisms of Action for Traditional and Alternative Agents. *Front Microbiol.* 2018; 9: 1351
52. Cannon R.D., Lamping E., Holmes A. R., Niimi K., Baret P. V., Keniya M. V., Tanabe K., Niimi M., Goffeau A., Monk B. C. Efflux-mediated antifungal drug resistance. *Clin Microbiol Rev.* 2009; 22(2): 291–321.
53. Ghannoum M.A., Rice L. B. Antifungal Agents: Mode of Action, Mechanisms of Resistance, and Correlation of These Mechanisms with Bacterial Resistance. *Clin Microbiol Rev.* 1999; 12(4): 501–517.
54. Grover N. D. Echinocandins: A ray of hope in antifungal drug therapy. *Indian J Pharmacol.* 2010; 42(1): 9–11.
55. White T.C., Marr K.A., Bowden R.A. Clinical, cellular, and molecular factors that contribute to antifungal drug resistance. *Clin Microbiol Rev.* 1998; 11(2):382-402.

56. Arendrup M.C., Patterson T. F. Multidrug-Resistant *Candida*: Epidemiology, Molecular Mechanisms, and Treatment. *J Infect Dis.* 2017; 216 (suppl_3): S445-S451.
57. Oxman D. A., Chow J. K., Frendl G., Hadley S., Hershkovitz S., Ireland P., McDermott L.A., Tsai K., Marty F.M., Kontoyiannis D.P., Golan Y. Candidaemia associated with decreased in vitro fluconazole susceptibility: is *Candida* speciation predictive of the susceptibility pattern? *J Antimicrob Chemother.* 2010; 65 (7), 1460–1465.
58. Cowen L. E., Sanglard D., Howard S. J., Rogers P. D., Perlin D.S. Mechanisms of Antifungal Drug Resistance. *Cold Spring Harbor Perspect Med.* 2015; 5(7): a019752.
59. Mansfield B. E., Oltean H. N., Oliver B. G., Hoot S. J., Leyde S. E., Hedstrom L., White T. C. Azole Drugs Are Imported By Facilitated Diffusion in *Candida albicans* and Other Pathogenic Fungi. *Plos Pathogens.* 2010; 6(9): e1001126.
60. Cowen L. E., Steinbach W.J. Stress, Drugs, and Evolution: the role of Cellular Signaling in Fungal Drug Resistance. *Eukaryot Cell.* 2008; 7 (5): 747-64.
61. Martel C.M., Parker J.E., Bader O., Weig M., Gross U., Warrillow A.G., Kelly D.E., Kelly S.L. A clinical isolate of *Candida albicans* with mutations in ERG11 (encoding sterol 14 α -demethylase) and ERG5 (encoding C22 desaturase) is cross resistant to azoles and amphotericin B. *Antimicrobial Agents Chemother.* 2010; 54(9):3578-83.
62. Sanglard D., Ischer F., Parkinson T., Falconer D., Bille J. *Candida albicans* mutations in the ergosterol biosynthetic pathway and resistance to several antifungal agents. *Antimicrob Agents Chemother.* 2003; 47:2404–2412.
63. Grossman N. T., Chiller T. M., Lockhart S. R. Epidemiology of echinocandin resistance in *Candida*. *Curr Fungal Infect Rep.* 2014; 8(4):243-248.

64. Prigent G., Aït-Ammar N., Levesque E., Fekkar A., Costa J.M., Anbassi S. E., Foulet F., Duvoux C., Merle J. C., Dannaoui E., Botterel F. Echinocandin Resistance in *Candida* Species Isolates from Liver Transplant Recipients. *Antimicrob Agents Chemother.* 2017; 61 (2). pii: e01229-16.
65. Quina A. S., Buschbeck M., Di Croce L. Chromatin structure and epigenetics. *Biochem Pharmacol.* 2006; 72(11):1563-9.
66. Santos R. H., Caldas C. Chromatin modifier enzymes, the histone code and cancer. *Eur J Cancer.* 2005; 41(16):2381-402.
67. Rai L. S., Singha R., Brahma P., Sanyal K. Epigenetic determinants of phenotypic plasticity in *Candida albicans*. *Fungal Biology Reviews.* 2018; 32 (1), 10-19.
68. Sterner D. E., Berger S. L. Acetylation of histones and transcription-related factors. *Microbiol Mol Biol Rev.* 2000; 64 (2): 435-459.
69. Peserico A., Simone C. Physical and Functional HAT/HDAC Interplay Regulates Protein Acetylation Balance. *J Biomed Biotechnol.* 2011; 2011: 371832.
70. Grozinger C. M., Schreiber S. L. Deacetylase enzymes: biological functions and the use of small-molecule inhibitors. *Chemistry & Biology.* 2002; 9: 3-16.
71. Seto E., Yoshida M. Erasers of Histone Acetylation: The Histone Deacetylase Enzymes. *Cold Spring Harb Perspect Biol.* 2014; 6(4): a018713.
72. Finnin M. S., Donigian J. R., Cohen A., Richon V. M., Rifkind R. A., Marks P. A., Breslow R., Pavletich N. P. Structures of a histone deacetylase homologue bound to the TSA and SAHA inhibitors. *Nature.* 1999; 401: 188–193.
73. Smith B. C., Denu J. M. Chemical mechanisms of histone lysine and arginine modifications. *Biochim Biophys Acta.* 2009; 1789(1): 45-57.

74. Smith B. C., Denu J. M. Sir2 Protein Deacetylases: Evidence for Chemical Intermediates and Functions of a Conserved Histidine. *Biochemistry*. 2006;45(1):272-82.
75. Serravallo M., Jagdeo J., Glick S. A. Sirtuins in dermatology: applications for future research and therapeutics. *Arch Dermatol Res*. 2013; 305(4):269-82.
76. Redondo P. M., Vaquero A. The diversity of histone versus nonhistone sirtuin substrate. *Genes Cancer*. 2013; 4(3-4): 148–163.
77. Garnaud C., Champleboux M., Maubon D., Cornet M., Govin J. Histone deacetylases and their inhibition in *Candida* species. *Front Microbiol*. 2016; 1238.
78. Kim J., Lee J.E., Lee J. S. Histone deacetylase-mediated morphological transition in *Candida albicans*. *J Microbiol*. 2015; 53(12):805-11.
79. Xiaofang L., Qing C., Huan M., Xiaowei Z., Yongnian S., Dongmei L., Weida L. The Rpd3/Hda1 family of histone deacetylases regulates azole resistance in *Candida albicans*. *J Antimicrob Chemother*. 2015; 70:1993-2003.
80. Smith W.L., Edlind T.D. Histone deacetylase inhibitors enhance *Candida albicans* sensitivity to azoles and related antifungals: correlation with reduction in CDR and ERG upregulation. *Antimicrob Agents Chemother*. 2002; 46:3532-9s.
81. Wurtele H., Tsao S., Lépine G., Mullick A., Tremblay J., Drogaris P., Lee EH., Thibault P., Verreault A., Raymond M. Modulation of histone H3 lysine 56 acetylation as an antifungal therapeutic strategy. *Nat Med*. 2010; 16:774-80.
82. Celic I., Masumoto H. The sirtuins Hst3 and Hst4p preserve genome integrity by controlling histone H3 Lysine 56 deacetylation. *Curr Biol*. 2006; 16 (13): 1280-9.

83. Calabrese E. C, Castellano S., Santoriello M., Sgherri C., Quartacci M. F., Calucci L., Warrilow A. G. S., Lamb D. C., Kelly S. L., Milite C., Granata I., Sbardella G., Stefancich G., Maresca B., Porta A. Antifungal activity of azole compounds CPA18 and CPA109 against azole-susceptible and -resistant strains of *Candida albicans*. J Antimicrob Chemother. 2013; 68: 1111-1119.
84. Eberharter A., Becker P. B. Histone acetylation: a switch between repressive and permissive chromatin. EMBO reports. 2002; 3: 224–229.
85. Wang X., Hayes J. J. Acetylation Mimics within Individual Core Histone Tail Domains Indicate Distinct Roles in Regulating the Stability of Higher-Order Chromatin Structure. Mol Cell Biol. 2008;28(1):227-36.
86. Stehr F., Felk A., Kretschmar M., Schaller M., Schäfer W., Hube B. Extracellular hydrolytic enzymes and their relevance during *Candida albicans* infections. Mycoses. 2000; 43 Suppl 2:17-21.
87. Hoyer L. L, Clevenger J, Hecht J. E, Ehrhart E. J., Poulet F. M. Detection of Als Proteins on the Cell Wall of *Candida albicans* in Murine Tissues. Infect Immun. 1999; 67(8): 4251–4255.
88. Singleton D. R., Fidel P. L. Jr., Wozniak K. L., Hazen K.C. Contribution of cell surface hydrophobicity protein 1 (Csh1p) to virulence of hydrophobic *Candida albicans* serotype A cells. FEMS Microbiology Letters. 2005; 15; 244 (2): 373-7.
89. Selving K., Alspaugh J. A. pH Response Pathways in Fungi: Adapting to Host-derived and Environmental Signals. Microbiology. 2011 Dec; 39(4): 249–256.
90. Baek Y.U., Martin S.J., Davis D.A. Evidence for novel pH-dependent regulation of *Candida albicans* Rim101, a direct transcriptional repressor of the cell wall beta-glycosidase Phr2. Eukaryot Cell. 2006; 5(9):1550-9.
91. Schneider S., Morschhäuser J. Induction of *Candida albicans* Drug Resistance Genes by Hybrid Zinc Cluster Transcription Factors. Antimicrob Agents Chemother. 2015; 59(1): 558–569.

92. Klis F.M., de Groot P., Hellingwerf K. Molecular organization of the cell wall of *Candida albicans*. *Med Mycol.* 2001; 39 Suppl 1:1-8.
93. Stuertvant J., Cihlar R., Calderone R. Disruption studies of a *Candida albicans* gene, ELF1: a member of the ATP-binding cassette. *Microbiology*, 1998; 144 (Pt8) :2311-21.
94. Marotta D. H., Nantel A., Sukala L., Teubl J. R., Rauceo J.M. Genome-wide transcriptional profiling and enrichment mapping reveal divergent and conserved roles of Sko1 in the *Candida albicans* osmotic stress response. *Genomic.* 2013; 102(4):363-71.
95. Su C., Lu Y., Liu H. Reduced TOR signaling sustains hyphal development in *Candida albicans* by lowering Hog1 basal activity. *Mol Biol Cell.* 2013; 24(3):385-97.
96. Nie X., Liu X., Wang H., Chen J. Deletion of EFG1 promotes *Candida albicans* opaque formation responding to pH via Rim101. *Acta Biochim Biophys Sin.* 2010; 42(10):735-44.
97. Zordan R., Miller M. G., Galgoczy D. J., Touch B. B., Johnson A. D. Interlocking Transcriptional Feedback Loops Control White-Opaque Switching in *Candida albicans*. *Plos Biol.* 2017; 5(10): e256.
98. Thaminy S, Newcomb B, Kim J, Gatbonton T, Foss E, Simon J, Bedalov A. Hst3 Is Regulated by Mec1-dependent Proteolysis and Controls the S Phase Check point and Sister Chromatid Cohesion by Deacetylating Histone H3 at Lysine 56. *J Biol Chem.* 2007; 282(52): 37805-14.

APPENDIX

LIST OF PUBLICATIONS

Papers

- Piccinelli A.L., Pagano I., Esposito T., Mencherini T., Porta A., **Petrone A. M.**, Gazzo P., Picerno P., Sansone F., Rastrelli L., Aquino R. P. HRMS Profile of a Hazelnut Skin Proanthocyanidin-rich Fraction with Antioxidant and Anti-*Candida albicans* Activities. *J Agric Food Chem.* 2016; 64 (3): 585-95.
- Porta A., **Petrone A.M.**, Morello S., Granata I., Rizzo F., Memoli D., Weisz A., Maresca B. Design and expression of peptides with antimicrobial activity against *Salmonella typhimurium*. *Cell Microbiol.* 2017; 19 (2).
- Concilio S., Sessa L., **Petrone A. M.**, Porta A., Diana R., Iannelli P., Piotto S. Structure Modification of an Active Azo-Compound as a Route to New Antimicrobial Compounds. *Molecules.* 2017; 22(6).
- De Falco G., Porta A., **Petrone A. M.**, Del Gaudio P., El Hassanin A., Commodo M., Minutolo P., Squillace A., and D'Anna A. Antimicrobial Activity of Flame-Synthesized Nano-TiO₂ Coatings. *Environ. Sci.: Nano.* 2017; 4, 1095-1107.
- Dal Piaz F., Bader A., Malafrente N., D'Ambola M., **Petrone A. M.**, Porta A., Ben Hadda T., De Tommasi N., Bisio A., Severino L. Phytochemistry of compounds isolated from the leaf-surface extract of *Psiadia punctulata* (DC.) Vatke growing in Saudi Arabia. *Phytochemistry.* 2018; 155: 191-202.

Presentation at conferences

- Porta A., **Petrone A. M.**, Morello S., Maresca B. A procedure to identify peptides with α -AMP activity. Microbiology 2015, 31st Meeting of SIMGBM. 23-26 September 2015, Ravenna, Italy.
- Gorrasi A., **Petrone A. M.**, Li Santi A., Montuori N., Ragno P. The urokinase receptor drives cell migration mechanisms in tumor cells. XV Workshop on Molecular and Cellular Biology of Plasminogen activation. 22-26 September, Rome, Italy.
- Manniello M.D., Simonetti A., **Petrone A.M.**, Porta A., Aquino R.P., Del Gaudio P., Russo P. Aerodynamic Properties and Drug Solubility of Dry Powders Prepared by Spray Drying: Clarithromycin Versus its Hydrochloride Salt. 3rd International TB-meeting “Inhaled Therapies for tuberculosis and other infectious diseases”. 14-16 October 2015, Parma, Italy.
- Bechlem H., Esposito T., Sansone F., **Petrone A. M.**, Porta A., Mencherini T., Benayache S., De Tommasi N. “*Mentha pulegium* extract: chemical composition, antioxidant and anti-*Candida albicans* activities”. SIF, XV Congress of the Italian society of phytochemistry jointly with 1st international Congress on Edible, Medicinal and aromatic plant (ICEMAP 2017). 28- 30 June 2017, Pisa, Italy.
- Habacher H., Bauer I., **Petrone A. M.**, Faserl K., Kremser L., Lindner H., Graessle S., Brosch G. Proteome-wide Profiling of Arginine Methylation in *Aspergillus nidulans*. Life Science PhD Meeting. 5th-6th April 2018, Innsbruck, Austria.